DESIGN, DEVELOPMENT, AND DELIVERY OF NOVEL RECOMBINANT PROTEINS FOR NEURON-TARGETED THERAPY AND NEURONAL DIFFERENTIATION

by
Paul A. Gramlich

A dissertation submitted to the Johns Hopkins University in conformity with the requirements for the degree of Doctor of Philosophy

Baltimore, Maryland
July 2015

Abstract

This thesis dissertation research has aimed to develop novel protein therapeutics with potential to treat neurological diseases for which there are currently limited available treatments and no cures including Parkinson's disease and neuronopathic Gaucher's disease. Although the individual chapters of this thesis had varied goals, all involved designing and expressing recombinant proteins, purifying the proteins, facilitating targeted and efficient protein delivery, and demonstrating *in vitro* activity.

The effective targeting of neuronal cell types requires effective delivery strategies. As a result, initial thesis work focused on the evaluation of cell-penetrating peptides (CPPs) and receptor-dependent neuronal membrane binding proteins to improve protein delivery. This work led to the discovery of a novel protein delivery vector, Tat-Tetanus Toxin Fragment C (Tat-TTC), a highly neuron-specific domain capable of dramatically enhancing the binding and internalization of recombinant proteins. Both fluorescent microscopy and quantitative fluorimetry were utilized to demonstrate that, with Tat-TTC, model protein GFP was bound and internalized by neuronal cell types at least an order of magnitude better than Tat-GFP or TTC-GFP alone. Since the Tat-TTC protein delivery vector was endocytosed, this research project addressed the issue of endosomal entrapment of cargo protein. Photochemical internalization (PCI) was used to facilitate the endosomal release of Tat-TTC-linked cargo presenting the option of using the delivery vector to target endosomes/lysosomes or cytosolic or nuclear intracellular targets.

Cell-penetrating peptide Tat and PCI were next utilized in the design, production, and delivery of recombinant transcription factors Mash1, Lmx1a, and Nurr1 intended for

neuronal differentiation. These transcription factors had been shown to transdifferentiate human fibroblasts to dopaminergic neurons (Caiazzo et al., 2011), the cell type lost in Parkinson's disease (PD) (Thomas, 2010). We hypothesized that direct protein delivery of Tat-linked transcription factors had the potential to generate dopaminergic neurons that would be safe for clinical cell-replacement therapy. Four transcription factors, Tat-Mash1, Tat-Mash1-GFP, Tat-Lmx1a, and Tat-Lmx1a-GFP were successfully expressed and purified from insoluble HEK293F cell lysate. The transcription factors were delivered to cells and endosomal escape was facilitated with PCI. Induction of promoter-reporter constructs with purified protein was limited, a finding which led us to question the bioactivity of the resolubilized factors. To address this issue, a cell-free mammalian expression system capable of producing high concentrations of soluble transcription factor was identified. In the future, this strategy could prove invaluable for transcription factor production.

Research into novel PD therapies led to my strong interest in Gaucher's disease (GD). Mutations in the *GBA1* gene encoding lysosomal enzyme glucocerebrosidase (GCase), leading to GD, has recently been shown to represent the greatest genetic risk factor for PD (Siebert et al., 2014). There is currently no available treatment for the neuronopathic type 2 and type 3 forms of GD. I aimed to develop a neuron-targeted recombinant GCase with the potential to cross the blood-brain barrier (BBB). Since the target for delivered protein was the lysosome, protein delivery vectors taken up by endocytosis were predicted to work well for GCase delivery, without any need for PCI. Seventeen GCase variants were designed and expressed in combination with a variety of protein delivery vectors. Cell-based assays using a GCase-knockout neuronal cell line

facilitated the identification of a rabies-derived peptide (RDP) linked GCase utilizing an IgA hinge linker region to remove steric hindrance by GCase on RDP. RDP-IgAh-GCase was shown to target GCase-knockout neurons ~2.5X better than Tat-GCase. Both RDP-IgAh-GCase and Tat-GCase reduced substrate glucosylsphingosine accumulation to wild-type levels with 72 hours of protein treatment, indicating the enzymes were appropriately trafficked to lysosomes and functional.

Thesis Advisors and Readers: Dr. Michael J. Betenbaugh, Dr. Paul S. Fishman

Thesis Committee Chair: Dr. Kevin Yarema

Thesis Committee: Dr. Honggang Cui, Dr. George Oyler

Acknowledgements

There are so many people that deserve thanks and acknowledgment for helping me over the past ~5 years in my graduate research. First, I'd like to thank my graduate research advisors Dr. Mike Betenbaugh and Dr. Paul Fishman. I respect Mike and Paul immensely both as scientific researchers and as people. Both of them were supportive of my hard work whether I got a good or bad result; their continued support kept my confidence up even when the data was less than promising. Mike Betenbaugh taught me the importance of collaboration, specifically, not being afraid to immerse myself in fields where I did not have the most expertise. Most of my graduate work has had neuroscience applications and before coming to Hopkins, my neuroscience knowledge mostly came from undergraduate courses. Mike is also a generally great guy and put me at ease meeting with him from the beginning. Paul Fishman has been a terrific mentor to me since I joined his lab in December of 2010. He has endless energy and to this day I'm not entirely sure how he's able to balance his clinical responsibilities as a neurologist with his research so well. Paul immediately recognized my ability and desire to work independently, but has always made himself available when I needed guidance despite his busy clinical schedule. Of the many things I've learned from Paul, I think the most important two are: 1) really learning to read and question scientific literature and 2) when to move on from an experiment or project that is not progressing appropriately. Along with Mike and Paul, I'd like to thank the rest of my thesis committee Dr. Kevin Yarema, Dr. Honggang Cui, and Dr. George Oyler for taking time out of their busy schedules to evaluate my dissertation.

talented group of undergraduates and master's students including Thuy-My Le and May

Sumi from Johns Hopkins and Julian Amin and Adam Zhao from the University of

Maryland. All of these students deserve credit for their contributions and assistance in

my research. Administrative staffs from the Johns Hopkins Department of Chemical and

Biomolecular Engineering and VA Research Service work very hard and often don't

receive the thanks they deserve. As a result, I'd like to take the time now to thank

everyone that has helped me from both institutions.

Research cannot take place without funding or valuable collaborators. I'd like to

thank the Department of Veteran's Affairs for funding my research via Paul Fishman's

VA grants. Importantly, I'd like to thank Dr. Wendy Westbroek and Dr. Ellen Sidransky

from the NIH, Dr. Ying Sun and Dr. Wujuan Zhang from Cincinnati Children's Hospital,

and Dr. Ricardo Feldman and Dr. Ola Awad from the University of Maryland School of

Medicine for their valuable collaboration on the development of the RDP-IgAh-GCase

enzyme. Wendy and Ellen provided me with the invaluable GCase-knockout neuronal

cell line and gave me the excellent opportunity to present my research for their

laboratory. Ying and Wujuan were critical collaborators for the glucosylsphingosine

substrate reduction work and were responsible for the LC-MS/MS analysis involved.

Ricardo and Ola provided me with iPSC-derived Gaucher neurons for initial study and

have been valuable consultants on the GCase delivery work.

Finally, I'd like to thank my friends and family for their support during my

graduate research. Along with old friends, I've made a lot of new friends in the ChemBE

department and in Baltimore as a whole; times with them made graduate school a lot less

stressful. There are too many people here to mention but they have all been valuable

Table of Contents

List of Figures

List of Tables

Chapter 1: Introduction

Derived from, or consisting of living entities, biologics are under widespread development for therapeutic use in the pharmaceutical industry. Contrary to traditional small molecule drugs, biologics are considerably less well-defined. They are a diverse class that can include gene therapeutic agents, proteins, or live cells. Recombinant proteins constitute most of the FDA-approved biologics. While direct protein delivery can have a powerful effect on phenotype, the effects are not permanent. As a result, protein delivery is widely considered to be safer than gene or cell-based approaches.

The motivation for this doctoral research was the development of recombinant proteins to enable new therapeutic strategies for diseases affecting the brain. With this goal in mind, I describe the design, development, and delivery of a novel neuronal cell type-specific protein delivery vector, a set of purified transcription factors for cell differentiation, and a neuron-targeted recombinant glucocerebrosidase (GCase) enzyme for neuronopathic Gaucher's disease (GD) treatment. While numerous challenges associated with the development of recombinant proteins exist, delivery was a major focus for each of the above research endeavors. Furthermore, design, production, and purification were addressed for each of the individual research goals. These three parameters had variable impacts on a protein-specific basis that will be discussed.

The highest profile, and most recent, achievement of this thesis research was the development of rabies derived-peptide (RDP) linked GCase containing a linker region from the IgA hinge domain (RDP-IgAh-GCase), the first neuron-targeted glucocerebrosidase. Although this recombinant enzyme neither utilized Tat-Tetanus Toxin Fragment C (Tat-TTC, Chapter 2) nor faced the challenges associated with transcription factor delivery

(Chapter 3), its development was successful as a result of experience gained in those two projects. The discovery of Tat-TTC provided a base that was extensively built upon during the screening of GCase variants employing numerous receptor-independent cell-penetrating peptides and receptor-dependent toxin and virus-derived protein delivery vectors. The goal set out in Chapter 3, to create a collection of recombinant Tat-linked transcription factors to promote neuronal differentiation, was never fully achieved. However, the assay development work to test transcription factor biological activity later served as the primer for some of the GCase functionality testing.

1.1.   Protein Delivery Vectors

Protein delivery vectors can be both receptor-independent and receptor-dependent and serve to target cargo proteins to a large variety of cellular compartments. Both classes of these vectors have been used in neuronal delivery although their mechanism, specificity, and capacity differ considerably.

1.1.1   Cell-penetrating peptides

Cell-penetrating peptides (CPPs) are short cationic peptides capable of penetrating the cell membrane in a receptor-independent manner (DeShayes et al., 2005). CPPs have been derived from a number of naturally occurring biological sources. The mechanism of CPP uptake has been extensively debated, especially whether or not the process is energy-dependent.

The first CPP discovered was Tat, an arginine and lysine-rich peptide derived from the HIV protein Tat (trans-activator of transcription). Frankel and Pabo, at The Johns Hopkins School of Medicine, unexpectedly discovered the membrane-penetrating ability of the intact purified Tat protein when attempting to develop a trans-activation assay for

Tat itself. When Tat was added to the extracellular medium of HL3T1 cells, expression of a reporter gene increased linearly with Tat dose, an unexpected result. This result was surprising because Tat were not predicted to enter the cell at all. Uptake was enhanced by lysosomotrophic agent chloroquine, indicating that membrane disruption increased the efficiency of the process (Frankel et al., 1988). The implications of this discovery for protein delivery were quickly identified and research began to determine exactly how much and what portion of the 86 amino acid Tat protein was necessary for membrane translocation. Initially, it was found that Tat amino acids 35-62 contained the region of interest (Anderson et al., 1993). Soon after, Fawell and colleagues recommended amino acids 37-72 for optimal delivery, although they found that regions 37-58 and 47-58 were also sufficient (Fawell et al., 1994). Other research groups confirmed that either 47-58 (Pepinsky et al, 1994) or 48-60 (Vivès et al, 1997) were effective. In the 48-60 sequence, it was found that any changes to the basic amino acids reduced membrane translocation potential (Vivès et al, 1997). It was later determined that amino acids 49-57, peptide sequence RKKRRQRRR, represented the shortest Tat-based peptide useful for cellular uptake. Although charge alone was not enough to reproduce this effect, polyarginine (R9) was found to be a very efficient CPP (Wender et al., 2000). The Tat CPP was shown to deliver proteins in a cell-type independent manner. β-galactosidase, a 120 kDa protein, was delivered across the blood-brain barrier (BBB) using Tat (Schwarze et al., 1999).

Over the years, the mechanism for Tat uptake has been controversial. It was initially reported that Tat and polyarginine were taken up directly into the cytosol by an energy-independent and unknown mechanism. However, it was later determined that even mild cell fixation led to artifactual uptake and that live cell imaging showed endosomal

Tat-linked cargo protein distribution (Richard et al., 2003). It is now generally accepted that Tat interacts electrostatically with cell surface proteoglycans (Heitz et al., 2009) and is internalized by receptor-independent lipid raft-dependent macropinocytosis (Kaplan et al., 2004; Wadia et al., 2004).

Although Tat and polyarginine are the most common CPPs used for protein delivery, a number of other protein-derived CPPs exist including transportan, penetratin, and VP22. Transportan is a 27 amino acid synthetic CPP consisting of a 13 amino acid N-terminal fragment of neuropeptide galanin and a 14 amino acid fragment of mastoparan, a wasp venom peptide toxin (Pooga et al., 1998). Penetratin is a 16 amino acid portion of the homeodomain of Antennapedia that is also capable of crossing the cell membrane. The 16 amino acid portion was found to be the minimal region capable of exhibiting the same penetrating properties as the entire 60 amino acid homeodomain (Derossi et al., 1994). VP22 is a 38 kDa structural protein of herpes simplex virus type 1 that can also freely penetrate the cell membrane; the C-terminal 34 amino acids were shown to be the critical portion of the molecule (Elliot et al., 1997). Although these are the more commonly used CPPs, numerous others that have been naturally derived or engineered exist, including Koposi FGF, Syn B1, FGF-4, nuclear localization signals (NLS), anthrax toxin derivative 254-amino acids peptide, diphtheria toxin binding domain, MPG, pep-1, WR peptide, and endotoxin A (Chauhan et al., 2007).

Upon discovery, transportan, penetratin, and VP22 were reported to be taken up directly by energy-independent mechanisms (Derossi et al., 1994; Deshayes et al., 2005; Elliot et al., 1997; Pooga et al., 1998). However, these early studies used cell fixation in their analysis; as a result, the internalization mechanisms may need to be revisited. In live

cell imaging Penetratin was found to be taken up through macropinocytosis (Jones et al., 2005; Maiolo et al., 2005). It is possible that, even for a specific CPP, the mechanism of cellular uptake could differ with the presence of cargo. It was found that, with live cell imaging, a R7 CPP could be taken up at 4ºC and observed as a diffuse signal in the cell, indicating that uptake could be direct. However, with a cargo peptide, internalization was almost totally through endocytosis (Maiolo et al., 2005).

Internalization of CPPs takes place quickly with maximum concentrations being reached in 1-3 hours, however, this can be slowed by the inclusion of cargo proteins (Jones et al., 2005; Zorko et al.; 2005). There have been some quantitative comparisons of CPP internalization in which magnitude of uptake was affected by a peptide cargo. In one study using FACS, the magnitude of uptake was compared with and without a cargo peptide. With the cargo peptide, polyarginine and transportan were taken up most efficiently, followed by penetratin and Tat. Without the peptide cargo the order was polyarginine = penetratin > Tat = transportan. However, penetratin and Tat were the least toxic, indicating that there are multiple factors to consider. As anticipated based on the mechanism, uptake of all peptides studied was found to be cell-type independent (Jones et al., 2005).

1.1.2 Receptor-dependent neuronal protein delivery vectors

Tat and other CPPs have been used to deliver cargo proteins to neuronal cell types because they don't require any specific receptor to bind. The lack of receptor can be a disadvantage if the intent is to specifically target neurons. Three neuronal protein delivery vectors have been utilized in this thesis: tetanus toxin fragment C (TTC), Tet1, and rabies-derived peptide (RDP). These delivery vectors vary in their size, binding affinity, and potential for *in vivo* delivery.

5

TTC is by far the largest of the neuronal binding domains, but it is also the best characterized. TTC is the non-toxic 50 kDa binding domain derived from the C-terminus of the heavy chain of tetanus toxin. It has been shown that TTC can enhance neuronal delivery of a cargo protein up to 1000x while retaining the retrograde transport and transsynaptic transport properties of tetanus toxin. As a result, delivery of proteins to the CNS with TTC leads not only to better binding, but to better distribution as well (Francis et al., 2004).

Gangliosides are sialic acid-containing glycosphingolipids that are present in neuronal membranes in high concentrations. It has long been known that tetanus toxin binding to neuronal membranes was mediated by complex gangliosides, especially tri- and tetra-siaylated gangliosides such as GT_{1b} (Rogers et al., 1981). Many neuroblastoma cell lines, with the exception of N18-RE-105 and PC12, bind tetanus toxin poorly because they only express monosialogangliosides to which the toxin does not bind well (Walton et al., 1988). Tetanus toxin binds gangliosides in two binding pockets, the "W" lactose-binding site and the "R" sialic acid-binding site. The Trp^{1289} and the Arg^{1226} are the key amino acids involved in the W and R binding pockets respectively (Chen et al, 2009). In early research, it was hypothesized that tetanus toxin might also have a protein receptor; these receptors were much later found to be both the SV2A/B receptors (Yeh et al., 2010) and P15 (Calvo et al., 2012; Miana-Mena et al., 2002). After cell binding with ganglioside and protein receptors, TTC is thought to be taken up via clathrin-mediated endocytosis (Calvo et al., 2012). In fact, when TTC-GFP is delivered to neuronal cells, all fluorescent signal (if observed) is entrapped in vesicles and therefore not distributed throughout the cytosol (Gillmeister et al., 2011; Gramlich et al., 2013).

While the 50 kDa TTC is non-toxic, its large size has the potential to decrease protein expression. Most importantly, TTC would be highly immunogenic as most individuals are immunized to tetanus toxin. The Boulis Laboratory recognized a need for shorter peptides capable of mimicking TTC's binding affinity. Using a phage display assay, the 12 amino acid Tet1 peptide sequence HLNILSTLWKYR, was identified for its ganglioside-binding properties. Tet1 does not have any direct homology to TTC. The Tet1 peptide has been found to bind trisialoganglioside GT_{1b} and can mediate retrograde transport to the neuronal cell body. Tet1 was found to bind differentiated PC12 cells, primary motor neurons, and dorsal root ganglion cells (Federici et al., 2007).

Tet1 has only been used for neuronal targeting of cargo in a few applications. The first application developed used Tet1-polyethylenimine (Tet1-PEI) to deliver nucleic acids to neuronal cells (Park et al., 2007). Tet1 was also successfully used to deliver polymersomes to nerves in the inner ear (Zhang et al., 2012b). To date, very limited protein delivery has been done using Tet1, although one recent paper investigated the feasibility of *in vivo* Tet1-mediated protein delivery using model protein GFP (Kassa et al., 2013). The Fishman laboratory was the first group to compare Tet1 protein delivery to TTC; unpublished results show that Tet1-GFP is bound and internalized significantly less than TTC-GFP (Mello et al., in preparation). The most recent Tet1 application integrated Tet1 into the capsid of an adenoviral vector, which improved transduction of motor neurons, decreased transduction of non-neuronal cells, and improved retrograde transport (Davis et al., 2015).

RDP is the neuronal delivery vector derived from the rabies virus glycoprotein (RVG) that was found to be most useful for the neuron-targeting of glucocerebrosidase in

this thesis. RVG is a 505 amino acid protein component of the rabies viral envelope that mediates neuron binding and internalization. The full-length glycoprotein after translation is 524 amino acids but the first 19 amino acids constituting the signal peptide are removed during post-translational processing (Maillard et al., 2002). All references to RVG amino acid sequences in the literature refer to the 505 amino acid glycoprotein. RVG has two nerve binding regions consisting of amino acid sequences 189-214 and 330-357 (Fu et al., 2013a).

References to RDP peptides in the literature can be confusing, because effective delivery peptides have been derived from both of the aforementioned neuron-binding sequences. To date, RVG-based delivery domains have been derived from amino acids 175-203 (Kumar et al., 2007; Liu et al., 2009; Gao et al., 2014; Gong et al., 2012; Xiang et al., 2011) and amino acids 330-356 (Fu et al., 2012; Fu et al., 2013a; Fu et al., 2013b). These RVG-derived peptides vary for a number of parameters including the nerve-binding region used, the presence of a nine-arginine sequence, and the application.

The first RVG-derived peptide was 41 amino acids long; it consisted of 29 amino acids derived from RVG sequence 175-203 and a R9 sequence connected by a 3 glycine linker. The R9 sequence was included to facilitate siRNA binding. Delivery of siRNA led to gene silencing in the brain, showing that this first RVG-derived peptide mediated delivery across the BBB (Kumar et al., 2007). The specific RVG-derived sequence was inspired by a 1990 paper that demonstrated the peptide could inhibit bungarotoxin binding to the nicotinic acetylcholine receptor (nAChR) (Lentz et al., 1990). The RVG-peptide alone was capable of crossing the BBB but because this peptide cannot bind siRNA, no comparison between delivery of RVG and RVG-R9 was done (Kumar et al., 2007). The

RVG-derived 29 amino acid peptide was utilized without the R9 peptide for nanoparticle-based gene delivery. While it was originally assumed that RVG uptake was nAChR-mediated, the nanoparticle delivery work showed that the GABA receptor also plays an important role. Uptake of the nanoparticles was found to be energy-dependent and facilitated by a clathrin- and caveolae-mediated endocytosis (Liu et al., 2009). Additional publications have also used this 29 amino acid RVG-derived peptide with (Gong et al., 2012) and without (Gao et al., 2014) the R9 peptide to deliver nucleic acids to the brain. A 43 amino acid peptide has been used to deliver protein β-galactosidase (Xiang et al., 2011).

Literature references to the RDP peptide all come from one research group and refer to a 39 amino acid sequence consisting of 27 amino acids derived from RVG, a 3 glycine linker region, and a 9 arginine peptide. The 27 amino acid peptide is RVG sequence 330-356 (Fu et al., 2012). RDP has been used to deliver several recombinant proteins including β-galactosidase, luciferase, brain-derived neurotrophic factor (BNDF) (Fu et al., 2012), GFP, and glial cell-derived neurotrophic factor (GDNF) (Fu et al., 2013b). All RDP-linked proteins were constructed with a flexible GGGSGGGS linker region (Fu et al., 2012; Fu et al., 2013b). Although not indicated in these publications, results in this thesis indicate that the linker region in RDP fusion proteins may be critical to biological activity (Chapter 4). RDP has also been used to deliver nucleic acids across the BBB (Fu et al., 2013a). Although the mechanism is not fully understood, RDP linked cargo proteins are thought to be taken up by clathrin-mediated endocytosis following GABA receptor binding (Fu et al., 2013b).

Although receptor-dependent neuronal targeting proteins and peptides TTC, Tet1, and RDP were used in this thesis and introduced at length, other neuronal delivery vectors have been described in the literature. KC2S, a 20 amino acid peptide derived from the loop 2 segment of Ophiophagus hannah toxin b, has been shown to bind nAChR receptors with similar affinity as the Kumar et al. 29 amino acid RVG-derived peptide. KC2S was shown to improve micelle-encapsulated drug delivery across the BBB (Zhan et al., 2010). Also, in an analogous way TTC is used, the C-terminal 51 kDa binding domain of botulinum toxin can also be used as a neuronal delivery vector (Drachman et al., 2010).

1.2. Photochemical Internalization (PCI) to Facilitate the Re-Distribution of Endocytosed Cargo Proteins

The cell membrane is not the only barrier to intracellular biological activity of protein delivery vector-linked cargos. As described at length in the previous section, after cell binding in a receptor-dependent or independent manner, most protein delivery vectors and their attached cargo are internalized via a variety of endocytotic mechanisms. Although CPPs do have the capability to escape endosomes following endocytosis, the vast majority of cargo proteins are sequestered in endosomal compartments and later trafficked to lysosomes for degradation. Escape from endosomes is the rate-limiting step in the delivery of CPP-linked macromolecules (El Sayed et al., 2008). Endosomal sequestering of proteins after endocytosis has been treated as both a barrier to be crossed, and a lysosomal delivery method in this thesis dissertation. For transcription factors, the target organelle was the nucleus, so endosomal entrapment had the potential to prevent biological activity of the delivered factors. The endosomal escape properties of Tat may not facilitate the nuclear delivery of a sufficient transcription factor concentration for intracellular

10

activity. Conversely, in the delivery of lysosomal enzyme GCase, the endosomes are the target since they will deliver GCase to the lysosome where it can be activated by saposin C and degrade glycosphingolipid substrates.

When the intracellular target for protein delivery vector-linked proteins is cytosolic or nuclear, methods to facilitate the endosomal escape of cargo become critical. Numerous strategies have been successfully utilized to enhance endosomal escape including fusogenic lipids, membrane-disruptive peptides, membrane-disruptive polymers, lysosomotrophic agents, and photochemical internalization (El-Sayed et al., 2008). Photochemical internalization (PCI) is a particularly interesting technique to rupture endosomes. Cells are treated with lipophilic photosensitizers that integrate in the cell membrane, and therefore, are localized in the endosomal membrane following endocytosis. The photosensitizers can be excited with specific wavelengths of light, causing a photochemical reaction that creates reactive oxygen species that damage endosomal membranes, releasing entrapped cargo (El-Sayed et al., 2008). PCI can be used to mediate the delivery of a large variety of macromolecules and other endosomally entrapped cargo (Selbo et al., 2010).

PCI was first described in 1999 using several different small molecule photosensitizers including $AlPcS_{2a}$, $TPPS_{2a}$, and $TPPS_4$. In this first paper, light was actually delivered with fluorescent tubes; $AlPcS_{2a}$ was excited with red light with 1.35 mW/cm^2 intensity and $TPPS_{2a}$ and $TPPS_4$ were excited with blue light with 1.5 mW/cm^2 intensity. When $TPPS_{2a}$ and horseradish peroxidase (HRP) were delivered together and PCI was mediated, ~60% of HRP was released into the cytosol. This publication also introduced a critical step in PCI: the incubation of cells in photosensitizer-free medium for

11

several hours before light treatment. This incubation period allows photosensitizer to diffuse out of the extracellular membrane, preventing cell lysis upon light treatment (Berg et al., 1999).

Despite the common practice of allowing excess photosensitizer to diffuse out of the cell membrane, some cytotoxicity is often observed in PCI. *In vitro*, PCI has been shown to efficiently mediate cytosolic release with reasonable levels of cytotoxicity, although the light intensity must be carefully controlled as too much intensity can kill cells (Gramlich et al., 2013). Some applications of PCI have taken advantage of the cytotoxic effects. PCI technology has been utilized in the delivery of chemotherapeutic agents to cancer cells (Selbo et al., 2010). Of particular recent interest, PCI has the potential for the treatment of drug-resistant cancers. Specifically, PCI can circumvent drug resistance due to efflux pumps, a common mechanism of resistance (Weyergang et al., 2015). PCI uses the same basic principle as the clinically-used photodynamic therapy. In photodynamic therapy, photosensitizers are delivered to tumors and excited, leading to cytotoxicity. The process can be well-controlled since singlet oxygen is around for only ~20 nanoseconds and has a very short range of action, ~10-20 nanometers. Photodynamic therapy has been shown to kill cancer cells three ways: direct killing of the cell, indirectly by vascular shutdown, and by a photosensitized-induced immune response. One of the limitations of photodynamic therapy is that light will penetrate a maximum of ~2 cm in low-pigmented tissue (Selbo et al., 2010). Tissue penetration is not a concern for *in vitro* work as cells are grown in a thin layer.

While the Berg group that invented and popularized PCI used a photosensitizer that was delivered at the same time, but not attached to the macromolecule of interest,

photosensitizers have been linked directly. Direct linkage of the photosensitizer to the cargo has been most successful when the cargo contains a CPP. When directly linked to CPPs, rhodamine has bene found to serve as a photosensitizer. Although 5(6)-carboxytetramethylrhodamine (TMR) was not found to serve as a photosensitizer alone or even attached to a K9 peptide, it was found to mediate endosomal release attached to CPPs Tat or R9 (Srinivasan et al., 2011). This result was supported when another study compared the endosomal rupture following light treatment of cells that had internalized either rhodamine-labeled Tat-GFP or rhodamine-labeled TTC-GFP. Endosmal rupture was only observed for the Tat-GFP containing cells (Gillmeister et al., 2013). The mechanism by which CPPs such as Tat improve PCI efficiency of a conjugated photosensitizer is not fully understood. It has been suggested that CPPs may increase singlet oxygen yield by a unknown mechanism (Srinivasan et al., 2011) while others feel that it is a function of the dual action of CPPs destabilizing the cell membrane and bringing the photosensitizer physically closer to the membrane (Meerovich et al., 2014). There are advantages and disadvantages to using photosensitizers that are directly conjugated. A strong argument for direct conjugation is that PCI will only be mediated in areas where the macromolecule of interest is sequestered (Gillmeister et al., 2013). Conversely, when photosensitizers are physically close to the cargo, reactive oxygen species could damage the delivered macromolecule along with the endosomal membrane. Overall, both conjugated (Endoh et al., 2008; Gillmeister et al., 2013; Matsushita et al., 2004) and unconjugated (Berg et al., 1999; Fretz et al., 2007; Gianolio et al., 2010; Shiraishi et al., 2006; Shiraishi et al., 2011; Wang et al., 2011) methods have been used successfully.

Light delivery to mediate PCI can be performed at a variety of scales. The original PCI experiments were performed using fluorescent tubes (Berg et al., 1999); a commercially available system called the Lumisource (PCI Biotech, Lysaker, Norway) uses this principle. The Lumisource is optimized to deliver uniform light intensity over the 45cm x 17cm treatment area. Uniform treatment is critical since high light intensity can lead to cytotoxicity. For smaller scale PCI experimentation, a fluorescent microscope can be used to deliver fluorescent light of the appropriate wavelength (Endoh et al., 2008; Gillmeister et al., 2011; Gramlich et al., 2013; Matsushita et al., 2004; Srinivasan et al., 2011).

1.3. Transcription Factor Delivery

Parkinson's disease (PD) has long been considered an ideal candidate for the development of cell-replacement therapy. Since the disease is caused by the loss of dopaminergic substantia nigra neurons, the introduction of healthy replacement dopaminergic neurons could provide a successful PD treatment (Thomas, 2010). Although complex genetic strategies exist to generate dopaminergic neurons, the genetic methods make these cells unfit for human transplantation due to safety concerns. The overexpression of transcription factors, especially those delivered via viral infection, greatly increases the chances of tumor formation after cell transplantation. We aimed to develop a method where the direct delivery of purified transcription factors could be used to generate neurons that would potentially be safe for human therapy.

1.3.1. The roles of transcription factors *Mash1*, *Lmx1a*, and *Nurr1* genes in general neuronal and dopaminergic differentiation

Caiazzo and colleagues directly converted human fibroblasts to functional dopaminergic neurons using the lentiviral delivery of proneural transcription factors *Mash1*, *Lmx1a*, and *Nurr1* (Caiazzo et al., 2011). Although the efficiency of the process was not high, this publication was particularly exciting since the source cells could be easily obtained without any regulatory concerns. Additionally, source fibroblasts could come from the patient in need of the transdifferentiated replacement cells. Although high risk, there was an enormous potential benefit of converting this transdifferentiation procedure from a lentiviral delivery to a protein delivery method. Each of the three transcription factors utilized for transdifferentiation have important roles in neuronal differentiation. If a method to produce and deliver biologically active transcription factor was developed, any one of the three transcription factors would be interesting to study independent of the other two.

Mash1 is a member of the basic helix-loop-helix (bHLH) family of transcription factors that play a critical role in the maintenance and differentiation of neural stem cells. There are two types of bHLH genes, the repressor and activator classes. The repressor bHLH genes include seven *Hes* genes that regulate both gliogenesis and neural stem cell maintenance. The activator class of bHLH factors includes Mash1, Math, NeuroD, and Neurogenin. These genes promote neurogenesis by binding to the E box. All activator bHLH transcription factors, including Mash1, need to form a heterodimer with bHLH factor E47 to become biological active (Kageyama et al., 2005). *Mash1* is expressed in both the peripheral and central nervous systems by both neural stem cells and post-mitotic

immature neurons. Significant insight regarding the role of Mash1 in neuronal differentiation was derived from *Mash1*-knockout mice. Mash1-deficiency is fatal at birth, so the development of the peripheral and central nervous systems can't be examined postnatal. At birth, most issues are observed in the peripheral nervous system. In the Mash1 deficient mice, neurons from the olfactory and autonomic systems were lost, although multipotent cells of each system still differentiated to neural precursors (Kageyama et al., 1997). Mash1 is inhibited by Hes1 through two distinct mechanisms. First, Hes1 can bind directly to the *Mash1* promotor to repress *Mash1* expression. Second, Hes1 forms a nonfunctional dimer with Mash1 activator E47 preventing Mash1-E47 dimer formation. *Hes1* expression is critical for the neural stem cell proliferation and maintenance. Without Hes proteins, premature neuronal differentiation is observed causing severe developmental problems (Kageyama et al., 2005). Although the overall roles of Mash1 and Hes1 in promoting neural stem cell proliferation and neuronal differentiation are understood, the mechanism by which this takes place is not fully characterized. During neural stem cell proliferation, the expression of *Mash1* and *Hes1* appears to oscillate until sustained Mash1 expression promotes differentiation (Vasconcelos et al., 2014)

P19 embryonal carcinoma cells have been used as a model for bHLH transcription factor-mediated neuronal differentiation *in vitro*. P19 cells are pluripotent and can be differentiated to neurons by transient transfection of numerous bHLH factors including *Mash1* (Farah et al., 2000). Mash1 has also been found to dramatically upregulate expression of cell cycle arrest factor Gadd45ɤ, a discovery that was utilized in the construction of the 281-EL2 *Mash1* reporter construct (Huang et al., 2010).

Lmx1a is a member of the large LIM-homeodomain (LIM-hd) family of transcription factors. All LIM-hd family members have two N-terminal LIM motifs that bind proteins allowing LIM-hd factors to form tissue-specific heterodimers and a C-terminal DNA-binding homeodomain. There are six groups of LIM-hd factors that are categorized by sequence homology, one of which is the Lmx group containing two members. Lmx1 group members Lmx1a and Lmx1b share the same homeodomain. As with Mash1, the study of a mouse model where *Lmx1a* was mutated provided some of the first evidence that Lmx1a had a critical role in neuronal differentiation. *Dreher* mice have one of eleven *Lmx1a* mutations which lead to abnormal pigmentation, deafness, and developmental issues in the cerebellum, hippocampus, and cortex (Koo et al., 2009). The loss of Lmx1a has been found to affect the formation of the roof plate, the inner ear, the cerebellum, and the choroid plexus. The number of dopaminergic neurons is also slightly reduced in *Dreher* mice (Griesel et al., 2011).

Transcription factor Lmx1a is a critical factor in the early stages of dopaminergic differentiation. Lmx1a induces the expression of msh homeobox 1 (*Msx1*), which itself induces the expression of neurogenesis-promoting *Ngn2* (Cai et al., 2009). In neural progenitor cells derived from embryonic stem cells, lentiviral expression of *Lmx1a* in combination with sonic hedgehog (Shh) and fibroblast growth factor 8 (FGF8) led to dopaminergic differentiation. Lmx1a has been found to directly bind the tyrosine hydroxylase promoter (Hong et al., 2014). Mesenchymal stem cells (MSCs) transduced with lentiviral vectors expressing *Lmx1a* and treated with Shh and FGF8 were also differentiated into dopaminergic neurons. Expression of *Lmx1a* in the MSCs upregulated *Sox2*, *Msx1*, *Ngn2*, and *hAsh1* (Barzilay et al., 2009). Although *Lmx1a* is the first

dopaminergic determinant factor expressed, it also has a role in the maturation of midbrain dopaminergic neurons. The discovery that Lmx1a regulates expression of the dopamine transporter gene was used to develop a *Lmx1a* reporter vector (Chung et al., 2012).

Nurr1, also commonly known as *NR4A2*, is a member of the nuclear receptor family of transcription factors. Nuclear receptor transcription factors are regulated by binding small lipophilic cofactors including steroid hormones, thyroid hormones, and retinoids. Even when the ligand is absent, nuclear receptors are found in the nucleus bound to co-repressors. Ligand-binding triggers a conformational change resulting in co-repressor dissociation and co-activator recruitment. Nurr1 is one of over 20 orphan nuclear receptors that do not have an identified ligand, although Nurr1's binding partner is known. For DNA binding, Nurr1 can bind as a monomer, homodimer, or heterodimer. Nurr1's heterodimerization partner is the retinoid X receptor (RXR). Since Nurr1's ligand binding pocket is entirely filled with hydrophobic amino acid side chains, it is thought that Nurr1 may act in a ligand-independent manner, a mechanism uncommon for nuclear receptor family members. Nurr1 may be indirectly influenced by ligands through binding partner RXR (Perlmann et al., 2004). Nurr1 binds DNA through a conserved domain consisting of two zinc fingers and has been shown to bind a NGFI-B response element (Rekha et al., 2014).

Nurr1 is critical for the normal development of ventral midbrain dopaminergic neurons. In homozygous *Nurr1* knockout mice, dopaminergic neurons were absent in the substantia nigra and animals died within 24 hours of birth (Jiang et al., 2005). Although no dopaminergic markers were observed in the knockout mice, a number of other dopaminergic transcription factors were expressed, indicating that Nurr1 was not an early

activator of a dopaminergic phenotype. Nurr1 also has roles outside dopaminergic development as the early death of knockout animals within 24 hours was not thought to be due to the lack of the dopaminergic neurons (Perlmann et al., 2004). Mice that are heterozygous for *Nurr1* knockout have reduced Nurr1 levels but can survive much longer, allowing more comprehensive study. As they age, these mice provide an interesting PD model (Jiang et al., 2005; Zhang et al., 2012a).

Overall, while Lmx1a is thought to be the first inducer of dopaminergic differentiation, Nurr1 is responsible for the maturation of the dopaminergic phenotype. Overexpression of *Nurr1* and *Pitx3*, another dopaminergic factor, has been found to promote the midbrain dopaminergic phenotype in embryonic stem cells; a result neither factor can fully induce on its own (Martinat et al., 2006). It has been discovered that Nurr1 is also critical for the maintenance of mature dopaminergic neurons, and loss of Nurr1 can lead to neuronal degeneration (Kadkhodaei et al., 2009). Nurr1 has a large variety of target genes that are affected on a Nurr1 concentration-dependent and gene-dependent manner (Johnson et al., 2011).

Decreases in *Nurr1* expression may contribute to PD pathogenesis, although it is not due directly to *Nurr1* mutation. Age-dependent decreases in Nurr1 levels are observed in dopaminergic neurons with PD pathology. Nurr1 is one of numerous transcription factors whose function is affected by α-synuclein overexpression. Interestingly, viral delivery of *Nurr1* has been shown to protect dopaminergic neurons against α-synuclein toxicity. Although the role of Nurr1 in PD is still under thorough investigation, it may be an interesting future PD therapeutic target (Decressac et al., 2013).

1.3.2. The delivery of transcription factors to mediate dopaminergic neuronal differentiation

There is a substantial literature on dopaminergic differentiation from a variety of cell sources. While a comprehensive review of the literature could be its own publication, the goal for this thesis is to briefly introduce the potential cell sources for dopaminergic neuron differentiation, methods for mediating the differentiation, and how transcription factor delivery has been used or can be used to enhance differentiation.

The first issue in generating mature dopaminergic neurons for cell replacement therapy is selecting the appropriate source cells for the differentiation process. This process is not as straightforward as choosing the ideal and/or most convenient source cell due to ethical, regulatory, and safety concerns. It is noteworthy that although the generation of dopaminergic neurons is introduced here, analogous methods can be utilized for the generation of other neuronal cell types. The first source of replacement dopaminergic neurons was fetal tissue. Although some initial studies where PD patients received fetal tissue from 6-8 week old human embryos delivered promising results, there are obvious issues limiting fetal tissue transplantation to proof-of-concept work only. Dopaminergic neurons have been generated using human embryonic stem cells (Thomas et al., 2010). The first method for differentiating hESCs to dopaminergic neurons was published in 2004, and used both co-culture with feeder cells, and the sequential addition of small molecules and growth factors (Perrier et al., 2004). Transcription factor delivery can also be used to differentiate hESCs to dopaminergic neurons. Retrovirus-mediated overexpression of each of dopaminergic transcription factors Lmx1a, Pitx3, and Nurr1 in hESC-derived neural progenitor cells led to the efficient generation of TH-position neurons

(Hong et al., 2014). Although the pluripotent nature of hESCs presents a number of options for the generation of dopaminergic neurons, there are also issues with hESC acquisition limiting their potential for cell-replacement therapy.

The discovery that induced pluripotent stem cells (iPSCs) could be generated through the viral-mediated overexpression of four transcription factors in fibroblasts presented an ethical way to obtain large quantities of pluripotent stem cells for neuronal differentiation (Takahashi et al., 2006). Human iPSC lines have already been used to generate neurons expressing dopaminergic markers under defined conditions. After iPSCs were differentiated to neural stem cells, about 30% of the iPSC-derived NSCs were tyrosine hydroxylase-positive (Swistowski et al., 2010). While scientifically exciting, this discovery still presented limitations; the integration of lentiviral DNA and the introduction of powerful viral promoters dramatically increase the possibility of unwanted genetic consequences (Zhou et al., 2009). These limitations were addressed using protein delivery. Direct delivery of the reprogramming factors as Tat-linked recombinant proteins has been used to generate iPSC lines without genetic modification (Kim et al., 2009; Nemes et al., 2014; Zhou et al., 2009).   The creation of protein-induced PSCs not only generated a safe and ethical source of pluripotent cells but it also demonstrated the potential for protein delivery of transcription factors to mediate cellular reprogramming. Although the direct protein delivery-mediated reprogramming was less efficient than the viral method (Kim et al., 2009), its success provided hope that recombinant transcription factors could be used in place of DNA overexpression for related applications. Protein-induced PSCs could be a safe and ethical source of cells for dopaminergic differentiation, and progress towards this goal has been made. From the piPSCs, 86.4% were differentiated into neural stem

cells. Of these piPSC-induced NSCs, 60-70% were differentiated into TuJ1+ cells and 35-45% of these TuJ1+ cells were TH+ (Rhee et al., 2011). Overall, 26% of the NSCs were differentiated into TH+ cells, a value comparable with hESC differentiation procedures (Swistowski et al., 2010). It has been shown that dopaminergic differentiation efficiency is similar for mESCs and mouse piPSCs (Kwon et al., 2014). Recombinant transcription factors could be a valuable asset in promoting dopaminergic differentiation and even enhancing current defined procedures involving sequential addition of small molecules and growth factors.

In 2010, the idea of converting somatic cells to pluripotent stem cells made further progress when the Wernig group at Stanford published the conversion of fibroblasts to functional neurons, without an intermediate multipotent or pluripotent stem cell state. Lentiviral delivery of *Mash1* alone was enough to induce immature neurons and the addition of *Brn2* and *Mytl1* improved efficiency close to 20% (Vierbuchen et al., 2010). This method has the potential to, in a straightforward manner, create patient-specific replacement cells. Soon after, it was discovered that the addition of *Lmx1a* and *FoxA2* led to the expression of dopaminergic markers with an overall transdifferentiation efficiency of ~10% (Pfisterer et al., 2011). This process was further streamlined when lentiviral expression of *Mash1*, *Nurr1*, and *Lmx1a* were used to generate dopaminergic neurons from several fibroblasts sources. The percentage of TH+ cells generated from mouse embryonic fibroblasts, human embryonic fibroblasts, and adult Parkinson's patient fibroblasts was 18%, 6%, and 3% respectively (Caiazzo et al., 2011). Analogous high-profile papers were published around this time where Alzheimer's disease (AD) skin fibroblasts were converted to neurons (Qiang et al., 2011), mouse and human fibroblasts were converted to

spinal motor neurons (Son et al., 2011), and differentiated hepatocytes were transdifferentiated to neurons (Marro et al., 2011). Although efficiency was very low, two microRNAs alone were shown to transdifferentiate fibroblasts to neurons. Efficiency of the process was improved with transcription factor delivery of *NeuroD2* alone, but more so with *Mash1* and *Myt1l* as well (Yoo et al., 2011). Small molecules have been used to improve transdifferentiation efficiency with viral overexpression of *Mash1* and *Ngn2* (Ladewig et al., 2012).

One of the major criticisms of the transdifferentiation process is that because the neurons generated do not proliferate and the efficiency is low, it is not a practical source of replacement neurons for transplantation. Efforts have been made to transdifferentiate fibroblasts to midbrain dopaminergic progenitor cells capable of expansion. This has been achieved through lentiviral expression of the Yamanaka reprogramming transcription factors Oct4, c-Myc, Klf4, and Sox2, followed by culturing in conditions to promote dopaminergic differentiation including the addition of Shh and FGF8. The induced dopaminergic progenitors could be differentiated to dopaminergic neurons through removal of medium growth factors. After 1-2 weeks of differentiation, ~27% of cells were TuJ1 and TH-positive (Kim et al., 2014). Very recently, fibroblasts have been transdifferentiated to dopaminergic progenitors without genetic modification using the protein transduction of recombinant Tat-linked Sox2 and Lmx1a, and a cocktail of small molecules. This publication represents the first time induced dopaminergic precursors were generated without genetic modification (Mirakhori et al., 2015).

1.4. Enzyme Replacement Therapy for Gaucher's Disease

Gaucher's disease (GD) is a lysosomal storage disease caused by mutations in lysosomal enzyme glucocerebrosidase (GCase). It is the most common lipid storage disease as well as the most common genetic disorder in the Ashkenazi Jewish population, although GD is observed in all ethnic groups (Hruska et al., 2008). As a result of the enzyme mutation, glycosphingolipid substrates glucosylceramide (GlcCer) and glucosylsphingosine (GlcSph) accumulate, leading to heterogeneous phenotypes. The effort to design RDP-IgAh-GCase required an understanding of the disease as well as numerous FDA-approved therapeutics that already exist for treatment of select disease subtypes. While numerous neuronopathic GD therapies have been proposed, none have shown promising clinical results. RDP-IgAh-GCase has the potential for fill a large void in the GD therapeutic toolkit.

1.4.1. Gaucher's disease

GD is classified into three types, only two of which affect the nervous system. Type 1 GD is the most common form where the reticulo-endothelial system is primarily affected. The GCase substrates accumulate in lysosomes causing macrophages to become dramatically enlarged. These engorged macrophages are historically known as "Gaucher cells." Types 2 and 3 GD both affect the central nervous system. In acute neuronopathic type 2, rapid neurodegeneration leads to death in infancy. Chronic neuronopathic type 3 GD patients can have variable symptoms but typically have some of the reticulo-endothelial issues of type 1 patients with some nervous system involvement. The neurologic symptoms of type 3 GD are variable. While symptoms can be severe, in less

severe cases, patients may only experience slowed horizontal saccadic eye movement (Sidransky, 2012).

A large number *GBA1*, the gene for GCase, mutations have been described; the disease is diverse both in genotype and phenotype. Of the nearly 300 GCase mutations identified, 203 are missense mutations, 18 are nonsense mutations, 36 are small insertions or deletions, 14 are splice junction mutations, and 13 are variants with 2 or more mutations. One of the reasons that phenotype is difficult to predict based on genotype is that most mutations are not found in the homozygous form and that some are found in a small sample size. Although uncommon, there are some correlations. GD patients with the N370S mutation typically do not have any neurological symptoms. Interestingly, some individuals that are homozygous for the N370S mutation are asymptomatic. Type 3 GD patients with visceral manifestations of the disease often carry the L444P and or the R463C mutations. Patients experiencing myoclonic epilepsy often carry the N188S or G377S mutations with a null or recombinant allele. Overall, most reasonably accurate phenotype predictions come from homozygous individuals. For example, homozygotes with the F213I or L444P often have Type 3 GD (Hruska et al., 2008). Mutations in *GBA1* can impact GCase multiple ways including one or a combination of activity, stability, trafficking to the lysosome, or interaction with GCase activators.

GCase is a 497 amino acid protein that has an unmodified polypeptide molecular weight of 56 kDa. The actual molecular weight of the protein extracted from different tissue sources has been found to be between 59 and 67 kDa as a result of variable post translational modifications (Grace et al., 1994). Specifically, GCase has 5 potential N-glycosylation sites at Asn-19, Asn-59, Asn-146, Asn-270, and Asn-462. The first four of

these sites are usually occupied in wild-type GCase. The N19 glycosylation site is the only one that has been shown to be critical for enzyme activity. Berg-Fussman and colleagues showed that enzymes with N19Q, N19E, or T21G mutations, where the glycosylation site was removed, had 3-60 fold decreases in enzyme activity. Folding effects due to the mutation and/or the lack of N19 glycosylation clearly prevented the formation of a fully catalytically active enzyme (Berg-Fussman et al., 1993). Two amino acids at the active site, E235 and E340, are critical to mediate the hydrolysis of glucosylceramide to glucose and ceramide (Dvir et al., 2003). Surprisingly, there is no strong correlation between residual enzyme activity and accumulated substrate in GD patients (Sidransky, 2012).

GCase requires two activators, negatively charged lipids and saposin C (SapC) for function *in vivo* (Berg-Fussman et al., 1993; Dvir et al., 2003). SapC is a small 80 amino acid, 9kDa glycoprotein that is derived from proteolysis of precursor protein prosaposin. If glycosylated at its N22 site, SapC can be 12kDa in size. The exact mechanism by which saposin C activates GCase is not fully understood. It is thought that SapC has two functions: binding GCase and helping it associate with the membrane, as well as extracting and solubilizing glycosphingolipid substrates to enable GCase-mediated hydrolysis. Negatively charged lipids in the cell membrane improve SapC membrane binding, further facilitating GCase activation (Tamargo et al., 2012). Select GCase mutations have been shown to affect the ability of SapC to activate GCase. For example, it was demonstrated that SapC was able to activate both wild-type and N370S GCase in the presence of high concentrations of anionic phospholipids. However, if anionic phospholipid concentration was reduced to ~20%, only wild-type and not N370S GCase was activated (Salvioli et al., 2005).

Until recently, there were relatively few cell and animal models for the study of GD. Although primary fibroblast cell lines with mutant GCase are available, there was not convenient source of Gaucher's neurons for *in vitro* study. This changed in 2012 when an induced pluripotent stem cell (iPSC) line was created from GD fibroblasts and it was demonstrated that these iPSCs could be differentiated into both Gaucher macrophages and Gaucher neurons (Panicker et al., 2012). Another exciting advance in *in vitro* study was the creation of a SV40-immortalized GCase-knockout neuronal cell line (Wendy Westbroek, personal communication). Although these cells have less true neuronal properties than the iPSC-derived Gaucher neurons, they can be expanded easily and cheaply for larger scale experimentation.

The first animal models for GD were chemically induced mouse models using conduritol-β-epoxide, a specific inhibitor of GCase activity. A GCase-knockout mouse model was made in 1992, and although these mice had very low enzyme activity, their lifespan was very short due to a previously unknown induced defect in skin permeability, causing the mice to die of dehydration. Recently, more complex genetic strategies have been utilized to generate knockout mice. One example of a more complex strategy was used to generate the K14 line, the first neuronal GD model. By breeding mice with a *loxP-Neo-loxP* cassette in the *GBA1* sequence with keratin-14-Cre transgenic mice, a line was made where GCase was knocked out except in skin where the K14 promoter drives excision of the *Neo* cassette (Farfel-Becker et al., 2011).

Although the study of GD is an important field itself, interest in the disease has grown considerably of late with the high profile discovery that *GBA1* mutations are the greatest genetic risk factor for Parkinson's disease. The mechanism by which GCase and

alpha-synuclein interact is not known. They seem to have a clear inverse relationship, although not a traditional enzyme-substrate connection (Siebert et al., 2014).

1.4.2. Type 1 Gaucher's disease therapy

Type 1 GD is currently treated by enzyme replacement therapy (ERT) with recombinant GCase. The original GCase for GD therapy was Ceredase (alglucerase, Genzyme), purified from human placental tissue. Genzyme later replaced Ceredase with Cerezyme (imiglucerase), a recombinant form of the enzyme with a single amino acid substitution of histidine for arginine at position 495 (Pastores, 2010). Cerezyme is produced in Chinese hamster ovary (CHO) suspension cells, a common cell line used for recombinant protein production. Both of the GCase products produced by Genzyme were sequentially deglycosylated after production to expose terminal mannose residues. This enzymatic modification takes advantage a mannose-binding lectin to target GCase to macrophages, the cell type most affected in Type 1 GD. Originally, treatment of patients with native GCase was not effective because the enzyme was cleared too rapidly by cell types that were not intended targets. The deglycoslyation procedure involved the sequential treatment of GCase with neuraminidase, β-galactosidase, and β-N-acetylglucosaminidase to expose mannose by removing sialic acid, galactose, and N-acetylglucosamine respectively (Furbish et al., 1981).

Since the release of recombinant Cerezyme, two biosimilars have been FDA-approved for GD ERT. VPRIV (velaglucerase alfa, Shire) was the first of the two biosimilars released. VPRIV is produced in a human fibroblast carcinoma cell line; mannose-terminal glycans are created due to the addition of mannosidase I inhibitor kifunesine to the extracellular medium during production. Elelyso (taliglucerase alfa,

Protalix Biotherapeutics) is produced in a recombinant carrot cell line and takes advantage of targeting to a storage vacuole where glycans are remodeled to contain terminal mannose residues (Tekoah et al., 2013). Aside from creating competition in the marketplace, the existence of multiple recombinant mannose-terminal GCase enzymes for ERT is important. When Genzyme had a large-scale bioreactor viral contamination, their Cerezyme supply became limited, creating a global shortage of the therapeutic protein (Branco Novo et al., 2012).

Although ERT is the preferred GD treatment method, two small molecule drugs also exist for GD treatment. Zavesca (miglustat, Actelion Pharmaceuticals) is an N-alkylated iminosugar that inhibits glycosylceramide synthase, an enzyme responsible for the production of glucosylceramide (GlcCer). By decreasing the amount of GlcCer that accumulates in lysosomes, the residual enzyme activity often present in Type 1 GD patients prevents excessive substrate accumulation. Zavesca was FDA-approved in 2002 for the treatment of type 1 GD patients that can't tolerate the ERT infusions (Ficicioglu et al., 2008; Pastores et al., 2010). Although Zavesca is taken orally, providing a very convenient therapeutic option for patients, its use was limited by gastrointestinal and neurological side effects. While neurological side effects were reversible when drug use was discontinued, 30% of patients experienced tremors and 15-20% of patients had peripheral neuropathy during treatment (Ficicioglu et al., 2008). When treated with Zavesca, patients displayed a wide tissue distribution including the CNS; this finding led to a clinical trial testing whether combinatorial treatments with Cerezyme and Zavesca could improve neurological symptoms of type 3 GD patients. In 2007, a report was published indicating that a 31 year old patient who received 200mg Zavesca 3x per day and 60 IU/kg Cerezyme every two

weeks experienced an improvement in his neurological symptoms without side effects (Capablo et al., 2007). While initially promising, the results of a 30 patient clinical trial released in 2008 indicated that this combinatorial treatment did not have a statistically significant neurological benefit compared to control patients that received Cerezyme only (Schiffmann et al., 2008).

Cerdelga (eliglustat, Genzyme) is a second small molecule glucosylceramide analogue that serves as a glucosylceramide synthase inhibitor. In 2014, it was FDA-approved for type 1 GD treatment. The development of Cerdelga is exciting, as it has been shown to have fewer unpleasant side effects than Zavesca, and clinical trials have shown similar efficacy to Cerezyme (Poole, 2014). Moving forward, ERT is still likely to remain the primary treatment method for type 1 GD patients since the long-term outcomes with ERT are better characterized and the current cost of Cerdelga is similar to Cerezyme (Sinha, 2014). Currently no clinical trials assessing Cerdelga in type 3 GD patients are in progress.

1.4.3. Potential neuronopathic Gaucher's disease treatments

Although no FDA-approved type 2 or type 3 GD therapies exist, a number of potential options have been investigated over the past several years. The strategies investigated for neuronopathic GD therapy can be generally organized in four categories: 1) direct infusion of mannose-terminal GCase to the CNS, 2) the design of novel strategies to deliver GCase across the BBB or improve neuronal binding, 3) small molecules that can potentially cross the BBB, and 4) gene therapy.

All FDA-approved recombinant GCase enzymes are engineered or modified to contain mannose-terminal N-glycans for macrophage targeting. Although very useful for

the treatment of systemic Gaucher's disease, they would not be predicted to preferentially bind neurons, possibly limiting the therapeutic potential of this strategy. An *in vitro* study testing Ceredase binding and internalization used cholinergic LA-N-2 cells, dopaminergic SH-SY5Y cells, and NHA astrocytes. Uptake of the Ceredase by the neuronal cell lines was found to be variable but uniformly inferior to the uptake by J774 macrophages. The LA-N-2 cells had the best binding, but half-maximal uptake occurred at approximately 7x the concentration of Ceredase compared to the macrophage cell line. The uptake by the LA-N-2 cells was found to be, at least in part, mannose-specific. Uptake of the Ceredase by the SH-SY5Y cells was significantly less, and no uptake was observed for the astrocyte cell line (Scheuler et al., 2002).

There has been a limited amount of *in vivo* CNS infusion of mannose-terminal GCase. Cabrera-Salazar and colleagues at Genzyme were able to reduce substrate and extend the life of K14 neuronopathic GD model mice from 15 to 23 days with intra-cerebroventricular infusion of reformulated Cerezyme three times, starting at postnatal day 1 (Cabrera-Salazar et al., 2010). Three young type 2 GD patients were given CSF infusions with Ceredase in the mid-1990s. Although the lifespan of one patient was possibly extended, two of the others suffered continued neurological decline (Erikson et al., 1997). Convection-enhanced delivery (CED) showed potential for improving GCase distribution after infusion since the slower diffusion of the large molecule was not limiting. In test rats, 53% of the infused GCase activity was detected immediately after infusion and 10% was detected after 18 hours (Zirzow et al., 1999). Further work showed effective and safe distribution of GCase activity in monkeys using CED (Lonser et al., 2005). CED has been used to deliver Cerezyme to the CNS of human patients. A young type 2 GD patient

received infusions at 10.5 and 13 months of age. The CED Cerezyme infusion was found to be safe and at 19 months the patient had a stable neurological baseline although neurologic symptoms were not necessarily improved (Lonser et al., 2007).

Since mannose-terminal GCase does not preferentially bind neurons or cross the BBB, some strategies have focused on engineering recombinant GCase enzymes for these purposes. Tat has the potential to improve GCase delivery and mediate crossing of the BBB (Schwarze et al., 1999). GCase-Tat was bound and internalized approximately 4 and 10 fold better than control GCase or Cerezyme in type 1 and type 2 Gaucher fibroblasts, respectively (Lee et al., 2005). Although promising, GCase-Tat was not delivered to any neuronal cell type nor was any reduction in substrate accumulation demonstrated. Another lysosomal enzyme, galactocerebrosidase (GALC), was delivered to primary mouse neurons using Tat as the protein delivery vector. The results of this study were less encouraging; less GALC-Tat was delivered compared to the control GALC protein, although the GALC-Tat delivery was less inhibited by the addition of mannose-6-phosphate. This indicated that Tat was mediating neuron binding (Zhang et al., 2008). Aside from Tat, the other strategy to delivery GCase across the BBB used the 38 amino acid low-density lipoprotein receptor binding domain of apolipoprotein B (Spencer et al., 2007). A portion of apolipoprotein E has also been shown to mediate BBB crossing (Böckenhoff et al., 2014).

While a clinical trial for Zavesca indicated that patients' neurological symptoms did not improve (Schiffmann et al., 2008), another glucosylceramide synthase small molecular inhibitor has recently showed promise in the K14 neuronopathic GD mouse model. Genzyme identified GZ 161, a propriety inhibitor, and found that it was able to

extend the life of K14 mice from 14 to 18 days and reduced substrate levels over 60% by the end of life. Although substrate levels were reduced, they were not normalized. The GZ 161 molecule was injected intraperitoneal (IP) and was found to cross the BBB (Cabrera-Salazar et al., 2012). Another small molecular therapeutic strategy involves chaperones that competitively inhibit glucocerebrosidase. They bind in the endoplasmic reticulum where GCase is less stable and improve lysosomal trafficking and enzyme activity (Sun et al., 2011). One chaperone, isofagomine, has been found to improve the activity of several mutant GCase variants including the L444P mutant common in neuronopathic GD (Khanna et al., 2010). The *in vivo* effects of isofagomine were evaluated in the 4L;C* neuronopathic mouse model that has homozygous V394L GCase mutations and no saposin C. Interestingly, while no decrease in substrate levels was observed (Sun et al., 2012) lifespan of the mice was extended ~34% with a 600 mg/kg/day isofagomine treatment given in their drinking water (Sun et al., 2011). Ambroxol, another chaperone, has been tested in a very small clinical trial for type 1 GD and proposed for neuronopathic GD treatment but not tested for that purpose (Zimran et al., 2013).

The final category of potential neuronopathic GD treatments is gene therapy. Gene therapy has long been an attractive idea for GD therapy since it has the potential to permanently cure the disease without need for repeat enzyme infusions over the patient's lifespan. The feasibility of gene therapy for type 1 GD was first demonstrated using CBE-induced mouse model (Marshall et al., 2002). Genzyme research has shown that intra-cerebroventricular delivery of adenoviral vectors expressing GCase increased the K14 mouse lifespan to 28.5 days compared to 15 days for the controls or 23 days for the mice

receiving three ICV infusions of enzyme beginning at postnatal day 1 (Cabrera-Salazar et al., 2010).

1.5.   Thesis Chapter Overview

This doctoral thesis is composed of three main chapters with a common theme: the design of therapeutic proteins and their delivery to the appropriate cellular compartments for biological activity. Chapter 2 discusses the design and development of Tat-TTC, a neuronal cell type-specific protein delivery vector that can target cargo proteins to either endosomal and lysosomal compartments or the cytosol utilizing photochemical internalization. In chapter 3, Tat-linked transcription factors were expressed with the intention of mediating neuronal differentiation. In principle, the generated neurons could be used to treat Parkinson's disease where this cell type is lost. The factors were delivered using the Tat CPP. Since transcription factors need to reach the nucleus to be biologically active, photochemical internalization was used to promote nuclear translocation. The delivery of GCase to neurons presented a number of protein delivery challenges that are discussed in chapter 4. Intracellularly, the targeted organelle for GCase is the lysosome so endosomal entrapment following uptake is preferred to cytosolic release. However, commercially available recombinant GCase enzymes that can bind neurons poorly already exist. The goal in chapter 4 was to develop a neuron-targeted and biologically active GCase, a therapeutic protein that has never been developed but for which there is a strong need. To accomplish this goal, seventeen different variants were assessed. The ability of Tat, TTC, and Tat-TTC protein delivery vectors to target GCase to neuronal cells was tested. A new peptide, RDP, was found to be most appropriate for a number of reasons to be discussed at length.

Chapter 2: Tat-Tetanus Toxin Fragment C: A Novel Protein Delivery Vector and its Use with Photochemical Internalization

2.1. Abstract

Protein delivery vectors can be grouped into two classes, those with specific membrane receptors undergoing conventional endocytosis, and cell penetrating peptides (CPPs) that have the capacity to cross cell or endosomal membranes. For both forms of vectors, translocation across a membrane is usually an inefficient process. In the current study, a novel vector combining the widely used CPP, Tat and the non-toxic neuronal binding domain of tetanus toxin (fragment C or TTC) was assessed for its capacity to deliver GFP as a test cargo protein to human neural progenitor cells (NPCs). These two functional membrane interacting domains dramatically enhanced internalization of the conjugated cargo protein. Tat-TTC-GFP was found to be bound or internalized at least 83-fold more than Tat-GFP and 33-fold more than TTC-GFP in NPCs by direct fluorimetry, and showed enhanced internalization by quantitative microscopy of 18 and 14 fold respectively. This preferential internalization was observed to be specific to neuronal cell types. Photochemical internalization (PCI) was utilized to facilitate escape of the endosome-sequestered proteins. The combined use of the Tat-TTC delivery vector with PCI led to both enhancement of neural cell type specific delivery to an endosomal target, followed by the option of efficient release to the cytosol.

2.2. Introduction

Vectors for delivery of proteins to living cells can be grouped into two classes. One group attempts to adapt the strategy of natural protein based toxins, such as plant derived ricin and bacterial toxins including botulinum toxin, tetanus toxin and diphtheria toxin. These toxins have a similar molecular design which includes: 1) a binding domain that recognizes a cell surface receptor, 2) a translocation domain that mediates passage through the plasma or endosomal membrane to deliver the toxin, and 3) a catalytic domain which mediates a toxic enzyme activity (Fishman, 2009; Sandvig et al., 2009). We have previously created delivery vectors based on the non-toxic binding domain of tetanus toxin, referred to currently as HC_C (C terminus of heavy chain), and also known as tetanus toxin fragment C or TTC (Francis et al., 2000; Francis et al., 2004; Li et al., 2009). The proteolytic activity of tetanus toxin comes from the toxin's light chain. Toxin with a mutation of amino acid Glu234 in the light chain, in combination with a wild-type heavy chain, was shown to be non-toxic (Li et al., 1994; Wang et al., 2012). The advantages of TTC as a vector are its neural specificity, moderate binding avidity with high capacity, and properties of retrograde axonal and trans-synaptic transport (Figueiredo et al., 1997; Fishman and Savitt, 1989; Francis et al., 1995). Neuronal binding properties of TTC stem from the binding of protein receptors and complex gangliosides. Binding pockets for complex gangliosides GD1b and GT1b are within the C-terminal 34 amino acids of TTC. The membrane association of TTC is dependent on pH and ganglioside content. Endocytosis of TTC is also depended on receptor proteins P15 and SV2A/B binding (Calvo et al., 2012; Miana-Mena et al., 2002; Yeh et al., 2010). TTC lacks the translocation domain of tetanus toxin and internalized proteins do not enter the free cytosolic

compartment (Figuererdo et al., 2000). Hybrid bacterial toxins incorporating a translocation domain identify the membrane translocation process as the limiting aspect of protein delivery to non-endosomal cytosolic targets (Barati et al., 2002; Box et al., 2003; Kern et al., 2011). An alternative to bacterial toxin domains as vectors to translocate cargo proteins across cell and endosomal membranes are small cationic peptides referred to as cell penetrating peptides (CPPs) (Reviews: Chauhan et al., 2007; Deshayes et al., 2005; Heitz et al., 2009; Zorko and Langel, 2005). The most widely used of these arginine rich peptides was originally derived from the trans-activator of transcription (Tat) protein of HIV (Frankel and Pabo, 1988). Tat has been used to deliver functional protein *in vitro* and *in vivo* (Fawell et al., 1994; Schwarze et al., 1999). Although over 20 Tat sequences have been used to mediate cell membrane translocation, the minimum sequence necessary is residues 49-57 of the Tat protein (Wender et al., 2000). Although the mechanism of the Tat peptide translocation remains controversial and may vary with cell type and cargo protein, the consensus is that Tat, like many other CPPs, is internalized through endocytosis (Chauhan et al., 2007). While lipid raft-dependent macropinocytosis is often mentioned as the mechanism by which Tat internalization occurs (Jones et al., 2005; Kaplan et al., 2005; Nakase et al., 2007; Wadia et al., 2004) clathrin-mediated endocytosis has also been suggested (Nakase et al., 2004; Rinne et al., 2007). Unlike bacterial toxins, CPP based protein delivery is usually non-specific for cell type or receptor, less avid, and less saturable.

There is a strong rationale to investigate molecules that would include domains from both types of vectors, potentially combining the properties of both. Such dual-domain molecules could potentially have enhanced uptake through the synergy of combined

binding domains as well as preserved cell-type specificity. There is also the potential of such vectors to impact both endosomal and cytosolic targets. Although CPPs are well documented to deliver functional proteins to cytosolic targets, their cytosolic entry is also frequently limited by endosomal trapping (Kaplan et al., 2005). Many estimates have >90% of Tat-linked cargoes trapped in endosomes (Wang et al., 2010). While Tat can mediate minimal cytosolic release of delivered protein, more efficient methods are frequently needed to significantly enhance intracellular availability. Methods described in the literature include: fusogenic lipids (Felgner et al., 1987), membrane-disruptive peptides (Wadia et al., 2004), membrane-disruptive polymers (Boussif et al., 1995), lysomotropic agents (Ciftci et al., 2001), and photochemical internalization (PCI) (Berg et al., 1999).

Photochemical internalization (PCI) is a powerful technique to improve the efficiency of macromolecule delivery when cytosolic release is desired. In PCI, a photosensitizer, usually with a porphyrin structure, preferentially locates to the cell membrane upon endocytosis (Fretz et al., 2007). Upon exposure to a specific frequency of light, photosensitizers induce the formation of reactive oxygen species, damaging the endosomal membrane and releasing endosome contents. Singlet oxygen's 10-20 nm range of action limits the oxidative damage to the endosomal membrane (Berg et al., 1999). The frequency of light applied is directly dependent on the photosensitizer used. PCI has been demonstrated in over 80 cell types (Selbo et al., 2010) using the following two strategies: chemically conjugating the photosensitizer to the macromolecule of interest or delivering unlinked photosensitizer in combination with the macromolecule. Both the conjugated (Endoh et al., 2008; Gillmeister et al., 2011; Matsushita et al., 2004) and unconjugated

(Berg et al., 1999; Fretz et al., 2007; Gianolio et al., 2011; Shiraishi et al., 2006; Shiraishi et al., 2011) approaches have been used successfully.

The current study aimed to develop an efficient strategy to deliver proteins to human neural progenitor cells (NPCs). Enhanced green fluorescent protein (GFP) was selected as a model protein for evaluating delivery. We wanted to examine whether a vector including both Tat and TTC might be bound and internalized by neural cells to a greater extent than mediated by either domain alone. TTC contains multiple neuronal-specific binding domains including two complex ganglioside binding sites and protein receptors (Chen et al., 2009; Miana-Mena et al., 2002; Yeh et al., 2010) while Tat binds in a receptor-independent manner. To test this hypothesis, three recombinant proteins were created and assessed: Tat-GFP, TTC-GFP, and Tat-TTC-GFP. To determine if the TTC containing recombinant proteins retained neuronal cell type-specific binding and internalization properties of TTC, N18-RE-105 neuroblastoma cells and 3T3 fibroblasts were also transduced with the three proteins of interest.

PCI was then utilized to mediate cytosolic release of the internalized recombinant proteins using incubation with unconjugated meso-tetraphenylporphine disulphonic acid dihydrochloride (TPPS$_{2a}$). Since the method involves the oxidative damage of membranes, PCI has the capability to cause high cytotoxicity. Often, PCI is utilized to enhance intracellular delivery of toxic drugs such as saporin or bleomycin in the setting of enhancing cancer cell death (Fretz et al., 2007; Wang et al., 2012). However, because the goal of the current study was to delivery high quantities of protein to viable cells, characterizing and limiting cytotoxicity was a point of emphasis. It has been suggested that ~50% of endosomally-entrapped protein can be released with subtoxic light treatment

(Selbo et al., 2010). With high toxicity, essentially total endosomal rupture can be achieved with our PCI method. However, with optimization of light treatment time and power, obvious cytosolic release was observed with acceptable levels of cytotoxicity.

2.3. Methods and Materials

2.3.1. Plasmid construction

The Tat-GFP construct was created by separately cloning sequences for Tat and Enhanced Green Fluorescent Protein (EGFP) into pGEX6P-3 (GE Healthcare). Oligonucleotides for the 11 amino acid Tat sequence were made by the University of Maryland at Baltimore Biopolymer Laboratory. This sequence represents residues 47-57 of the HIV-1 protein Tat. *Tat* was cloned into the BamHI-EcoRI sites of pGEX6P-3. *EGFP* was amplified from Clontech vector pEGFP-1 and cloned into the EcoRI-SalI sites of the *Tat*-containing pGEX6P-3. This created plasmid pGEX6P3_Tat_GFP.

To create the TTC-GFP construct, *TTC* and *EGFP* were cloned into the pGEX4T-3 bacterial expression vector. *TTC* was amplified from cDNA generously provided by Dr. Neil Fairweather of Imperial College (Makoff et al., 1989). Similar to construction of pGEX6P3_Tat_GFP, *EGFP* was amplified from pEGFP-1. *TTC* was cloned into pGEX4T-3 with BamHI and BglII-NotI sites that were designed in the primers. Subsequently, *EGFP* was cloned into pGEX4T-3 with BglII and NotI sites. The final vector was named pGEX4T3_TTC_GFP.

The pGEX4T3_Tat_TTC_GFP construct was created by inserting the *Tat* sequence into pGEX4T3_TTC_GFP using the same strategy employed in the creation of pGEX6P3_Tat_GFP. All expression vectors were sequenced to confirm all cloned fragments were in-frame and not mutated.

2.3.2. Expression and purification of recombinant proteins

Bacteria transformed with the expression vectors for Tat-GFP, TTC-GFP, and Tat-TTC-GFP were cultured to an OD600 of 0.6 at 37°C. At this point, cultures were induced with 0.1mM IPTG (isopropyl-β-D-thiogalactopyranoside, Invitrogen) and grown overnight at 25°C. After ~21 hours of growth, cultures were harvested by centrifugation. After discarding the supernatant, cell pellets were frozen at -80°C until purification. Cell pellets were thawed and lysed with 1mg/mL lysozyme (Sigma), 1% Triton X-100 and brief sonication. After cell lysis, the lysate was centrifuged at 14,000 RPM for 30 minutes and pelleted insoluble cell debris was discarded. The GST-linked proteins in the soluble fraction were purified using Glutathione Sepharose 4B resin according to the manufacturer's protocol (GE Healthcare). Following purification, the GST was cleaved off Tat-GFP using PreScission Protease (GE Healthcare) and dialyzed against 1X PBS. The GST was cleaved off TTC-GFP and Tat-TTC-GFP using Thrombin (GE Healthcare). Protein quality was confirmed by SDS-PAGE (Figure 2.1) and protein concentrations were determined by Bradford Assay using the Coomassie Protein Assay Reagent (Thermo Scientific).
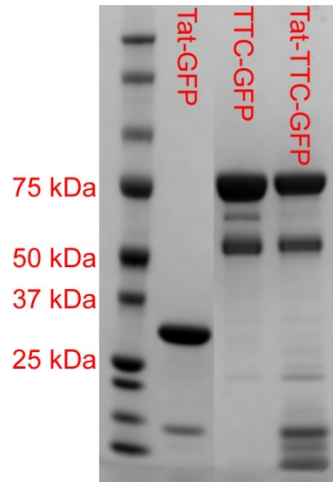
Figure 2.1: SimplyBlue Safestain of 6.5 µg purified proteins of interest. The expected molecular weights of Tat-GFP, TTC-GFP, and Tat-TTC-GFP are 28.6 kDa, 80.7 kDa, and 82.3 kDa respectively. Tat-GFP ran between the 25 kDa and 37 kDa standard bands while both TTC-GFP and Tat-TTC-GFP ran above the 75 kDa standard band of the Precision Plus All Blue Protein Standard (Roche). These proteins have been run on 4-12% Bis Tris SDS-PAGE gels (Life Technologies) many times with highly consistent results. The image of the gel was cropped to remove additional (identical) elutions.

2.3.3. Cell culture and protein transduction

Human neural progenitor cells (hNPCs, Lonza) were cultured in hNPC starting medium (Ebert et al., 2008). Shortly after vial thaw (2-5 days), passage 4 neurospheres were dissociated with Accutase (Sigma) and expanded as single cells. For protein treatment, NPCs were re-plated in poly-L-lysine-coated 8-well chambered coverglasses (Nunc) and allowed to expand 4-7 days until cells reached a density of ~25,000 cells/cm^2. The NPCs were plated in 50% hNPC starting medium and 50% MEM (Gibco) supplemented with 5% horse serum.

N18-RE-105 cells were grown in DMEM (Gibco Catalog #11965) supplemented with 10% Fetal Bovine Serum (FBS, Gibco), 1X HAT Supplement (Sigma), and 1:100 Penn/Strep (Gibco). The cell line was subcultured twice per week to avoid culture

overgrowth. The 3T3 fibroblasts were cultured in DMEM (Gibco Catalog #11995) supplemented with 10% FBS (Gibco) and 1:100 Penn/Strep (Gibco). Due to the faster growth rate of 3T3 cells, they were subcultured three times per week. Both N18-RE-105 and 3T3 cells were plated in poly-L-lysine-coated 8-well Lab Tek Chambered Coverglasses and allowed to expand for two days until they reached ~25,000 cells/cm^2. All cell culture growth was performed in a humidified incubator at 37°C and 5% CO_2.

Cells were treated with Tat-GFP, TTC-GFP, and Tat-TTC-GFP for 18 hours in either fresh 4% serum media (N18-RE-105 and 3T3 cells) or hNPC starting medium (NPCs) and incubated at 37°C and 5% CO_2. Serum concentration was reduced for N18-RE-105 and 3T3 cells to limit interference with CPP internalization (Eiríksdóttir et al., 2010). Cells were treated with 20μg/mL protein for all work except the dose-response experiment. After the overnight incubation, cells were washed three times and imaged live. The NPCs were washed with 70% DMEM (Gibco Catalog #11965), 30% F12 (Gibco Catalog #11765), 1:50 B27 (Gibco), and 1:100 Penn/Strep (Gibco). This is the hNPC starting medium without growth factors or heparan sulfate. N18-RE-105 and 3T3 cells were washed using reduced 4% serum media with otherwise identical supplements to the 10% serum media in the appropriate DMEM formulation.

2.3.4. Assaying cell-associated protein

To determine how much of each protein was bound or internalized by NPCs, cells were treated with 7 different concentrations of each protein: 0, 0.512, 1.28, 3.2, 8, 20, and 50 μg/mL in a total 2mL working volume in poly-L-lysine-coated 6-well plates (Corning). NPCs for this experiment were plated in standard hNPC Starting Medium. Duplicate wells were treated for all protein concentrations. After the overnight incubation, cells were

washed quickly and thoroughly with 1X PBS, detached with Accutase (Sigma), and lysed with 60μL M-PER Mammalian Protein Extraction Reagent containing Halt Protease Inhibitor (Thermo Scientific). Duplicate wells were lysed using the same 60μL volume of M-PER reagent to concentrate the lysate. This was done because pilot experiments indicated that fluorescence was not above background when low numbers of cells were lysed. As a result, this experimental procedure aimed to concentrate samples as much as reasonably possible. Samples were diluted 1:7 in 1X PBS to get enough volume to load 100μL/well in triplicate in black 96-well plates (Microfluor 2, Thermo Scientific) and read on the Victor 3 Multilabel Counter (Perkin Elmer). GFP was excited at 485nm and emission was read at 535nm. Cell-associated fluorescence (which includes both internalized protein and protein that remained bound to the cell surface) was quantitated by comparing fluorescence with a standard curve created with the appropriate protein diluted in 1X PBS containing the identical concentration of M-PER in the lysed samples. Each standard curve contained blank buffer and 12 protein concentrations ranging from 5.24E-4 to 12.5 μg/mL. Total protein concentration was determined by Bradford Assay using Coomassie Protein Assay Reagent (Thermo Scientific).

2.3.5. Fluorescent microscopy and image quantitation

All fluorescent microscopy was performed using an Axio Observer Z1 Motorized fluorescent microscope (Carl Zeiss, Inc.) and HBO 100 Mercury Arc Lamp. Zeiss Filter #10 was used for GFP excitation and emission (excitation: 450-490nm BP, emission: 515-565nm BP). Fluorescent images were taken with a Zeiss AxioCam MRm monochrome camera (1.3 megapixel, 12 bits/pixel) using the Zeiss C-Apochromat 40x/1.2 W Korr objective.

Image quantitation was performed using Zeiss Axiovision Software Version 4.6.3. Each of NPCs, N18-RE-105 cells, and 3T3 cells were treated with Tat-GFP, TTC-GFP, and Tat-TTC-GFP as described above. Image quantitation was utilized to quantitatively determine cell type specificity because sensitivity was not an issue and fluorescent signal is readily evident for all combinations of protein and cell type.

For accurate fluorescent quantitation, images should be acquired under identical conditions unless there is a compelling reason for not doing so (Cromey, 2010). For the current study, all images were taken under identical microscope and software conditions with the exception of camera exposure time. For NPCs and N18-RE-105 cells, the fluorescent signal intensity following Tat-GFP/TTC-GFP treatment and Tat-TTC-GFP treatment was very different. For the appropriate Tat-TTC-GFP exposure time, signal was not present for the other two proteins. Conversely, at the appropriate Tat-GFP/TTC-GFP exposure time, Tat-TTC-GFP signal was totally saturated. Therefore, for each cell line/protein combination 11-14 images were taken with an appropriate exposure time where signal was clear but not saturated.

For each cell line/protein combination, 45-58 cells were selected for quantitation. To avoid bias in cell selection, all cells were chosen for quantitation from the phase contrast image. Cells were only selected for quantitation if they were sufficiently separated from other cells to insure all fluorescent intensity originated from the cell of interest. To determine signal intensity, the entire cell was outlined using the "outline splice" feature of Axiovision. Phase contrast images were taken for all images for which fluorescent quantitation was performed. Furthermore, cells were outlined for densitometry using the phase contrast. To accurately account for background, local background was determined

next to each cell (Waters, 2009). All cell fluorescent intensities were normalized to their local background. Since the fluorescent signal saturation was minimized, normalized signal intensities were approximated as directly proportional to time (Schönhuber et al., 1997). This approximation provided an effective basis upon which to compare cell type specificity of the Tat-TTC-GFP protein. This method was appropriate due to scaling; it was used to compare protein internalization on the order-of-magnitude scale to determine cell type specificity. Furthermore, this linear approximation was not required for the 3T3 cells since imaging with the same camera exposure time was possible for all proteins.

2.3.6. Photochemical internalization

Photochemical internalization (PCI) was mediated in NPCs following protein transduction using photosensitizer $TPPS_{2a}$ and fluorescent light delivered by the Zeiss Axio Observer Z1 through the Zeiss Fluar 2.5x/0.12 objective and Zeiss Filter #47 (excitation: 426-446 BP). Light intensity was attenuated using the manual attenuator wheel of the Zeiss Axio Observer Z1 fluorescent microscope. The wheel has six neutral density settings which from settings 1-6 represent 100%, 70%, 50%, 40%, 20%, and 2% maximum light intensity. To mediate PCI, fluorescent light was delivered with neutral density filter setting 4 or 5 (ND4, ND5) in place representing 40% and 20% maximum light intensity respectively. The peak excitation wavelength of photosensitizer $TPPS_{2a}$ is 420nm. To prepare a 2mg/mL $TPPS_{2a}$ solution, 10mg $TPPS_{2a}$ was dissolved in 1mL 0.1N NaOH. Once in solution, the $TPPS_{2a}$ was diluted to 2mg/mL with 1X PBS pH=7.3. Aliquots of the $TPPS_{2a}$ solution were frozen at -20°C and thawed immediately before use (Berg et al., 2010). The protein transduction procedure preceding PCI was performed as described above, except $TPPS_{2a}$ was added at the same time as the protein at a final concentration of

0.2μg/mL. Once photosensitizer was added, all procedure steps were performed in subdued light. After the 18 hour incubation, cells were washed three times as described with hNPC starting medium without growth factors or heparan sulfate. The NPC cultures were then incubated four additional hours in hNPC starting medium to facilitate the diffusion of excess photosensitizer from the cell membrane. Cultures were then washed one additional time, given fresh hNPC starting medium, and treated with fluorescent light to mediate PCI.   To image cells before and after PCI, three representative fields were selected before and after light treatment using the C-Apochromat 40x/1.2 W Korr objective.

2.3.7. Cytotoxicity of photochemical internalization

The cytotoxicity of PCI was determined using an LDH assay, the Cytotoxicity Detection Kit (Roche). Protein transduction and PCI were performed for each protein of interest in NPCs. Although cells for the cytotoxicity experiments were plated in hNPC Starting Medium, beginning with the protein treatment, hNPC Starting Medium without F12 was used because sodium pyruvate in the F12 medium would have interfered with the LDH assay. The 30% F12 was replaced with the appropriate sodium pyruvate-free DMEM formulation. The cytotoxicity of PCI for NPCs was determined by LDH assay 24 and 48 hours after light treatment in two experiments.   First, NPCs were treated with photosensitizer and 20 μg/mL Tat-GFP. PCI was mediated for 10, 30, and 60 seconds with ND4 and ND5. Subsequently, NPCs treated with TTC-GFP and Tat-TTC-GFP were subjected to 3 light conditions: 10, 30, and 60 second light treatments with only ND4. All experimental conditions included duplicate wells although a few conditions had only one well due to cell loss in the extensive washing required preceding PCI. After photochemical

internalization, media samples were collected after 24 and 48 hours of incubation at 37°C and 5% CO_2. Percent cytotoxicity was calculated according to manufacturer's recommendations: Percent cytotoxicity = ((Test condition – Low Control)/(High Control)) *100, where the low control is an identical sample that did not receive a light treatment and the high control received a 1% Triton X-100 treatment.

2.4. Results

2.4.1. Qualitative description of protein internalization in NPCs

When NPCs were treated with equal protein concentrations by weight, it was observed that Tat-TTC-GFP was internalized considerably more than either Tat-GFP or TTC-GFP. NPCs treated with the proteins of interest could not be photographed using the same camera exposure time without saturating Tat-TTC-GFP signal (Figure 2.2). When a 750 ms exposure time was used to image treated NPCs, Tat-TTC-GFP signal was saturated in most cells (Figure 2.2C). Instead, a 100 ms exposure was needed to observe the punctuate Tat-TTC-GFP distribution (Figure 2.2D) in NPCs. At this exposure time, Tat-GFP and TTC-GFP fluorescence was not visible. The punctuate protein fluorescence in NPCs is consistent with the common observation of endosomal entrapment (Gillmeister et al., 2011). With the imaging conditions used, cytosolic fluorescence was not observed for any of the three proteins of interest.
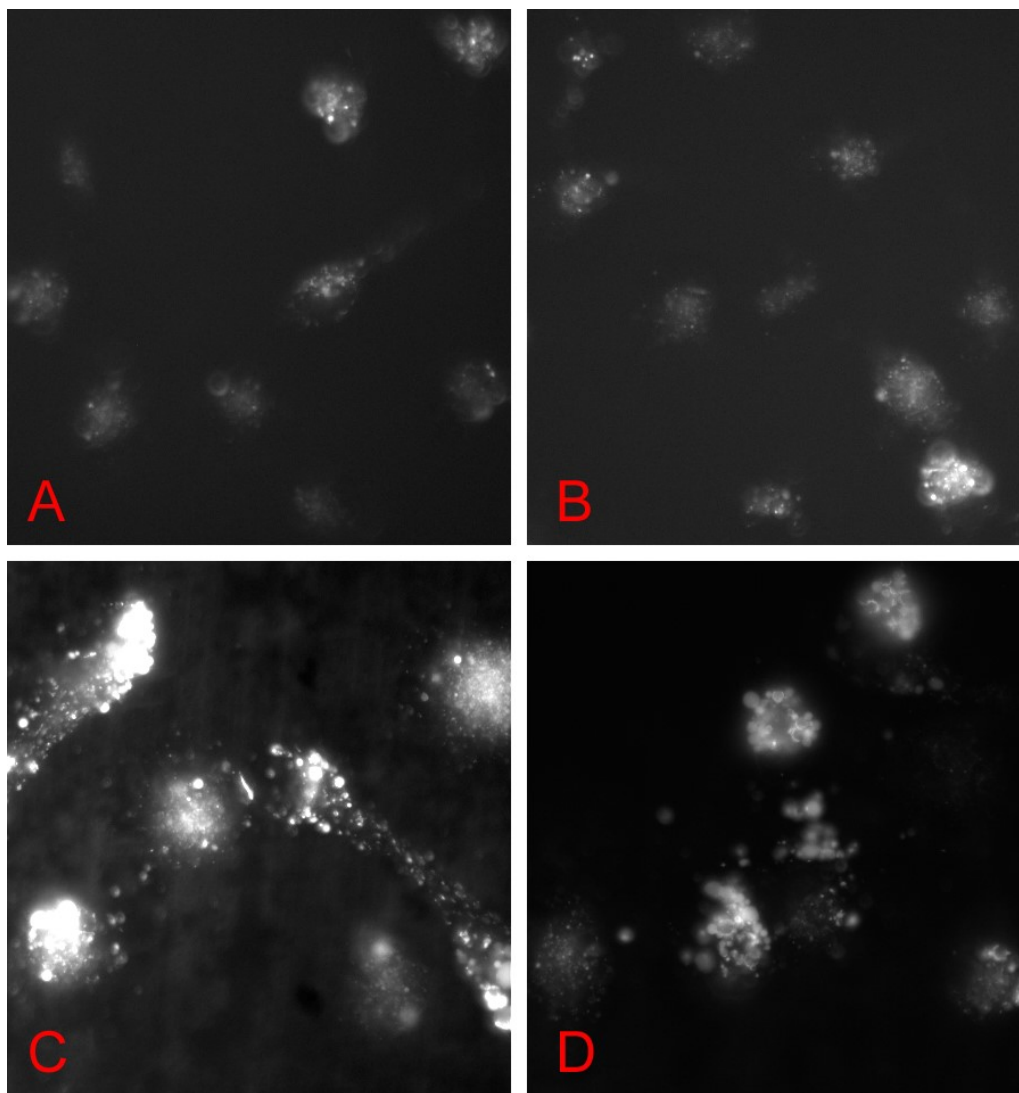
Figure 2.2: A qualitative comparison of GFP internalization in NPCs. (A) Tat-GFP, 750 ms exposure (B) TTC-GFP, 750 ms exposure (C) Tat-TTC-GFP, 750 ms exposure (D) Tat-TTC-GFP, 100 ms exposure. 400X fluorescent images were taken with a Zeiss AxioCam MRm monochrome camera (1.3 megapixel, 12 bits/pixel) using the C-Apochromat 40x/1.2 W Korr objective.

2.4.2. Quantitation of cell-associated protein in NPCs

The concentration of Tat-GFP, TTC-GFP, and Tat-TTC-GFP present in protein-treated NPC lysate was determined by quantitative fluorimetry. For each of the three recombinant proteins, normalized lysate fluorescence was compared to a standard curve of the treated protein. Fluorescence of background samples for the protein standards and

49

negative control protein lysates were subtracted from the protein standards and lysates to obtain normalized fluorescence values. For each sample, 58-89 µg total lysate protein was collected. Although comparable quantities of total protein were collected for all treatment conditions, when lysates were read on the fluorimeter, no incubation concentrations of Tat-GFP or TTC-GFP gave clear fluorescence signal in the cell lysates over background. Since the quantity of cell associated Tat-GFP and TTC-GFP could not be directly quantitated, the lowest concentration at which cell associated Tat-GFP or TTC-GFP would have been detected was estimated using the sensitivity of the standard curve for each of the proteins (Figure 2.3A). This analysis determined the minimum concentrations of Tat-GFP or TTC-GFP that would have been readily detected in the lysates. To conservatively determine a maximum possible Tat-GFP or TTC-GFP concentration, the standards for which fluorescence was approximately twofold greater than the ~180 RFU background were determined. For standard concentrations 0.0082, 0.0205, and 0.0512 µg/mL Tat-GFP and TTC-GFP, fluorescence was 252.00, 362.00, and 619.33 and 229.67, 292.67, and 382.67 in RFUs, respectively. Conservatively, the maximum Tat-GFP concentration in the lysate for any treatment condition was found to be 0.0205 µg/mL. With a similar conservative estimate, the maximum TTC-GFP concentration present in any culture supernatant must be at most 0.0512 µg/mL. In contrast, cell lysate from all six Tat-TTC-GFP treatment concentrations had normalized average fluorescence values well above the background. In order to determine the concentration of Tat-TTC-GFP in the cell lysate, the concentration of Tat-TTC-GFP was plotted against the independent variable, normalized average fluorescence, to generate a standard curve. For a more accurate concentration determination, a second-order polynomial was fit to the standard curve (Figure 2.3B).
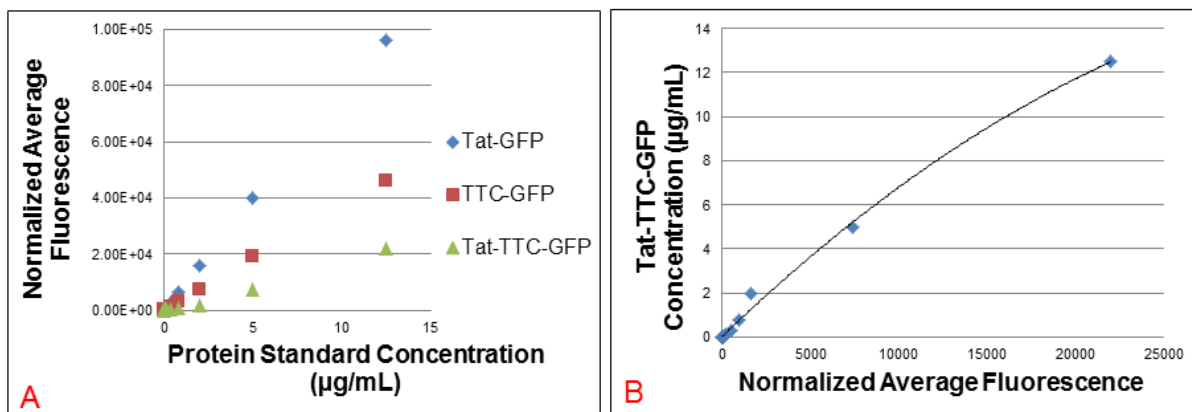
Figure 2.3: Standard curves for quantitation of GFP fluorescence. (A) Plots of the fluorescence versus protein standard concentration for each of the test proteins. (B) Second-order polynomial fit of the Tat-TTC-GFP standard curve with normalized average fluorescence as the dependent variable. Tat-TTC-GFP concentration in cell lysate was determined from the equation $y = 7.79E\text{-}4(x)\text{-}9.63E\text{-}04(x^2)$. All standard curves were generated by plotting the average of triplicate protein samples. The triplicate samples exhibited very minimal variability.

The quantities of Tat-TTC-GFP detected in NPC cell lysate were divided by the total concentration of protein collected for each sample. From this data, a dose-response curve was generated plotting cell associated Tat-TTC-GFP per total lysate protein (ng/µg) versus the concentration of Tat-TTC-GFP provided in the media (µg/mL) (Figure 2.4). When cells were incubated with 20µg/mL, 9.71ng of cell associated Tat-TTC-GFP was detected per microgram total lysate protein representing 0.89% of total incubated fluorescent protein.

For the 20 µg/mL Tat-TTC-GFP treatment condition, 1.70 µg/mL Tat-TTC-GFP was detected in the cell lysate. Using this data, the increase in protein bound and internalized by the cells can be approximated based upon the estimates of maximum cell associated Tat-GFP and TTC-GFP (0.0205 µg/mL and 0.0512 µg/mL respectively). When NPCs were treated with 20 µg/mL of purified protein, Tat-TTC-GFP was bound or internalized at least 83-fold greater than Tat-GFP and 33-fold more than TTC-GFP. The

51

dose-response curve for Tat-TTC-GFP indicates the approximately linear cellular association does not continue beyond 20 µg/mL treated Tat-TTC-GFP (Figure 2.4).
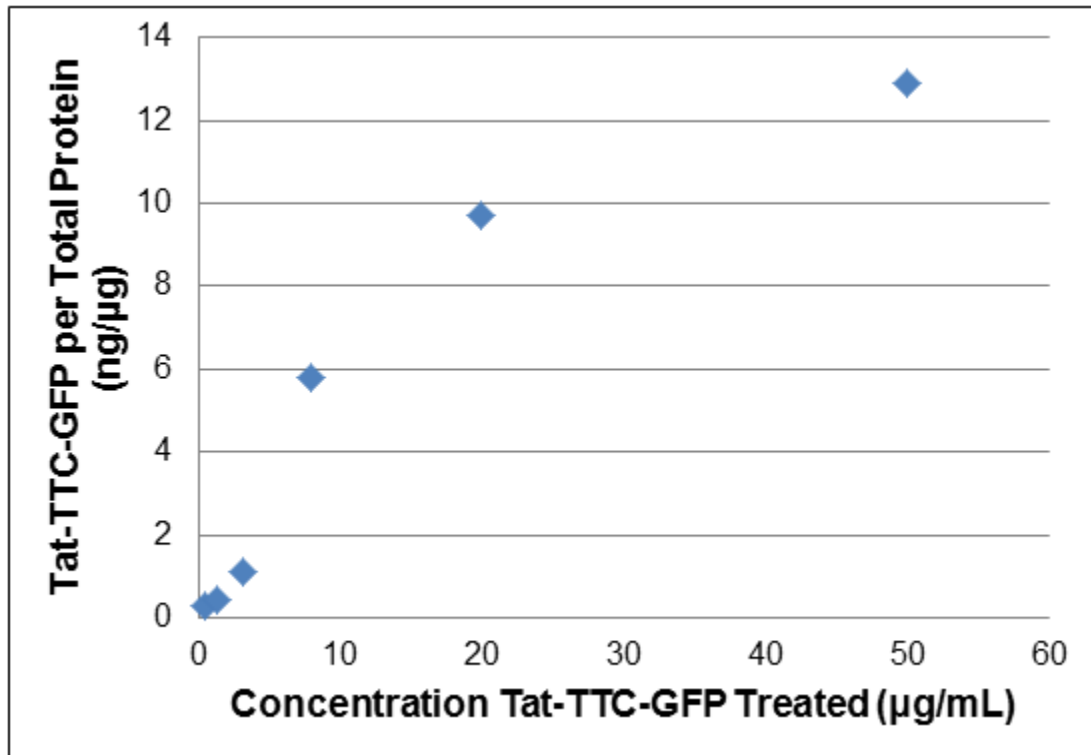
Figure 2.4: Dose-response curve for Tat-TTC-GFP. Each data point represents the lysate from pooled duplicate wells of six-well plates containing NPCs treated with varied concentrations of Tat-TTC-GFP. All fluorimetry was performed on triplicate samples which exhibited very low variability.

2.4.3. Enhanced Tat-TTC-GFP internalization is specific to neural cell types that bind TTC

In order to examine the cell type specificity of Tat-TTC-GFP binding, NPCs, N18-RE-105 neuroblastoma cells, and non-neuronal 3T3 fibroblasts were incubated with Tat-GFP, TTC-GFP and Tat-TTC-GFP. Qualitatively, Tat-TTC-GFP-treated N18-RE-105 cells exhibited much brighter fluorescence than either Tat-GFP or TTC-GFP-treated N18-RE-105 cells. Conversely, Tat-TTC-GFP did not seem to be preferentially internalized in 3T3 cells. As in our earlier experiments, marked differences in fluorescence intensity

necessitated different exposure times to image Tat-TTC-GFP internalization in NPCs and

N18-RE-105 cells (Figure 2.5).
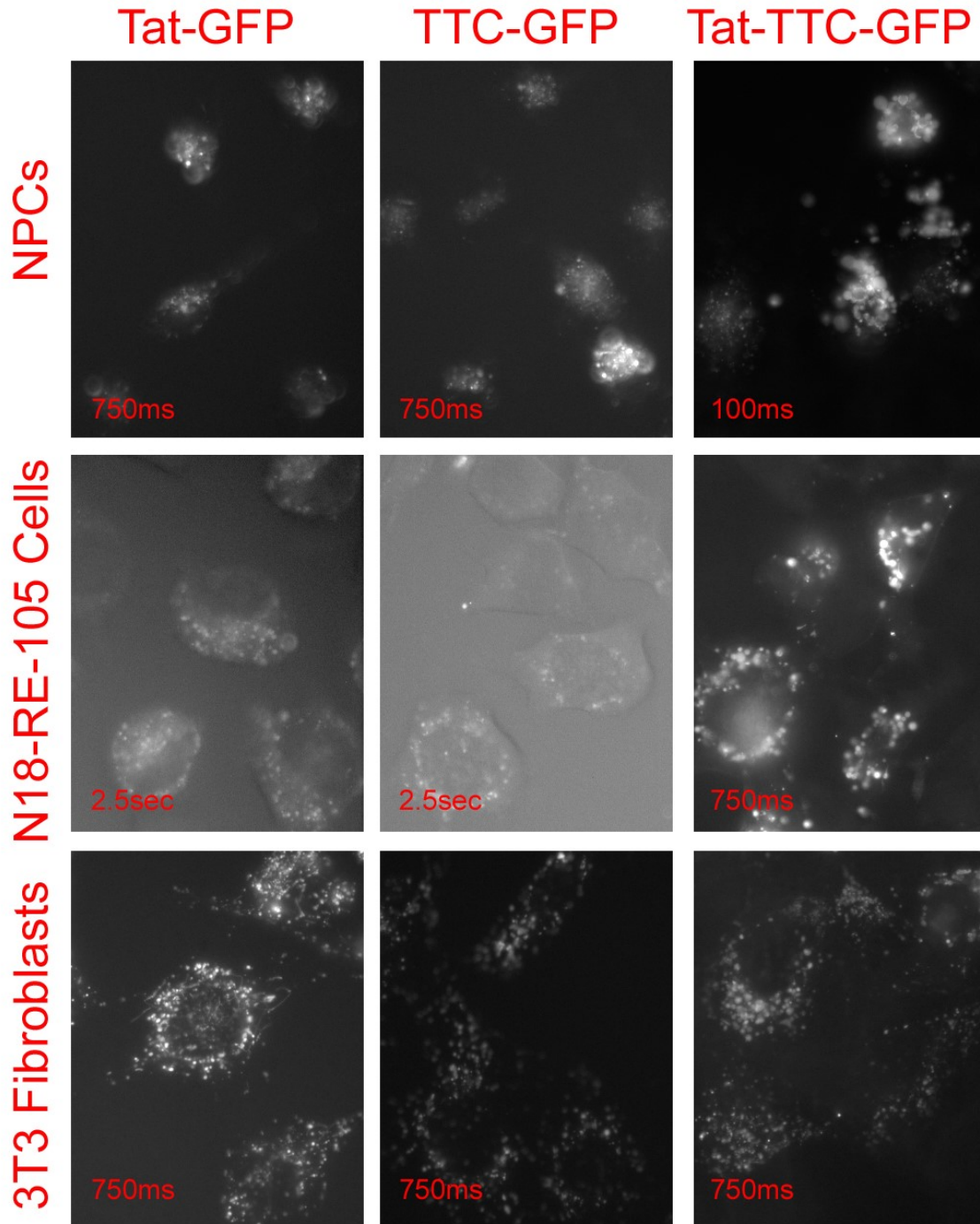
Figure 2.5: Representative fields used for quantitation of fluorescence of internalized proteins in NPC, N18-RE-105, and 3T3 cells. Camera exposure times are shown, and were chosen to limit signal saturation. All images are 400X magnification.

For NPCs and N18-RE-105 cells, Tat-TTC-GFP fluorescence was greater than an order of magnitude above either Tat-GFP or TTC-GFP fluorescent intensity. No increase in Tat-TTC-GFP internalization was observed compared to Tat-GFP internalization in 3T3 cells (Table 1). This fluorescence quantitation indicated that enhanced internalization of Tat-TTC-GFP is specific to neuronal cell types that bind TTC.

Cell Type	Protein	Exposure Time (ms)	Normalized Density	Scaled Normalized Density	**Fold Increase (to Tat-GFP)**
NPC	Tat-GFP	749.83	285.29	285.29	**1.00**
	TTC-GFP	749.83	358.23	358.23	**1.26**
	Tat-TTC-GFP	99.90	686.80	5155.12	**18.07**
N18-RE-105	Tat-GFP	2499.84	106.51	106.51	**1.00**
	TTC-GFP	2499.84	61.94	61.94	**0.58**
	Tat-TTC-GFP	749.83	438.27	1461.13	**13.72**
3T3	Tat-GFP	749.83	371.08	371.08	**1.00**
	TTC-GFP	749.83	94.48	94.48	**0.25**
	Tat-TTC-GFP	749.83	224.68	224.68	**0.61**

Table 2.1: Summary of fluorescence image quantitation data for NPC, N18-RE-105, and 3T3 cells treated with Tat-GFP, TTC-GFP, and Tat-TTC-GFP.

2.4.4. Photochemical internalization meditates the endosomal release of entrapped proteins in NPCs

Photochemical internalization (PCI) was used to mediate the cytosolic release of Tat-GFP, TTC-GFP, and Tat-TTC-GFP in NPCs. Pilot experiments were performed to optimize the light treatment conditions that promoted the best balance of endosomal release and cell viability. Using the Zeiss Axio Observer Z1 microscope, light intensities from 2% to 100% and treatment times up to five minutes were investigated (data not shown). These initial experiments indicated that treating cells with 20% and 40% maximum light intensity

for up to 60 seconds facilitated endosomal rupture while maintaining cell viability. For the higher light intensities and 60 second light treatment, nearly total endosomal release (Figure 2.6) but extremely high cell toxicity were observed. This observation made it clear that working with higher intensities and longer treatment times was not necessary and excessive.
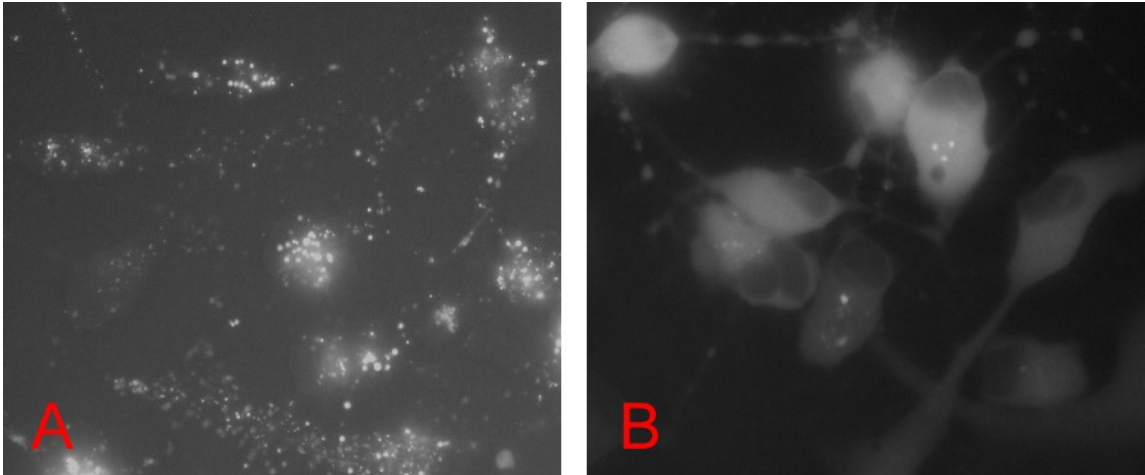
Figure 2.6: NPCs treated with 20µg/mL Tat-GFP before (A) and after (B) PCI with 60 seconds of maximum-intensity light treatment. Minimal endosomal entrapment was observed post-PCI. All images were taken at 400X magnification with a 1.5 s camera exposure time. The displayed images are representative fields, not the same cells pre- and post-PCI.

While treatment times up to 60 seconds with 20%-40% maximum intensity light did not mediate total endosomal rupture, redistribution of all three proteins, (Tat-GFP, TTC-GFP, and Tat-TTC-GFP) from a punctate to a more uniform distribution was clearly observed (Figure 2.7). Visually, clear GFP redistribution was observed for the 30 second treatment with 40% intensity and the 60 second treatment with 20% and 40% intensity (data not shown).
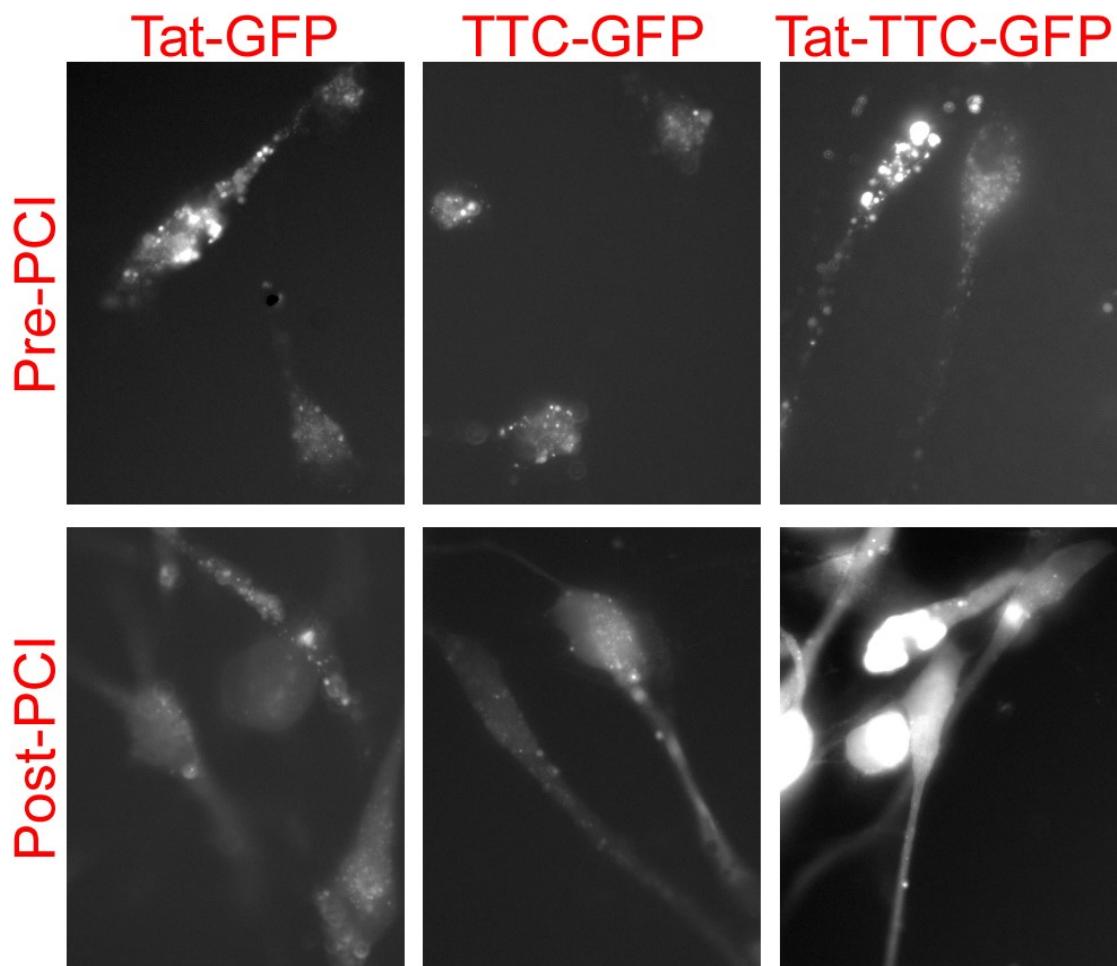
Figure 2.7: PCI facilitates the cytosolic redistribution of Tat-GFP, TTC-GFP, and Tat-TTC-GFP in NPCs. Light treatment was performed for 60 seconds with neutral density setting #4 representing 40% maximum light intensity. All images were taken at 400X magnification with a 750 ms camera exposure time. Images are representative fields and not the same cells pre- and post-PCI.

Two key observations were made from experiments at different light intensities where NPCs were treated with Tat-GFP only. First, 40% intensity treatment for 10-60 seconds resulted in higher cytotoxicity than the corresponding 20% intensity treatment. Second, cell survival was very similar for the 24 and 48 hour samples regardless of light exposure paradigm (Figure 2.8A). Based upon this experiment with Tat-GFP, NPCs were treated with either TTC-GFP or Tat-TTC-GFP confirming the initial observation that light

intensity and treatment time were the only important factors determining cytotoxicity. While lower cytotoxicity levels sixty seconds after light treatment were generally observed with TTC-containing vectors, no obvious difference in cytotoxicity was observed based upon which protein was used. For all proteins over both experiments, treatment times between 10 and 60 seconds with 40% light intensity yielded percent cytotoxicities of 0.5-6.3%, 23.2-35.4%, and 46.4-71.3% respectively. Interestingly, the 24 and 48 hour cytotoxicity data sets were very similar (Figure 2.8B). All cytotoxicity data is summarized below (Table 2.2).
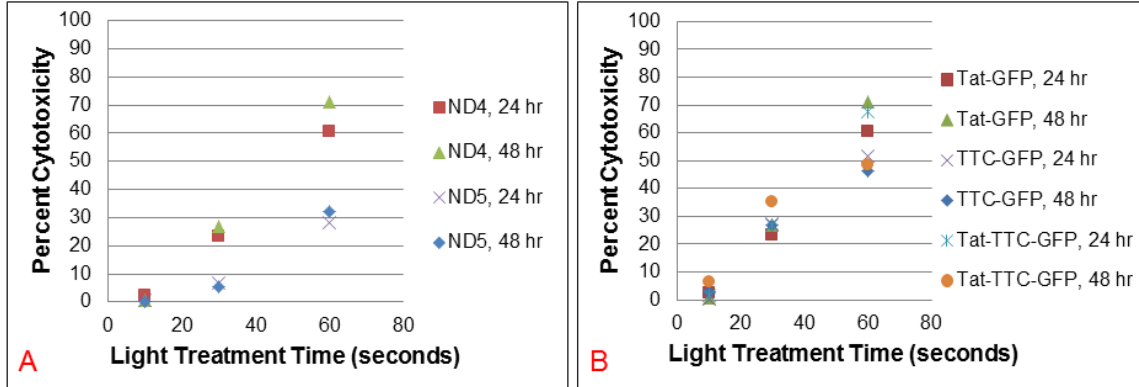
Figure 2.8: PCI cytotoxicity for NPCs was assayed 24 and 48 hours after light treatment. (A) NPCs were treated with Tat-GFP and subjected to light treatments with neutral density settings #4 (ND4) and #5 (ND5) representing 40% and 20% maximum light intensity respectively. (B) PCI cytotoxicity for NPCs treated with Tat-GFP, TTC-GFP, or Tat-TTC-GFP. PCI was mediated with 40% maximum light intensity only. LDH assay for all cell lysates was performed in triplicate with minimal variability.

Control cultures were evaluated to examine for any potential cytotoxic effect of the photosensitizer and/or light treatment. LDH absorbance was nearly identical for cells that did not receive treatment of any kind and cells treated with photosensitizer and protein but not exposed to light. An additional set of control cells were treated only with the maximum intensity light used in the study: 60 seconds with 40% intensity. This control indicated that

cells receiving light exposure without protein or photosensitizer treatment experienced

very minimal cell death (data not shown).

Light Intensity (% Maximum)	Time After Treatment (hours)	Protein	Light Treatment Time (s)	Percent Cytotoxicity
20%	24	Tat GFP	10	0.72
	24	Tat GFP	30	6.77
	24	Tat GFP	60	28.15
40%	24	Tat GFP	10	2.46
	24	Tat GFP	30	23.15
	24	Tat GFP	60	60.51
40%	24	TTC GFP	10	0.48
	24	TTC GFP	30	27.27
	24	TTC GFP	60	51.59
40%	24	Tat-TTC-GFP	10	1.68
	24	Tat-TTC-GFP	30	26.75
	24	Tat-TTC-GFP	60	67.41
20%	48	Tat GFP	10	0.2
	48	Tat GFP	30	5.62
	48	Tat GFP	60	32.02
40%	48	Tat GFP	10	0.58
	48	Tat GFP	30	26.99
	48	Tat GFP	60	71.29
40%	48	TTC GFP	10	2.91
	48	TTC GFP	30	26.65
	48	TTC GFP	60	46.37
40%	48	Tat-TTC-GFP	10	6.28
	48	Tat-TTC-GFP	30	35.41
	48	Tat-TTC-GFP	60	48.74

Table 2.2: Compilation of cytotoxicity data for NPCs 24-48 hours after binding/internalization of Tat-GFP, TTC-GFP, or Tat-TTC-GFP and light treatment to mediate photochemical internalization. The ND4 and ND5 filters referenced in the text refer to 40% and 20% maximum light intensity respectively.

2.5. Discussion

Our observation that Tat considerably increases protein internalization in conjunction with TTC is reasonable when considering the mechanism of TTC binding itself. TTC promotes high-capacity neuron-specific binding using multiple binding sites for a variety of neuronal receptors (Fishman, 2009). Two carbohydrate binding pockets interact with complex gangliosides (Chen et al., 2009). TTC can also interact with N-glycosylated P15 and the recently determined SV2A/B protein binding site (Miana-Mena et al., 2002; Yeh et al., 2010). TTC has been previously combined to a non-specific vector as a ternary complex with plasmid DNA and PEI to improve the transfection efficiency of neurons (Oliveira et al., 2010). Although the exact mechanism of Tat is not fully understood, Tat is commonly thought to mediate cellular uptake in a receptor-independent manner (Jones et al., 2005; Kaplan et al., 2005; Nakase et al., 2007; Wadia et al., 2004). The addition of Tat to the TTC-GFP vector may provide an additional binding site to enhance the membrane association of TTC without interfering with the membrane binding properties of TTC.

While the mechanisms for Tat and TTC uptake are different, upon cellular internalization both Tat and TTC-conjugated proteins are sequestered in endosomal vesicles. Tat is able to promote limited endosomal escape, while TTC is unable to mediate endosomal membrane translocation (Gillmeister et al., 2011). The minimal escape afforded by Tat is not sufficient for many potential applications of protein transduction. In the current study, all test proteins were internalized in endosomal vesicles and cytosolic GFP fluorescence was not observed following treatment even with Tat conjugated proteins. This finding is consistent with our previous study of Tat-GFP and TTC-GFP where

conjugation of rhodamine to Tat-GFP was required to observe cytosolic fluorescence. Even with the rhodamine tag, quantitation of the distribution of Tat-GFP was not significantly different from that of TTC-GFP (Gillmeister et al., 2011). Thus, facilitating the cytosolic release of entrapped proteins was an additional goal of the current study, because maximizing internalization is not very useful if the protein is not biologically available. As mentioned in the introduction, the method of Tat-conjugated cargo protein internalization remains controversial. While endocytosis is clearly involved, both lipid raft-dependent macropinocytosis and clathrin-mediated endocytosis have been implicated (Jones et al., 2005; Kaplan et al., 2005; Nakase et al., 2007; Rinne et al., 2007; Wadia et al., 2004). While the mechanism of endocytosis was not determined for the recombinant proteins in the current study, the localization of Tat-GFP, TTC-GFP, and Tat-TTC-GFP was consistent with past observations of endosomal entrapment for both Tat and TTC-conjugated cargo proteins.

Multiple domains have also been previously used to improve CPP-linked delivery. Plasmid DNA delivery was increased through covalent linkage of a polyarginine CPP and a piggyBac transposase (Lee et al., 2011). Branched CPPs exhibited higher biological activity for the delivery of PNAs (Saleh et al., 2010). Tat conjugated to an integrin-binding motif increased DNA transfection efficiency with lipofectamine 5-fold over transfection with lipofectamine alone (Renigunta et al., 2006). The delivery of siRNA was enhanced by the addition of a CPP and fatty acid to a protein nucleic acid (PNA). The CPP mediated internalization while the fatty acid facilitated endosomal escape (Shiraishi et al., 2011). Similarly, antisense oligonucleotide delivery was enhanced using stearylated CPPs (Hassane et al., 2011). Dimerization of CPPs was found to facilitate direct transport over

endocytosis. This effectively increased internalization of protein and eliminated the need for endosomal escape (Geisler et al., 2011). A novel peptide CAYHRLRRC was identified for the delivery of therapeutic agents preferentially to leukemia and lymphoma cells. This peptide contained a region for lymph node targeting and a sequence for cell penetration (Nishimura et al., 2008).

While Tat promotes cellular uptake of protein in many cell types, TTC is a highly efficient delivery vector for only neuronal cell types with the appropriate receptors. As a result, Tat-TTC-GFP appears to significantly increase GFP internalization in only cell types that bind TTC. This hypothesis was confirmed by treating N18-RE-105 and 3T3 fibroblast cells with all three proteins of interest and imaging the cells to compare internalization. N18-RE-105 neuroblastoma cells express complex gangliosides including GT_{1b} and have been previously used as a positive control for TTC-binding (Walton et al., 1988). The 3T3 cell line has also been previously used as a negative control for non-specific TTC binding (Oliveira et al., 2010). Both visual observations and fluorescent quantitation confirmed that Tat-TTC-GFP was preferentially internalized in NPCs and N18-RE-105 cells but not in 3T3 cells, where TTC linked proteins showed no superiority over Tat linkage alone (Table 1). Direct fluorometic measurements of cell lysates were highly consistent with the quantitative microscopy data sets demonstrating enhanced protein internalization with the recombinant combination of Tat and TTC. The approach utilizing fluorimetry although more direct, does not measure solely recombinant protein that is internalized, but also includes protein that remains on the cell surface after washing. Tat-TTC-GFP was internalized or bound at least 83-fold higher than Tat-GFP and at least 33-fold higher than TTC-GFP. These estimates are comparable to an order of magnitude

enhancement of internalization for Tat-TTC-GFP over Tat-GFP and TTC-GFP respectively by quantitative microscopy.

This combined Tat-TTC delivery strategy represents a novel method to increase internalization of a full-length protein over a control CPP-protein conjugate for neuronal cell types. Previous approaches have been considered to increase both CPP internalization as well as transduction into the cytosol. Dimeric cationic amphiphilic CPP P11LRR was found to mediate cellular uptake ~30-fold over Tat. At higher concentrations this CPP also exhibited direct transport to the cytosol over endocytosis (Geisler et al., 2011). Another CPP modification strategy to improve uptake and cytosolic availability attached the GKPILFF sequence of Cathespin D to CPP R8. This R8-CathD CPP was internalized 5-fold over the R8 CPP itself. The inverted R8-CathD CPP was internalized 18-fold over the R8 CPP. Both of these modified CPPs were found to increase endosomal escape over the control (Takayama et al., 2009). These studies did not investigate whether uptake was still enhanced with conjugation to a cargo protein (Manosroi et al., 2011).

Successful strategies to enhance the delivery of full length proteins are less prevalent in the literature. One study found that 10% DMSO pretreatment increased FITC-Tat uptake 2 to 4-fold depending on the cell line used. Tat-GFP uptake was also shown to increase significantly following the DMSO pretreatment although quantitative results were not provided (Wang et al., 2010). Nanovesicular systems of liposomes and niosomes were used to deliver Tat-GFP to HT-29 colon carcinoma cells. When loaded into elastic anionic niosomes, Tat-GFP was internalized 2.8-fold more than unloaded Tat-GFP (Manosroi et al., 2011). Numerous gene delivery systems have utilized Tat in conjunction with other functional domains to increase membrane binding or nucleic acid delivery. The use of

multiple binding domains was successful although the outputs, such as splice-correction, are difficult to compare to direct protein internalization (Hassane et al., 2011; Lee et al., 2011; Renigunta et al., 2006). Indeed, the Tat-TTC protein delivery vector provides a dramatic advancement in the efficiency of protein delivery to neuronal cell types.

We recognize that the rationale for combining TTC and Tat may appear counterintuitive since the entire 100 kDa heavy chain of tetanus toxin, which contains both the membrane binding (TTC) and translocation domains of tetanus, could have been used to deliver the model cargo protein GFP. There are a number of reasons why we chose to investigate the use of Tat as a membrane binding and translocation domain. First and most importantly, our laboratory and others have found that the heavy chain of tetanus toxin does not efficiently mediate the membrane translocation when conjugated to a cargo protein. Second, Tat provides a receptor-independent binding domain to act in conjunction with the receptor-dependent TTC. Third, use of the heavy chain over Tat-TTC essentially doubles the size of the binding domain and would likely lead to increased difficulties in protein expression.

Different strategies for promoting the endosomal escape of cargo macromolecules have been examined and evaluated in the literature with varying effectiveness (El-Sayed et al., 2009). We chose to use PCI because of its potential to induce cytosolic release with very high efficiency, and its lack of a requirement for further modification of the protein to be delivered. To mediate PCI in the NPCs, photosensitizer TPPS$_{2a}$ was delivered in combination but not linked to the proteins of interest. PCI methods employing linked photosensitizers have also been used with success, but diminished fluorescence within the endosomes has been observed (Matsushita et al., 2004).

Our method for mediating PCI using a fluorescent microscope proved very efficient at facilitating the release of protein from the endosomes. When maximum intensity light was delivered for 60 seconds, virtually total endosomal rupture was observed. While powerful, this method was highly cytotoxic and required further optimization for practical use. Experimentation with a wide range of combinations of light intensity and treatment time allowed us to identify the range in which PCI was efficient with acceptable cytotoxicity. No toxicity was observed for protein and photosensitizer treatment without PCI. Treating NPCs with 20-40% maximum intensity light for 0-60 seconds yielded cytotoxicity from less than 1% to 70%. Furthermore, the cytotoxicity profiles indicate further optimization of cytosolic release and cytotoxicity is possible. This study demonstrates that effectively mediating PCI while maintaining 80% cell viability is clearly possible. Toxicity in samples treated with light for 60 seconds, especially 48 hours after light treatment, appeared to be lowest when TTC-conjugated proteins were delivered, an observation that could be due to the described neuroprotective properties of TTC (Calvo et al., 2012).

The PCI toxicity observations reported here are consistent with the relatively limited available data from the literature. Light doses leading to 30-50% toxicity are recommended for photochemical transfections (Berg et al., 2010). Tat conjugated to 5(6)-carboxytetramethylrhodamine (TMR) was found to be an efficient photosensitizer, mediating endosomal release within a few hundred milliseconds upon light treatment. However, extremely high toxicity was observed from this treatment (Srinivasan et al., 2011). Another application of PCI was using photosensitizer $TPPS_{2a}$ to promote the endosomal escape of saporin delivered in liposomes. The method alone without saporin

found 45-120 second light treatments caused 20-50% cytotoxicity 48 hours after treatment. As we observed, longer light treatments yielded more cell death (Fretz et al., 2007). PCI using a macromolecule-linked photosensitizer method has also been found to be toxic. An Alexa Fluor 546 fluorophore was conjugated to a U1A RNA-binding domain for siRNA delivery. PCI was mediated to enhance delivery and 22 hours after light treatment, ~40% cytotoxicity was observed (Endoh et al., 2008).

2.6. Conclusions

Cellular uptake and cytosolic release are two major challenges to protein transduction efficiency (El-Sayed et al., 2009). In the current study, the use of multiple functional binding domains and photochemical internalization (PCI) effectively addressed both of these challenges to enhance protein delivery in neural progenitor cells (NPCs). Cellular association and internalization of GFP was dramatically enhanced by the addition of both Tat and TTC domains, while the specificity of neural cell delivery of TTC was preserved. The combination of a small CPP and a receptor specific vector yielding enhanced binding and internalization, and retention of cell-specific binding, could apply to a variety of receptor specific vectors and cell types.

None of the vectors, including the hybrid vector in the current study, demonstrated detectable translocation to the cell cytosol. This limitation was successfully addressed with the application of PCI. The PCI procedure outlined here is probably not cell type specific, and could be useful to anyone interested in macromolecule delivery. The combinatorial use of multiple binding domains and PCI could be an invaluable tool for direct protein delivery in a wide variety of settings spanning cell type, cargo protein and sub-cellular target.

Chapter 3: Production and Delivery of Recombinant Transcription Factors

3.1.   Abstract

The last decade has seen a dramatic improvement in genetic-modification based strategies for stem cell differentiation. While exciting, any cell generated by a differentiation approach that involves genetic modification is unsuitable for human transplantation. Genetic modification, especially with the introduction of powerful viral promoters, increases the risk of tumor formation. This is an outcome that would outweigh any therapeutic effects provided by the delivered cells. The current study proposed that neuronal differentiation could be mediated through the direct treatment of cells with cell-penetrating peptide-linked recombinant transcription factors. While a protein delivery approach faces a number of additional challenges, it would generate cells that are safe for human therapy.

In pursuit of mediating neuronal differentiation with a protein-based approach, Tat-linked Mash1 and Lmx1a with and without GFP were expressed via transient transfection of HEK 293F cells and purified from the insoluble fraction of cell lysate. The biological activity of transcription factors was evaluated by testing for nuclear delivery following protein transduction and photochemical internalization and evaluating the induction of reporter gene expression after transcription factors were delivered by either co-transfection with the reporter vector or directly as a purified protein. The majority of designed transcription factors induced reporter expression following co-transfection. However, these results could not be reproduced with direct protein delivery, calling the efficiency of protein delivery and/or the functionality of the transcription factors produced into question.

The first step towards overcoming these limitations has been successfully accomplished; a new mammalian cell *in vitro* translation kit was successfully used to produce high concentrations of soluble Tat-Mash1 and Tat-Mash1-GFP. The use of an *in vitro* transcription factor production method has not been described in the literature. This finding could be critical for future efforts to mediate neuronal differentiation with defined purified factors.

3.2. Introduction

Cell-replacement therapy has long been considered an exciting option for neurodegenerative disease therapy. In cell-replacement therapy, the neuronal cell type lost due to the disease would be delivered; as the new cells integrate with the rest of the nervous system the disease phenotype would become less severe and possibly even reversed. Parkinson's disease (PD) is characterized by the loss of dopaminergic neurons from the substantia nigra, affecting 1% of individuals over the age of 60. Currently, PD is viewed as an ideal candidate for cell replacement therapy (Thomas, 2010).

Despite the potential for cell-replacement therapy for PD, there are a number of limiting factors that include obtaining stem cells to differentiate and the safety of the differentiation process. The discovery of induced pluripotent stem cells (iPSCs) as an alternative to human embryonic stem cells (hESCs) in recent years has made cell replacement therapy a more viable therapeutic option since a potentially limitless supply of stem cells for differentiation could be available without any ethical or regulatory concerns regarding the source of the cells. In 2006, the Yamanaka lab discovered that the infection of fibroblasts with lentiviral vectors expressing transcription factors Oct4, Sox2, c-Myc, and Klf4 induced pluripotency (Takahashi et al., 2006).

Although iPSCs potentially alleviate the concerns of sourcing large quantities of stem cells, they present safety issues. The lentivirus-mediated genetic manipulation and overexpression of transcription factors dramatically enhances the tumor-forming potential of transplanted cells. Even when the transcription factor gene sequence can be removed after differentiation, safety concerns are not fully alleviated. In 2009, an iPSC line was generated by the direct delivery of the four purified transcription factors. Critically, these protein-induced PSCs (piPSCs) were capable of indefinite expansion (Zhou et al., 2009). These transcription factors were expressed with an 11 amino acid polyarginine sequence to facilitate binding and internalization of the purified transcription factors.

In 2010, the idea of iPSC creation as a source of stem cells from which dopaminergic neurons could be generated was taken a step farther when the Wernig laboratory published the direct conversion of fibroblasts to neurons without an intermediate pluripotent state. Originally, it was thought that this direct conversion would be impossible. To test their hypothesis that such a direct conversion was possible, 19 different transcription factor lentiviral expression vectors were created. From this pool, it was found that a combination of three was necessary to facilitate neuronal transdifferentiation: *Mash1 (AsclI)*, *Brn2*, and *Mytl1* (Vierbuchen et al., 2010). After this discovery was published, two methods describing the generation of dopaminergic neurons directly from fibroblasts were developed. The first published method used the initial transdifferentiation cocktail plus dopaminergic factors *FoxA2* and *Lmx1a* (Pfisterer et al., 2011). The second published method generated dopaminergic neurons directly from fibroblasts directly via delivery of *Mash1*, *Lmx1a*, and *Nurr1* (Caiazzo et al., 2011).

The differentiation of stem cells or transdifferentiation of fibroblasts has traditionally been done in a method analogous to the creation of iPSCs. Expression vectors for transcription factors of interest are transfected into cells or lentiviral vectors are used to force continuous high level transcription factor expression. While genetic manipulation is a powerful strategy for modifying cellular phenotypes, genetically modified dopaminergic neurons are not a practical source of replacement cells for PD patients. As a result, there is a need for a method to induce neuronal differentiation or transdifferentation without genetic modification. To accomplish this goal, the lab aimed to express and purify a library of recombinant transcription factors. In 2011, it was reported that microRNA (miRNA) alone was capable of mediating transdifferentiation of fibroblasts to neurons. However, this process was inefficient without the expression of at least NeuroD2 with two miRNAs (Yoo et al., 2011). Even in this miRNA-based system, purified transcription factors would be an asset to improve efficiency. The use of protein treatment of transcription factors to induce transdifferentiation has only very recently been shown. Dopaminergic precursor cells were induced from fibroblasts using a complex procedure involving small molecules and Tat-linked Sox2 and Lmx1a (Mirakhori et al., 2015). This work was published only a month before this thesis was completed and unfortunately was not a useful reference when the work was completed from 2011-2012.

The long-term goal of the project was to design, express, and purify a small library of cell-penetrating peptide-linked functional transcription factors for the differentiation or transdifferentiation of source cells to dopaminergic neurons. Initially, Mash1, Lmx1a, and Nurr1 were chosen for study based on Caiazzo et al. published in 2011. However, each of these transcription factors has an important role in neuronal development and would be

interesting even independently of the others. Mash1 (AsclI) is a member of the bHLH family of transcription factors and controls various stages of the neurogenesis process including neuronal differentiation, migration, axon guidance, and synapse formation (Vasconcelos et al., 2014). Lmx1a is a critical factor involved in dopaminergic differentiation. It was the first dopaminergic determinant transcription factor expressed and it binds to the tyrosine hydroxylase promoter (Barzilay et al., 2009). Nurr1 is a member of the nuclear receptor superfamily and regulates the differentiation, migration, and maturation of mesencephalic dopaminergic neurons (Li et al., 2011).

In pursuit of the goal of mediating neuronal differentiation using purified transcription factors, expression vectors for Tat-Mash1, Tat-Mash1-GFP, Tat-Lmx1a, Tat-Lmx1a-GFP, Tat-Nurr1, and Tat-Nurr1-GFP were designed. Recombinant Tat-linked variants for each factor were designed with and without GFP because GFP had the potential to improve protein expression and enabled the binding and internalization of the transcription factors to be assessed. The downside of adding GFP was a potential negative impact on transcription factor activity. Transcription factors were expressed via the transient transfection of HEK 293F suspension cells and purified from the insoluble fraction of the cell lysate. The functionality of recombinant Mash1 and Lmx1a proteins was assessed. While all transcription factors besides Tat-Mash1-GFP were functional when delivered by co-transfection, the purified proteins were not observed to have any significant activity. For future work, alternate expression systems were assessed with the goal of producing high-levels of soluble transcription factors. A commercially available HeLa cell lysate *in vitro* translation system was identified for its potential for soluble transcription factor production. The results of this study show that before neuronal

differentiation can be mediated with defined purified transcription factors, the issues of production, solubility, and delivery efficiency must be addressed.

3.3.   Materials and Methods

3.3.1. Creation of pSecTag2a-based transcription factor expression vectors

Expression vectors for six Tat-linked transcription factors were created: Tat-Mash1, Tat-Mash1-GFP, Tat-Lmx1a, Tat-Lmx1a-GFP, Tat-Nurr1, and Tat-Nurr1-GFP. All were created using a modified pSecTag2a (Life Technologies) containing Tat in the 5' end of the multiple cloning site. The pSecTag2a expression vector possesses a number of features that lend it itself to the expression of recombinant transcription factors including an IgK signal peptide to facilitate secretion, a myc epitope tag to enable easy detection, and a 6x His tag for affinity purification.

The human *Mash1* gene was recovered from a fibroblast cell line infected with a lentivirus generated by GeneCopoeia. RNA was purified from fibroblast cells and cDNA was generated. *Mash1* was amplified using PCR and cloned into pSecTag2a containing the *Tat* sequence using HindIII and BamHI restriction sites. Restriction sites were designed into the PCR primers for cloning. This completed sequence was confirmed and given the name pTagTat_Mash1.   The completed pTagTat_Mash1 was used to create pTagTat_Mash1_GFP. The sequence for *EGFP* was cloned into the backbone via BamHI and NotI restriction sites.

Each of the pTagTat_Lmx1a, pTagTat_Lmx1a_GFP, pTagTat_Nurr1 and pTagTat_Nurr1_GFP constructs were created using an analogous procedure with the same starting expression vector and added HindIII and BamHI restriction sites. Human *Lmx1a*

cDNA was purchased from Origene for use as a PCR template. Similarly, pTagTat_Nurr1 and pTagTat_Nurr1_GFP were created

3.3.2. Cell culture

HEK 293F suspension cells grown in CD CHO medium (Life Technologies) were adapted into Freestyle 293 medium (Life Technologies) since CD CHO contains an anti-clumping agent that inhibits transfection. HEK 293F suspension cells were passaged in Freestyle 293F medium three times per week seeding at 2-4E5 cells/mL and passaging before the cells exceeded the cell density of 2E6 cells/mL. Cultures were vortexed for 30 seconds before each passage to break up cell clumps.

Neural Progenitor Cells (NPCs) and select immortalized cell lines were used to evaluate the transcription factors binding/internalization and functionality. NPCs and 3T3 cells were cultured as described in Chapter 2, Section 2.3.3. SK-N-BE(2)C neuroblastoma cells were grown in 50% EMEM medium (ATCC) and 50% F12 medium (Gibco) supplemented with 10% fetal bovine serum (Gibco). The cells were subcultured twice per week.

3.3.3. Transient expression of recombinant Tat-linked transcription factors in HEK 293F suspension cells

Tat-linked transcription factors were produced by transient transfection of HEK 293F cells using 293fectin reagent (Life Technologies). One day before transfection, cells were seeded at 7E5 cells/mL in either 40mL in a 125mL vented non-baffled shake flask or 160mL in a 500mL vented non-baffled shake flask. Cultures were grown overnight until a cell density of 1.2E6-1.5E6 cells/mL was reached. At this time, 3.0E7 cells were

transfected in a final volume of 30mL with 30μg of DNA complexed with 293fectin at a 2:1 ratio of 293fectin reagent and plasmid DNA.

Transfected cultures were maintained at 37ºC and 5% CO2 for 2-3 days before being harvested. Samples of medium and cells were taken daily during production for evaluation of protein secretion and yields before purification. Cell-free medium was collected and stored at 4ºC pending evaluation of its transcription factor content. The cell pellet was washed 1X with an equal volume of 1X PBS pH = 7.4 and frozen at -80ºC.

Small-scale samples were lysed with M-PER protein extraction reagent (Pierce) and centrifuged at 14,000xg for 15 minutes to collect the soluble fraction of the lysate. The insoluble pellet was dissolved in SDS-containing sample loading buffer (Invitrogen) in preparation for SDS-PAGE analysis. Samples of cell-free medium, soluble lysate, and insoluble lysate were evaluated for protein content by western blotting for the myc epitope tag.

3.3.4. Purification of Tat-Mash1 and Tat-Lmx1a from the soluble and insoluble fractions of HEK 293F producer cells

Tat-Mash1, Tat-Mash1-GFP, and Tat-Lmx1a-GFP were purified from both the soluble and insoluble lysates where as Tat-Lmx1a was only purified from the insoluble lysate as no soluble material was detected. Frozen cell pellets were lysed with 1mL M-PER protein extraction reagent for every 100mg cell pellet. Insoluble material was dissolved by adding 1mL 1X PBS pH = 7.4 containing 8M Urea for each 100mg of wet insoluble pellet, vortexing vigorously, and sonicating 30 seconds with 1 second pulses at 50% power. After centrifugation at 15,000xg for 10 minutes, any material not re-solubilized was discarded.

Proteins were purified using HisPur Ni-NTA Resin (Pierce) and purification buffers of 1X PBS pH = 7.4 (20mM sodium phosphate, 300mM NaCl) containing varied concentrations of imidazole. Equilibration, wash, and elution buffers contained 10mM, 25mM, and 250mM imidazole respectively. All buffers used for purification of insoluble lysates contained 8M urea.

Protein was purified from soluble and insoluble lysates by adding an appropriate amount of equilibration buffer and binding 0.5mL Ni-NTA resin overnight at 4ºC. Following batch binding, the resin/lysate suspension was poured into a 2mL column and allowed to drain by gravity flow. After the flow-through was applied over the resin one additional time, the resin bed was washed 3-4 times with two bed volumes of wash buffer until the A280 reading reached baseline followed by 3-4 elutions. Later purifications used only 3 washes and elutions after that was determined to be more than sufficient. Elutions of interest were dialyzed against 1X PBS pH = 7.4 using 10kDa MWCO Slide-A-Lyzer cassettes (Pierce) to remove 8M urea. Final elutions were quantitated by Bradford assay. Densitometry was not performed on the specific bands because bands were not visible by coomassie staining.

3.3.5. Protein transduction and nuclear delivery of recombinant factors using photochemical internalization (PCI)

Nuclear Tat-Mash1-GFP and Tat-Lmx1a-GFP delivery was attempted in NPCs by mediating photochemical internalization (PCI) following protein transduction. NPCs were plated on poly-L-lysine-coated 8-well chambered coverglasses and allowed to expand 6 days to ~2.5E4 cells/cm². After the six days, cells were treated with purified protein. In the first experiment, cells were treated with either 1μg/mL Tat-GFP or 1μg/mL Tat-

Lmx1a-GFP and 0.2μg/mL photosensitizer TPPS$_{2a}$ in NPC starting medium. Since Tat-Mash1-GFP purification yields were higher, in the second experiment, NPCs were treated with 1, 2.5, or 5μg/mL Tat-GFP or Tat-Mash1-GFP and 0.2μg/mL photosensitizer TPPS$_{2a}$ in NPC starting medium.

Following an 18 hour overnight protein treatment, cells were washed three times in NPC starting medium without growth factors and incubated for 4 hours in NPC starting medium without photosensitizer at 37ºC and 5% CO_2 in preparation for light treatment to mediate PCI. Before PCI, three representative 400X images were taken for each treated well using the Zeiss Axio Observer Z1 fluorescent microscope. PCI was mediated using the Fluar 2.5x/0.12 objective and Zeiss filter set #47 (excitation 426nm-446nm) by delivering 20-40% maximum intensity light for either 30 or 60 seconds. Following PCI, cells were returned to the 37ºC incubator for four hours when 400X "post-PCI" images were taken to observe GFP signal after endosomal release.

3.3.6. Promoter/reporter assays to test functionality of transcription factors delivered by cotransfection

Promoter/reporter assays were chosen as the most straightforward test for transcription factor functionality. These promoter/reporter experiments were made possible by the generous gift of two reporter constructs for Mash1 and Lmx1a respectively. The 281-EL2 Mash1 reporter plasmid was provided by the Turner Lab and consists of a region of the *Gadd45γ* promoter upstream of luciferase (Huang et al., 2010). The Lmx1a DAT-A reporter construct consists of a region of the dopamine transporter (*DAT*) gene repeated 14 times upstream of a luciferase (Chung et al., 2012). This DAT-A reporter was a generous gift from Kwang-Soo Kim.

In preparation for co-transfection of the reporter plasmids and transcription factor-expressing plasmids, 10,000 cells/well of 3T3 or SK-N-BE(2)C cells were plated in 96-well plates in antibiotic-free medium and allowed to double overnight. At least 30 minutes before transfection, the culture medium was removed from all wells and 100µL Opti-MEM medium (Gibco) was added. Each well was transfected with complexes of plasmid DNA and Lipofectamine 2000 in OptiMEM medium (Life Technologies). Master mixes were prepared where single wells received 200ng total of plasmid, 100ng of each of a reporter plasmid and transcription factor-expressing plasmid, and 0.5µL Lipofectamine 2000. To test background luciferase expression, reporter plasmids were co-transfected with pCMV-MCS, an empty vector. Six hours after transfection, complex-containing medium was discarded and fresh antibiotic-containing culture medium was added. The Britelite Plus kit (Perkin Elmer) was used to assay luciferase activity 48-72 hours after transfection.

3.3.7. Promoter/reporter assays to test functionality of transcription factors delivered via protein treatment

Two experiments were designed to test Tat-Mash1 and Tat-Mash1-GFP protein functionality using the 281-EL2 reporter vector. Both experiments were initiated by transfecting 3T3 cells in 6-well plate format with the reporter vector. Cells were transfected by creating complexes where each well received 4µg plasmid DNA and 10µL Lipofectamine 2000. Complexes were added to 1.5mL OptiMEM medium in a volume of 0.5mL OptiMEM. All other steps of the reporter plasmid transfection were analogous to the procedure described in Section 3.3.6. Transfected cells were incubated at 37ºC and 5% CO_2 for 24 hours at which time protein treatment was performed. For protein treatment and possible light treatment to mediate PCI, cells needed to be in 8-well chambered

coverglasses. Cells transfected with 281-EL2 were dissociated using TrypLE Express and counted. Master mixes containing protein with and without TPPS$_{2a}$ were created and used to resuspend transfected cells to plate 3.37E4 cells/well in poly-L-Lysine coated chambered coverglasses. Cell density was calculated so the 8-well coverglasses were approximately 80% confluent. PCI was mediated after an 18 hour protein treatment; the light treatment condition chosen was 20% maximum lamp power for 60 seconds. The Britelite Plus kit was used to assay luciferase expression 24 hours after PCI.

Although the two experiments performed had a similar design, they varied in their protein treatment conditions. For the first experiment, 3T3 cells were treated with 1μg/mL Tat-Mash1 or Tat-Mash1-GFP with or without 0.2μg/mL TPPS2a. For each protein treatment condition and negative control, duplicate wells either did or did not undergo PCI. Mash1 protein was diluted in 3T3 base medium containing 4% FBS instead of the standard 10% FBS for all protein transduction experiments.

For the second experiment, cells were treated with cell lysate instead of purified protein. Purified protein was only obtained in reasonable amounts from the insoluble fraction of cell lysates. Due to concerns that protein derived from insoluble material might not be properly folded, cells were treated directly with lysate containing soluble protein. HEK 293F cell pellets from transient transfections were lysed by freeze/thaw to ensure the soluble protein was present in a buffer that would not be cytotoxic to the treated 3T3 cells. A pilot experiment was performed to determine what lysis method would harvest soluble Tat-Mash1 and Tat-Mash1-GFP comparably to M-PER lysis buffer (Figure 3.1).

Lane Description:

1. Precision Plus Standard
2. Tat-Mash1, M-PER
3. Tat-Mash1, Freeze/Thaw
4. Tat-Mash1, Sonication
5. Tat-Mash1, Freeze/Thaw + Sonication
6. Tat-Mash1-GFP, M-PER
7. Tat-Mash1-GFP, Freeze/Thaw
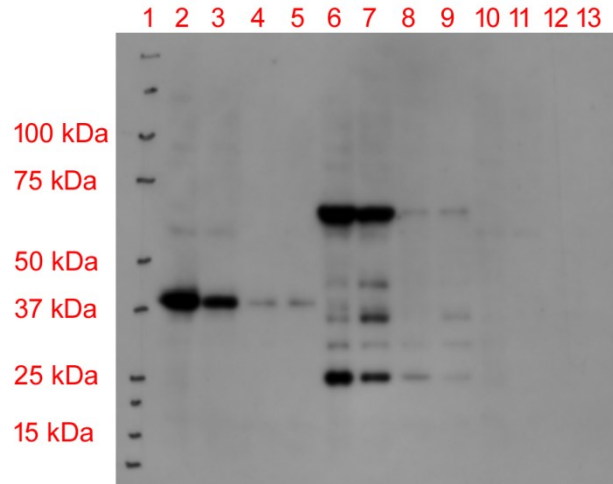
8. Tat-Mash1-GFP, Sonication
9. Tat-Mash1-GFP, Freeze/Thaw + Sonication
10. Negative, M-PER
11. Negative, Freeze/Thaw
12. Negative, Sonication
13. Negative, Freeze/Thaw + Sonication

Figure 3.1: Comparison of soluble protein yields from selected lysis techniques. HEK 293F pellets transiently transfected with pTagTat_Mash1, pTagTat_Mash1_GFP, or the untransfected negative control were thawed and lysed. Cell pellets were lysed by either M-PER lysis buffer treatment, freeze-thaw, sonication, or a combination of freeze-thaw and sonication. Equal volumes of soluble lysate were run on a 4-12% Bis Tris SDS-PAGE gel and analyzed by anti-myc western blotting (5 minute exposure). Expected sizes were Tat-Mash1= 33.6 kDa and Tat-Mash1-GFP= 60.5 kDa.

Tat-Mash1, Tat-Mash1-GFP, and negative control transiently transfected cell pellets contained between 25-33 million cells. Frozen cell pellets were thawed and resuspended in 133μL 1X PBS pH = 7.4 for each 1E6 cells and subjected to four freeze/thaw cycles in a dry ice/isopropanol bath. Whole cell lysate was centrifuged at 14,000xg for 15 minutes to remove any insoluble material. Each well containing 3.37E4 cells/well was treated with 75μL soluble lysate in 300μL total medium. As with the first

experiment, TPPS$_{2a}$ was added to the master mix for duplicate wells for one set of each protein treatment condition so that PCI could be mediated. Besides the protein treatment, the second experiment was identical to the first experiment.

3.3.8. Production of soluble Tat-Mash1 using *in vitro* translation

Two *in vitro* translation systems were selected to attempt to improve the production of soluble Tat-Mash1 and Tat-Mash1-GFP. The first system, the One-Step High Yield IVT Kit (Pierce), used HeLa cell lysate. The second was the Expressway Cell-Free Expression System (Life Technologies) using *E. coli* cell lysate. Both systems were coupled *in vitro* transcription and translation kits requiring the input of only plasmid DNA. Furthermore, both IVT systems could be tested at the small scale but scaled-up to produce quantities of protein potentially enabling significant experimentation.

The expression vector chosen for the HeLa IVT kit was pT7CFE1 (Pierce) containing a C-terminal 6x His sequence for purification. The *Tat-Mash1-myc* or *Tat-Mash1-GFP-myc* sequences were amplified out of pTagTat_Mash1 or pTagTat_Mash1_GFP via PCR. Restriction sites NdeI and SalI were engineered into the PCR primers for cloning into pT7CFE1.

For the *E. coli* IVT system, *Tat-Mash1* and *Tat-Mash1-GFP* were cloned into pEXP5-CT/TOPO using the pEXP5-CT/TOPO TA Expression Kit (Life Technologies). The final pEXP5_TatMash1 construct was confirmed to be the correct sequence. It was found that the final pEXP5_TatMash1GFP construct contained an isoleucine to valine point mutation at amino acid #390 within the *GFP* sequence. While this construct would not have been suitable for experimentation, it was used for an initial evaluation of the IVT system.

The Pierce IVT reactions were setup according to manufacturer's recommendations. All reactions were performed in the recommended tube setup where the outer tube contained 1X dialysis buffer prepared in nuclease-free water. For the HeLa IVT kit, each 100µL reaction consisted of 50µL HeLa lysate, 10µL accessory proteins, 20µL reaction mix, 8µL 0.5µg/µL plasmid DNA, and 12µL nuclease-free water. The HeLa IVT kit was also tried with half of the plasmid DNA in the mix above being replaced by the 281-EL2 reporter vector to see if the promoter-reporter system could be activated in the IVT reaction. All reactions were incubated at 30ºC for 24 hours without mixing.

Expressway *E. coli* IVT reactions were also performed according to manufacturer's recommended parameters. Each 50uL reaction contained 20µL *E. coli* slyD extract, 25µL 2X reaction buffer, 1.25µL 50mM amino acids without methionine, 1µL 75mM methionine, 1µL T7 enzyme mix, 1µL of 1µg/µL plasmid DNA, and 0.75µL nuclease-free water. Reactions were incubated at 30ºC and 300RPM for 30 minutes at which time 50µL of 1X feed buffer were added. The feed buffer master mix contained 100µL IVPS Feed Buffer, 6µL 50mM amino acids, 4µL75mM methionine, and 90µL nuclease-free water. Reactions were incubated at 30ºC and 300RPM 5.5 additional hours at which time they were stored at 4ºC awaiting SDS-PAGE.

Production yields from all IVT reactions were assessed using anti-Myc western blotting following SDS-PAGE. HeLa IVT reactions were centrifuged for 5 minutes at 10,000 RCF; insoluble pellets were discarded and the soluble supernatant was transferred to a fresh tube for analysis. Expressway reactions were sampled for a "whole lysate" analysis then also centrifuged at 10,000 RCF to remove soluble fraction for analysis.

3.4.   Results

3.4.1.   Transient expression of Mash1, Lmx1a, and Nurr1

Recombinant transcription factors were expressed by the transient transfection of HEK 293F suspension cells. While the pSecTag2a base expression vector contained an IgK signal peptide to facilitate recombinant protein secretion, it was critical to determine if the produced transcription factors were secreted into the extracellular medium. Past Fishman Laboratory experience expressing Tat-NeuroD2 and Tat-NeuroD2-GFP with the pSecTag2a vector indicated that expressed NeuroD2 was translocated to the nucleus and not secreted despite the presence of the secretion signal (Gillmeister, 2009).   This phenomenon was observed for all expressed transcription factors; a representative image for Tat-Mash1-GFP is provided below along with a representative image of a comparator secreted protein (Figure 3.2).
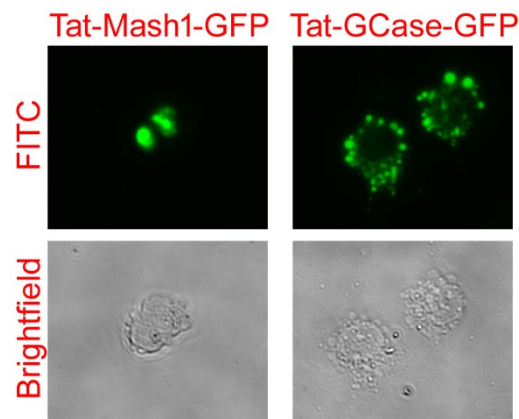
Figure 3.2: Transcription factors expressed in HEK 293F cells are translocated to the nucleus and not secreted. Tat-Mash1-GFP fluorescence is found almost exclusively in the nucleus of producer cells. Tat-GCase-GFP is a recombinant enzyme expressed and secreted in HEK 293F producer cells using the pSecTag2a vector (P. Gramlich Thesis Chapter 4). Images were taken using the Zeiss Axiovert 40 CFL microscope and 20X objective.   Exposure times for the images were 372ms and 2000ms respectively for Tat-Mash1-GFP and Tat-GCase-GFP.

Equal volumes of cell-free medium, soluble lysate, and insoluble lysate were run on 4-12% SDS-PAGE gels to determine the fraction containing the majority of the final product. The soluble and insoluble lysates were ~4x more concentrated than the cell-free medium. Overall, the vast majority of produced protein was found in the insoluble lysate. Detectable signal in the cell-free medium was not observed for Tat-Lmx1a, Tat-Lmx1a-GFP, or Tat-Mash1. At higher western blot exposure times, some Tat-Mash1-GFP was found in the cell-free medium although it was insignificant compared to even the quantity found in the soluble lysate (data not shown). Small quantities of each transcription factor were observed in the soluble lysate, with the maximum amount observed at day 2. While observable, the amount of soluble protein was far less than the insoluble protein. Total production was much higher for Mash1 compared to Lmx1a; the Lmx1a western blot is a 30 second exposure while the Mash1 western blot is a brief 1 second exposure (Figure 3.3).
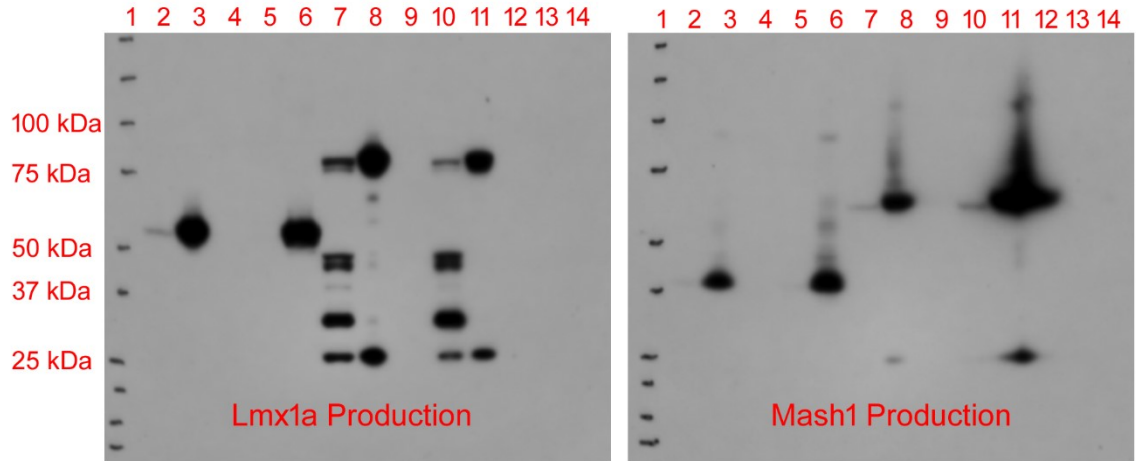
Lane Description:

1.	Precision Plus Standard	8.	GFP, Insoluble Lysate Day 2
2.	Soluble Lysate, Day 2	9.	GFP, Cell-Free Medium, Day 3
3.	Insoluble Lysate, Day 2	10.	GFP, Soluble Lysate, Day 3
4.	Cell-Free Medium, Day 3	11.	GFP, Insoluble Lysate, Day 3
5.	Soluble Lysate, Day 3	12.	Negative Cell-Free Medium, Day 3
6.	Insoluble Lysate, Day 3	13.	Negative Soluble Lysate, Day 3
7.	GFP, Soluble Lysate Day 2	14.	Negative Insoluble Lysate, Day 3

Figure 3.3: The majority of transiently expressed Mash1 and Lmx1a transcription factors was found in the insoluble fraction of the cell lysate. HEK 293F cells transiently transfected with pTagTat_Lmx1a, pTagTat_Lmx1a_GFP, pTagTat_Mash1, and pTagTat_Mash1_GFP were lysed with M-PER protein extraction reagent to harvest soluble lysate. Insoluble material was dissolved in the concentrated sample loading buffer. Cell-free medium, soluble lysate, and insoluble lysate samples were run on 4-12% Bis-Tris gels and analyzed by anti-Myc epitope tag western blotting. The westerns above are not the same exposure time; Lmx1a exposure time was 30 seconds while Mash1 exposure time was 1 second. Samples labeled "GFP" refer to the Tat-Lmx1a/Mash1-GFP variant. Expected sizes are: Tat-Mash1= 33.6 kDa, Tat-Mash1-GFP= 60.5 kDa, Tat-Lmx1a= 50.9 kDa, and Tat-Lmx1a-GFP= 77.8 kDa.

Tat-Nurr1 and Tat-Nurr1-GFP expressed at too low a level to support any experimentation. Even with a 10 minute western blot exposure time, only relatively light bands were observed in the insoluble fraction of Tat-Nurr1 and Tat-Nurr1-GFP. HEK 293F cells expressing Nurr1 were harvested after 2 days in an attempt to maximize any

soluble protein although none was observed. The limited quantity of protein expressed

was all found in the insoluble lysate (Figure 3.4).

Lane Description:

1. Precision Plus Standard
2. Tat-Nurr1 Soluble, Day 1
3. Tat-Nurr1 Insoluble, Day 1
4. Tat-Nurr1 Medium, Day 2
5. Tat-Nurr1 Soluble, Day 2
6. Tat-Nurr1 Insoluble, Day 2
7. Tat-Nurr1-GFP Soluble Day 1
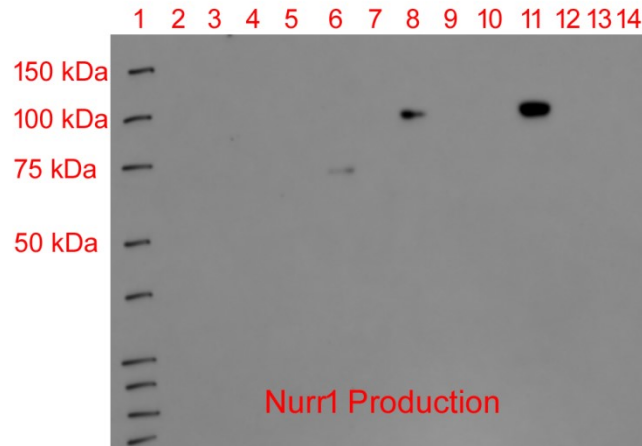
8. Tat-Nurr1-GFP Insoluble Day 1
9. Tat-Nurr1-GFP Medium, Day 2
10. Tat-Nurr1-GFP Soluble, Day 2
11. Tat-Nurr1-GFP Insoluble, Day 2
12. Negative Control Medium, Day 2
13. Negative Control Soluble, Day 2
14. Negative Control Insoluble, Day 2

Figure 3.4: Tat-Nurr1 and Tat-Nurr1-GFP expressed poorly and were found only in the insoluble lysate. HEK 293F cells were transiently transfected with pTagTat_Nurr1 and pTagTat_Nurr1_GFP. Equal volumes of cell-free medium, soluble lysate, and insoluble lysate were loaded on 4-12% Bis Tris SDS-PAGE gels and analyzed for production using anti-myc western blotting. The film exposure time for the western blot was 10 minutes; the long exposure time was necessary to observe any signal at all. Expected sizes were Tat-Nurr1= 74.7 kDa and Tat-Nurr1-GFP= 101.7 kDa.

3.4.2. Transcription factor purification

The insoluble fractions of the cell lysate for Tat-Lmx1a and Tat-Lmx1a-GFP were

solubilized in 1mL 1X PBS containing 8M Urea per 0.1g wet insoluble pellet. The

purification input is shown for the two proteins respectively in lanes 3 and 12 (Figure 3.5).

Almost all of the purified protein was found in Elution #1 with very little observed loss in the flow-through or washes. Purification efficiency appeared to be higher for Tat-Lmx1a-GFP compared to Tat-Lmx1a. Purification samples were also run on 4-12% Bis Tris gels and subjected to Simply Blue Safestain but the method was not sensitive enough to detect bands for the proteins of interest.
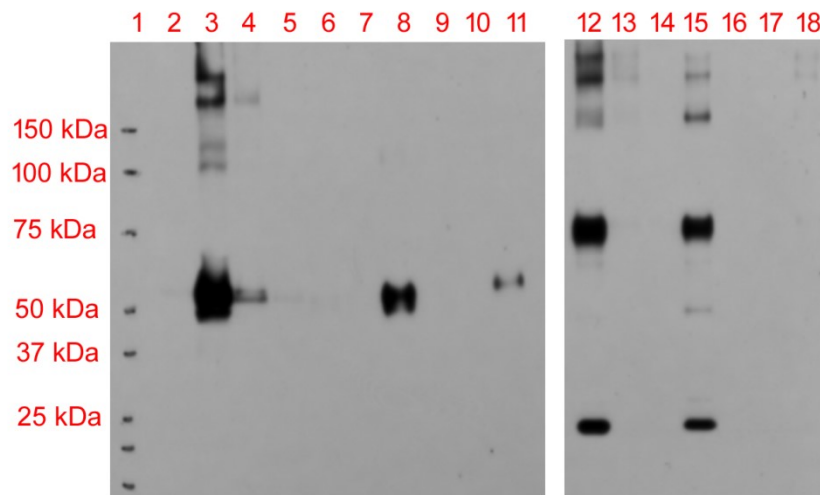
Lane Description:

1. Precision Plus Standard
2. Tat-Lmx1a Soluble Lysate
3. Tat-Lmx1a Insoluble Lysate
4. Tat-Lmx1a Flow-Through
5. Tat-Lmx1a Wash 1
6. Tat-Lmx1a Wash 2
7. Tat-Lmx1a Wash 4
8. Tat-Lmx1a Elution 1
9. Tat-Lmx1a Elution 2

10. Tat-Lmx1a Elution 3
11. Tat-Lmx1a Elution 4
12. Tat-Lmx1a-GFP Insoluble Lysate
13. Tat-Lmx1a-GFP Flow-Through
14. Tat-Lmx1a-GFP Wash 1
15. Tat-Lmx1a-GFP Elution 1
16. Tat-Lmx1a-GFP Elution 2
17. Tat-Lmx1a-GFP Elution 3
18. Tat-Lmx1a-GFP Elution 4

Figure 3.5: Purification of Tat-Lmx1a and Tat-Lmx1a from the insoluble fraction of the cell lysate. Frozen cell pellets from HEK 293F cells transiently transfected with pTagTat_Lmx1a and pTagTag_Lmx1a_GFP and harvested at day 3 were thawed, lysed with MPER protein extraction reagent, and the insoluble material was dissolved in 1X PBS pH = 7.4 containing 8M Urea. Equal volumes of selected purification samples were run on 4-12% Bis Tris SDS-PAGE gels and assayed with anti-myc western blotting. The blots shown above are 30 second exposures.

The insoluble lysates containing Tat-Mash1 and Tat-Mash1-GFP were purified using the HisPur Ni-NTA resin and purification samples were analyzed. The anti-myc westerns indicated that while all elutions contained some Tat-Mash1 or Tat-Mash1-GFP, significant protein was lost in both the flow-through and the first wash. The amount of protein lost relative to the amount of protein in the final elutions was greater for Tat-Mash1 compared to Tat-Mash1-GFP. Initial input samples were very bright and not included in Figure 3.6 (Figure 3.3). Due to signal intensity, experimentation was performed with Tat-Mash1 elutions 1 and 3 and Tat-Mash1-GFP elutions 1-3.

Lane Description:

1. Precision Plus Standard
2. Tat-Mash1 Flow-Through
3. Tat-Mash1 Wash 1
4. Tat-Mash1 Wash 3
5. Tat-Mash1 Elution 1
6. Tat-Mash1 Elution 2
7. Tat-Mash1 Elution 3
8. Tat-Mash1 Elution 4
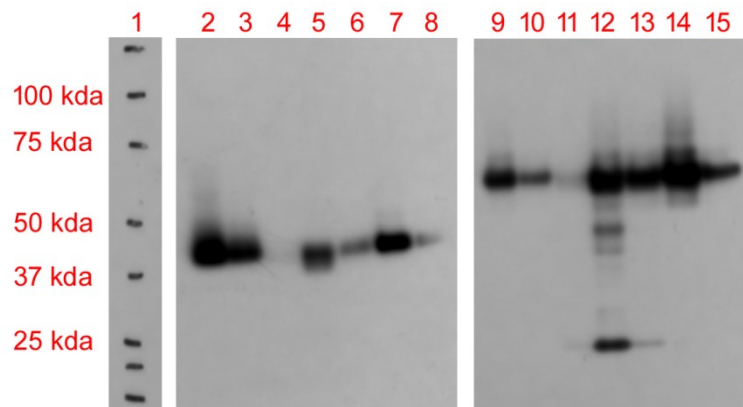
9. Tat-Mash1-GFP Flow-Through
10. Tat-Mash1-GFP Wash 1
11. Tat-Mash1-GFP Wash 3
12. Tat-Mash1-GFP Elution 1
13. Tat-Mash1-GFP Elution 2
14. Tat-Mash1-GFP Elution 3
15. Tat-Mash1-GFP Elution 4

Figure 3.6: Purification of Tat-Mash1 and Tat-Mash1-GFP from the insoluble fraction of the cell lysate. HEK 293F cells transfected with pTagTat_Mash1 and pTagTat_Mash1_GFP were harvested after 3 days and frozen until cell lysis. Equal volumes of purification fractions were run on 4-12% Bis Tris SDS-PAGE gels and analyzed by anti-myc western blotting. The exposure time for the blots shown above was very short, approximately one second.

3.4.3. Tat-Lmx1a-GFP is delivered to the nucleus following protein transduction and photochemical internalization

After production, transcription factor functionality was assessed. Unlike enzymes where protein functionality is assessed using relatively straightforward enzyme assays, transcription factor function cannot be assaying using a simple well-controlled cell-free *in vitro* system. During production, it was clear that the majority of Tat-Lmx1a-GFP or Tat-Mash1-GFP was translocated to the nucleus. As a result, the first question we aimed to answer is whether purified Tat-Lmx1a-GFP and Tat-Mash1-GFP were transported to the nucleus following protein transduction and photochemical internalization (PCI).

For both Tat-Lmx1a-GFP and Tat-Mash1-GFP, NPCs were treated with 1μg/mL purified protein for 18 hours. Tat-GFP was included in both experiments as a control for cytosolic localization following PCI. The first experiment using Tat-Lmx1a-GFP and Tat-GFP gave the clearest result. Before PCI, GFP signal was punctate for both proteins while four hours after PCI, Tat-GFP signal was distributed throughout the cell while Tat-Lmx1a signal was localized to the nuclear compartment (Figure 3.7). This same experiment was performed for Tat-Mash1-GFP but results were far less clear. While after PCI, Tat-GFP was located throughout the cytosol, Tat-Mash1-GFP distribution was heterogeneous. Furthermore, protein precipitation at higher concentrations made effective qualitative comparisons more difficult.
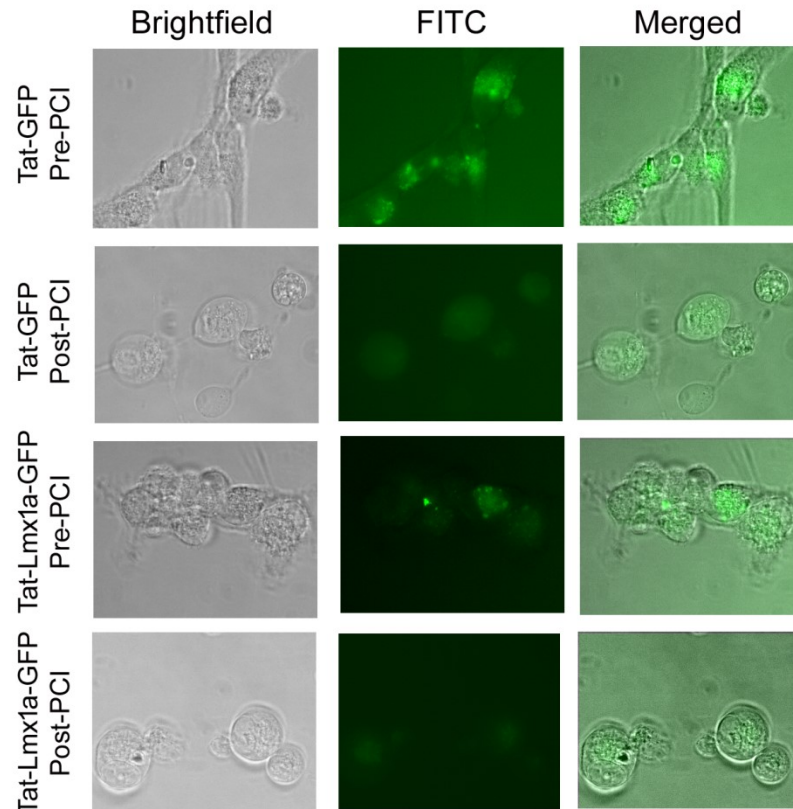
Figure 3.7: Qualitative comparison of Tat-Lmx1a-GFP and Tat-GFP intracellular distribution before and after photochemical internalization. Following 18 hours of protein treatment with 1µg/mL purified Tat-Lmx1a-GFP or Tat-GFP, cells were washed, incubated for four hours in photosensitizer-free medium, and treated with light at 20% maximum intensity for 60 seconds to mediate PCI. Several representative images were taken before and after PCI to determine the distribution of GFP signal. 400X fluorescent images were taken with a Zeiss AxioCam MRm monochrome camera (1.3 megapixel, 12 bits/pixel) using the C-Apochromat 40x/1.2 W Korr objective.

3.4.4. Promoter/Reporter assays to test functionality of transcription factors delivered by co-transfection

Promoter/reporter vectors provided the most straightforward test of recombinant transcription factor functionality. Using the 281-EL2 Mash1 reporter vector and the DAT-A Lmx1a reporter vector, transcription factor functionality was assessed in 3T3 fibroblasts and SK-N-BE(2)C neuroblastoma cells. Before any recombinant protein was delivered,

transcription factor was delivered by co-transfection with the reporter vector. Initially, 3T3 fibroblasts were transfected with vectors for *Tat-Mash1*, *Tat-Mash1-GFP*, *Tat-Lmx1a*, and *Tat-Lmx1a-GFP* and the appropriate reporter vector and luciferase expression was assayed 48-72 hours later. Tat-Mash1 was found to clearly induce luciferase expression, with average increases over the background of 2.39-2.79 fold after 48-72 hours. Conversely, Tat-Mash1-GFP did not convincingly induce luciferase expression. With co-transfection of *Tat-Mash1-GFP* and 281-EL2, luciferase production increased 0.76-1.39 fold after 48-72 hours. Neither Tat-Lmx1a nor Tat-Lmx1a-GFP induced luciferase expression over the background value in 3T3 cells. In fact, the transfection of *Lmx1a* inhibited luciferase expression in 3T3 cells. After 72 hours, *Tat-Lmx1a* and *Tat-Lmx1a-GFP* transfected 3T3 cells expressed luciferase 0.41X and 0.17X background levels respectively (Figure 3.8).
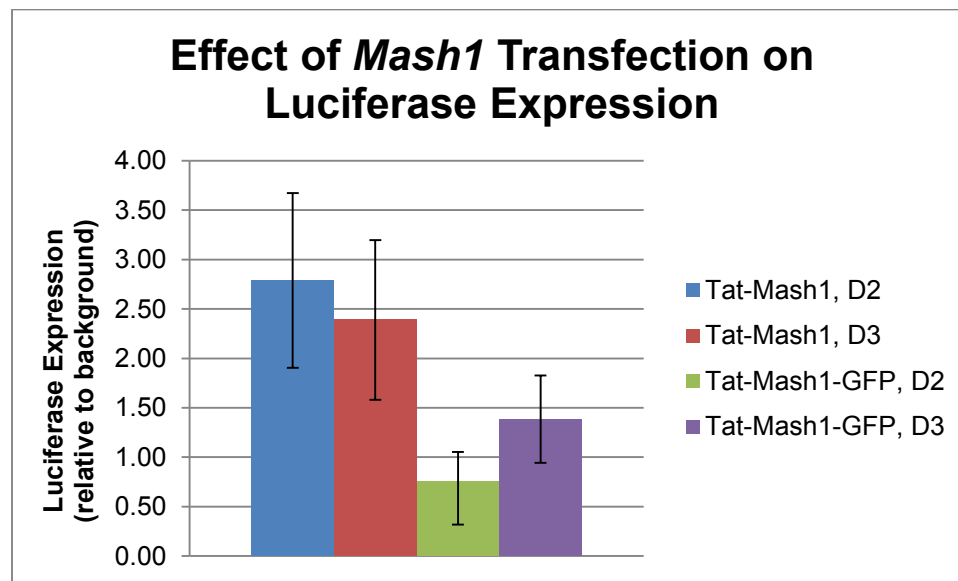
Figure 3.8: Induction of luciferase expression from Mash1 reporter vector 281-EL2 when 3T3 fibroblasts were co-transfected with pTagTat_Mash1 or pTagTat_Mash1_GFP. Following transfection, 3T3 cells were maintained at 37ºC and 5% CO2 for 48-72 hours at which time luciferase expression was analyzed. The data in the chart above represents triplicate data points repeated twice for the day 2 values and three times for the day 3 values. Error bars (standard error) show that while trends were reproducible, specific data points exhibited variability.

To test whether Tat-Lmx1a and Tat-Lmx1a-GFP were not functional or whether the DAT-A promoter/reporter vector functioned in a cell type-specific manner, all four transcription factor expression vectors were co-transfected with the appropriate reporter vectors in SK-N-BE(2)C neuroblastoma cells. This was the cell line used in the paper where the DAT-A vector was described (Chung et al., 2012). In the SK-N-BE(2)C cells, Tat-Mash1 and Tat-Mash1-GFP induced reporter expression 1.88X and 1.65X over the background value. Tat-Lmx1a and Tat-Lmx1a-GFP also induced luciferase expression 4.91X and 3.34X respectively. This experiment clearly showed that the DAT-A reporter vector must be used with the SK-N-BE(2)C cell line while 281-EL2 is likely less cell-type specific (Figure 3.9).
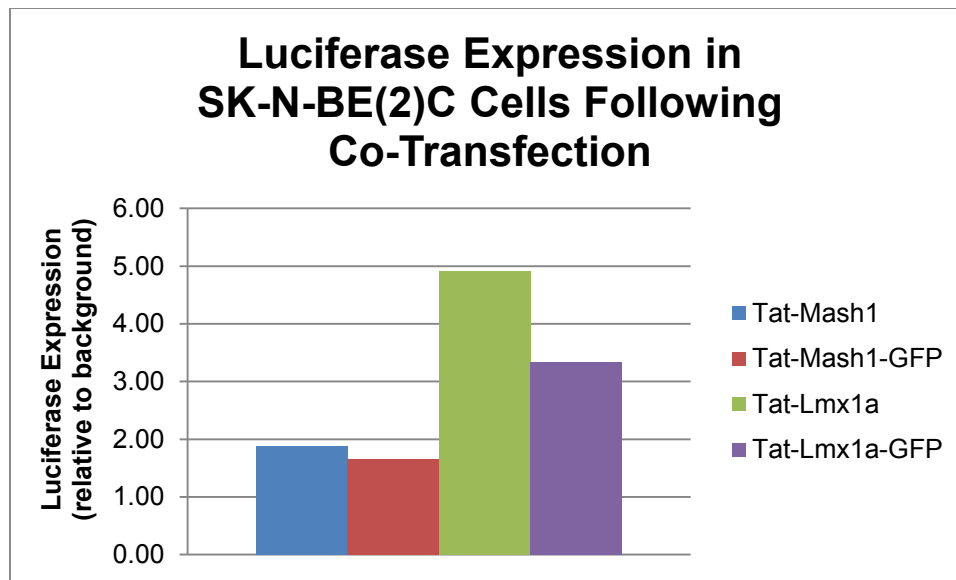
Figure 3.9: Induction of luciferase expression 48 hours after the co-transfection of SK-N-BE(2)C cells with transcription factor expression vectors and promoter/reporter vectors. Following transfection, cells were maintained at 37ºC and 5% $CO2$ for 48 hours at which time luciferase expression was analyzed using the Perkin-Elmer Britelite Plus kit. All data points in the above chart represent the average of triplicate samples; the experiment was performed once.

3.4.5. Direct protein treatment of 281-EL2 reporter vector-transfected 3T3 cells to test Tat-Mash1 and Tat-Mash1-GFP functionality

Co-transfection of 3T3 cells with 281-EL2 and with pTagTat_Mash1 or pTagTat_Mash1_GFP indicated that while Tat-Mash1 was able to induce reporter expression, Tat-Mash1-GFP was not. As a result, the functionality of Tat-Mash1 was confirmed while the functionality of Tat-Mash1-GFP was called into question. The next set of experiments aimed to determine whether, when delivered directly, protein Tat-Mash1 could induce luciferase expression in 281-EL2 transfected 3T3 cells.

Both experiments were conducted using identical procedures with the exception of the protein treatment step. In the first experiment, 1 μg/mL Tat-Mash1 or Tat-Mash1-GFP purified from the insoluble lysate were added to 281-EL2 transfected 3T3 cells. The protein treatment conditions were not found to increase luciferase expression; in fact luciferase expression was observed to be slightly lower than the baseline with protein treatment (Figure 3.10).
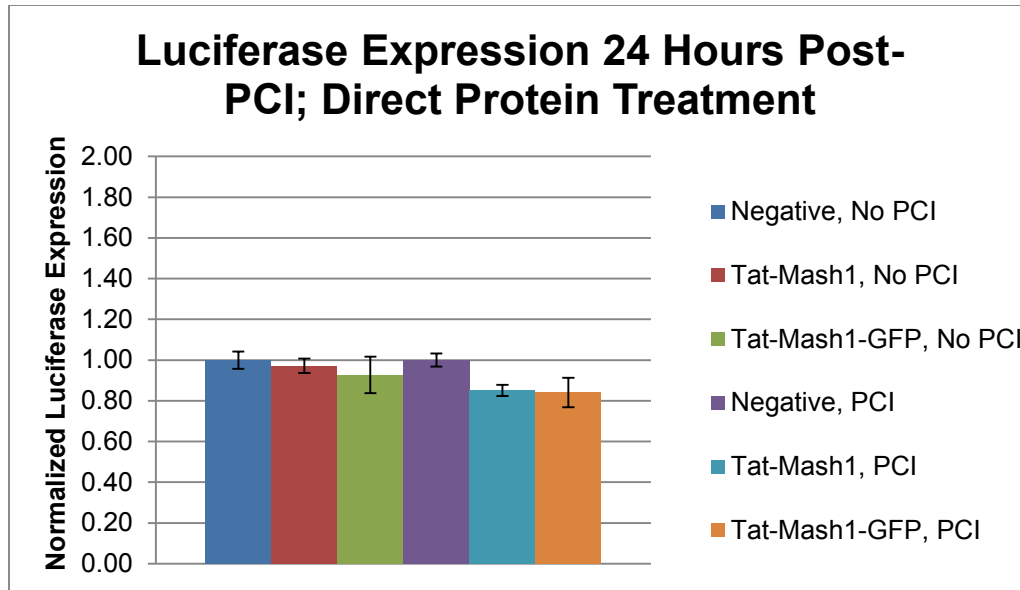
Figure 3.10: Reporter gene expression following the treatment of 281-EL2 transfected 3T3 cells with purified Tat-Mash1 or Tat-Mash1-GFP. 3T3 fibroblasts were transfected with reporter vector 281-EL2 and 24 hours later treated with 1 µg/mL Tat-Mash1 or Tat-Mash1-GFP. Following the 18 hour protein treatment, cells were washed for 4 hours and light treatment was performed (for half of the samples). Luciferase expression was assayed 24 hours after PCI. All data points above represent the average of duplicate samples with data normalized to the untreated control. PCI decreased baseline luciferase expression across the board; the PCI-treated untreated control had 38.1% the luciferase activity of the untreated control without PCI.

The results of the first experiment raised major questions regarding whether the proteins purified from the insoluble fraction of the lysate were functional. As a result, the experiment was repeated with soluble lysates harvested by freeze-thawing producer cells in 1X PBS pH = 7.4 so the soluble lysate could be directly added to 3T3 fibroblast medium. Unlike in the first experiment, Tat-Mash1 and Tat-Mash1-GFP treated wells had slightly higher luciferase expression than the negative controls. Without PCI, results were variable, but with PCI, Tat-Mash1 and Tat-Mash1-GFP both gave 16-19% higher luciferase expression. While this value is somewhat consistent with co-transfection data for Tat-Mash1-GFP delivery, it is not consistent with co-transfection data for Tat-Mash1 delivery.

Overall, while the soluble protein may have led to a small increase in reporter expression with PCI, increases were not of the same magnitude seen when transcription factors were delivered by co-transfection.
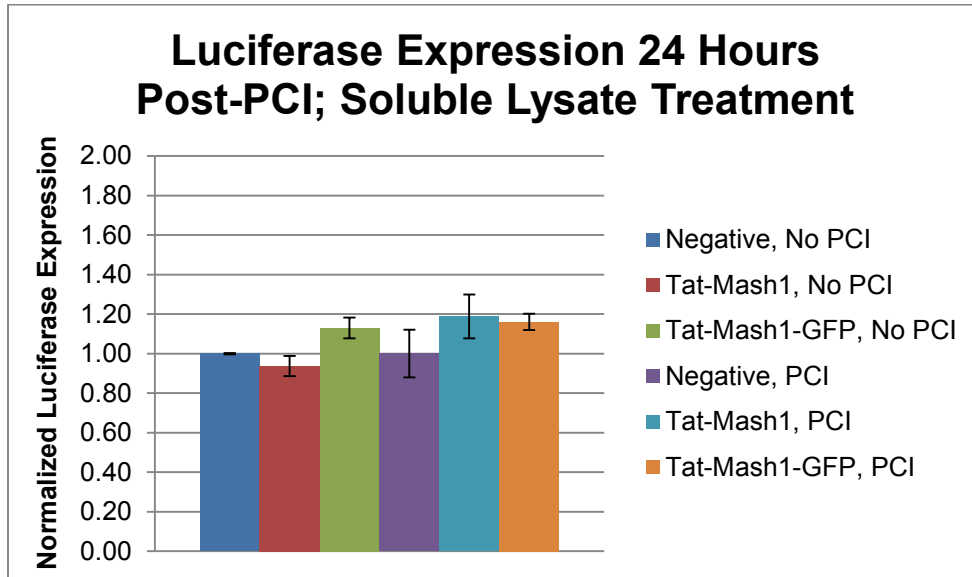
Figure 3.11: Reporter gene expression following the treatment of 281-EL2 transfected 3T3 fibroblasts with soluble lysate of HEK 293F producer cells containing either Tat-Mash1 or Tat-Mash1-GFP. 3T3 cells were treated with 25% soluble lysate and 75% 3T3 medium containing only 4% FBS. All data is reported as the average of duplicate conditions, normalized to the appropriate untreated control. PCI decreased baseline luciferase expression in the negative controls; the untreated control subjected to PCI had 34.4% of the baseline luciferase expression of the control on which PCI was not performed.

3.4.6. Production of soluble Tat-Mash1 and Tat-Mash1-GFP using *in vitro* translation

Commercially available *in vitro* translation (IVT) systems were pursued for the production of Tat-Mash1 and Tat-Mash1-GFP in an attempt to improve protein solubility during production to yield a much higher concentration of soluble product. Two commercially-available systems were assessed, the One-Step High Yield IVT Kit (Pierce)

using HeLa cell lysate and the Expressway Cell-Free Expression System (Invitrogen) using

E. coli cell lysate.

The mammalian lysate system yielded excellent soluble expression of both Tat-Mash1 and Tat-Mash1-GFP at the expected sizes. The majority of the produced protein was soluble (Figure 3.12). Furthermore, far more soluble protein was produced than through the transient transfection of HEK 293F cells (Figures 3.3, 3.12). In an additional experiment, the 281-EL2 reporter vector was added to the IVT reaction as well to determine if soluble protein could induce luciferase expression. No luciferase induction was observed; this could very well be due to the absence of coactivators (data not shown).
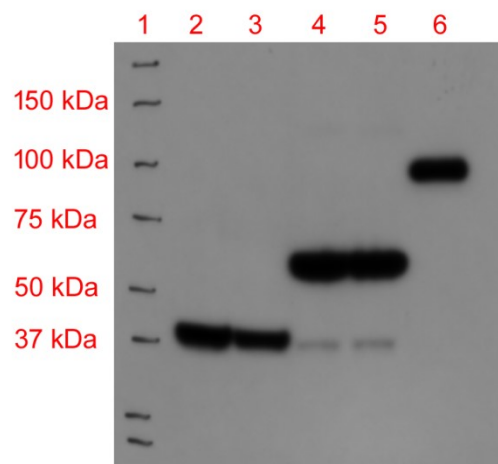
Lane Description:

1. Precision Plus Standard
2. Tat-Mash1, Total IVT Reaction
3. Tat-Mash1, Soluble IVT Fraction

4. Tat-Mash1-GFP, Total IVT Reaction
5. Tat-Mash1-GFP, Soluble IVT Fraction
6. Tat-GCase-GFP Western Control

Figure 3.12: Expression of soluble Tat-Mash1 and Tat-Mash1-GFP using a HeLa cell lysate *in vitro* translation system. At the conclusion of the IVT reactions, a sample of the whole reaction was taken (total IVT), and the remaining reaction was centrifuged. The supernatant was removed to yield the soluble fraction. Equal volumes of both the total reaction and soluble fraction were loaded onto 4-12% Bis Tris SDS-PAGE gels for each of Tat-Mash1 and Tat-Mash1-GFP. The anti-myc western blot shown above was a 3 second exposure to film.

The *E. coli* IVT system had significantly less overall and soluble protein production. While most of the protein was soluble in the HeLa IVT system (Figure 3.12), the majority of Tat-Mash1 and Tat-Mash1-GFP produced in the Expressway system was removed with centrifugation after the IVT reaction was concluded. Tat-Mash1-GFP appeared to express in a full-length form but there were numerous truncated products observed on the anti-myc western blot (Figure 3.13).
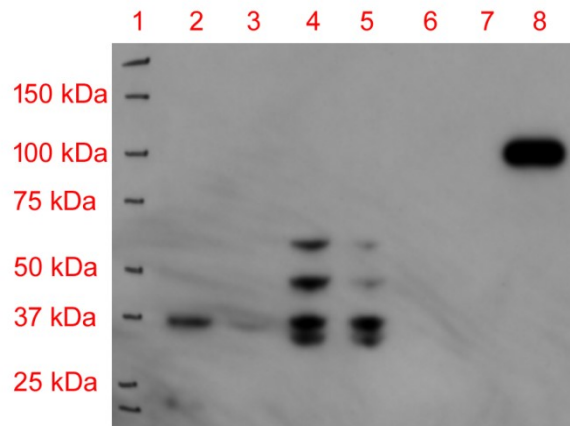
Lane Description:

1. Precision Plus Standard
2. Tat-Mash1, Total IVT Reaction
3. Tat-Mash1, Soluble IVT Fraction
4. Tat-Mash1-GFP, Total IVT Reaction
5. Tat-Mash1-GFP, Soluble IVT Fraction
6. Negative, Total IVT Reaction
7. Negative, Soluble IVT Reaction
8. Tat-GCase-GFP Western Control

Figure 3.13: Expression of Tat-Mash1 and Tat-Mash1-GFP using the Expressway *E. coli in vitro* translation system. Equal volumes of the total IVT reaction and the soluble fraction of the IVT reaction were run on a 4-12% Bis Tris SDS-PAGE gel and analyzed by anti-myc western blotting. The western blot shown above was a 10 second exposure to film.

3.5. Discussion

The goal of the research presented in this chapter, to design, express, and purify transcription factors to mediate neuronal differentiation through direct protein treatment,

was not accomplished. Although numerous factors contributed to this goal not being met, the low expression of soluble and/or functional protein, and the efficiency of protein delivery, were the most glaring. Neuronal differentiation via genetic approaches is an already inefficient process made even more difficult by low protein delivery and quality. The results presented in sections 3.4.1 to 3.4.6 clearly point out the flaws in the transcription factor production methods employed. A method to produce high levels of soluble Tat-Mash1 and Tat-Mash1-GFP was identified: the HeLa cell lysate IVT system. Despite the failure to demonstrate purified transcription factor functionality, this chapter provides a framework that could be used in the future development of a protein-based neuronal differentiation procedure and contains significant results.

Mammalian expression vectors for Tat-Mash1, Tat-Mash1-GFP, Tat-Lmx1a, Tat-Lmx1a-GFP, Tat-Nurr1, and Tat-Nurr1-GFP were designed using pSecTag2a. Proteins were expressed via the transient transfection of HEK 293F suspension cells. Bacterial expression was not explored for Mash1, Lmx1a, or Nurr1 as a result of past issues expressing transcription factors in bacteria in the Fishman laboratory. Tat-NeuroD2 was not expressed in a full length form (Gillmeister et al., 2009) and Tat-Lmx1a was totally insoluble once 8M urea was removed (Fishman Lab, unpublished data). During the expression work, Tat-Mash1-GFP and Tat-Lmx1a-GFP were observed only in the nucleus of producer cells, despite the presence of the signal peptide (Figure 3.2). This same phenomenon was observed during the expression of Tat-NeuroD2-GFP (Gillmeister et al., 2009). The vast majority of expressed Tat-Mash1, Tat-Mash1-GFP, Tat-Lmx1a, and Tat-Lmx1-GFP was found in the insoluble fraction of the HEK 293F producer cell lysate (Figure 3.3). Tat-Nurr1 and Tat-Nurr1-GFP expressed at very low levels insufficient for

any experimentation (Figure 3.4). Mash1 soluble protein production was better than Lmx1a but the insoluble protein fraction still contained the majority of the final product. Insoluble proteins were solubilized using 8M urea-containing buffers and purified by Ni-NTA affinity chromatography. Purified Tat-Lmx1a and Tat-Lmx1a-GFP were concentrated in single elutions (Figure 3.5). Tat-Mash1 and Tat-Mash1-GFP purification yields were much higher compared to Lmx1a, with purified protein distributed over several elutions (Figure 3.6).

We hypothesized that the transcription factor insolubility was directly related to the translocation of the factors to the producer cell nucleus. In the nucleus, the transcription factor could bind DNA and interact with other factors creating complexes that could fall out of solution upon cell lysis. One potential approach to improve solubility could be to inhibit nuclear importation pathways during protein production. Importazole (2,4-diaminoquinazoline) is a small molecular inhibitor of the importin-β nuclear importation pathway (Soderholm et al., 2011). Preliminary data showed that importazole addition did not improve soluble protein production. Additionally, overall protein production was inhibited with increased importazole concentrations (Fishman Lab, unpublished results). However, with further development, inhibition of nuclear importation could be a strategy to improve transcription factor solubility.

Initially, the ability of Tat-Mash1-GFP and Tat-Lmx1a-GFP to translocate to the cell nucleus following protein transduction and photochemical internalization was assessed. Nuclear transport of transcription factor after release from endosomes would not have been a confirmation of protein functionality, but it would have been a promising observation. Nuclear importation has been used to test transcription factor functionality in

published literature (Tachikawa et al., 2004). While Tat-Lmx1a-GFP was found in the nucleus 4 hours after PCI, Tat-Mash1-GFP was not. Promoter/reporter assays were chosen as a relatively straightforward approach to quantitatively test transcription factor function, and had been used previously by other labs (Koya et al., 2008; Lan et al., 2014). When 3T3 cells were co-transfected with the appropriate reporter construct, only Tat-Mash1 was reproducibly able to induce reporter gene expression. Tat-Mash1-GFP was not able to induce luciferase expression in 3T3 cells (Figure 3.8). However, it was able to induce reporter expression in SK-N-BE(2)C cells (Figure 3.9). As a result, while GFP appears to reduce the activity of Tat-Mash1, it does not totally eliminate it. Tat-Lmx1a and Tat-Lmx1a-GFP were only able to induce luciferase expression from the DAT-A reporter vector using the SK-N-BE(2)C cells, indicating that promoter/reporter system activation was cell-type specific (Figure 3.9).

Purified transcription factor function was tested using Tat-Mash1 due to the much higher expression level compared to Tat-Lmx1a or Tat-Lmx1a-GFP. Two protein delivery approaches were attempted with Tat-Mash1 to reproduce co-transfection results, but neither was able to do so effectively (Figures 3.10, 3.11). Comparing the two experiments, the treatment of 3T3 cells with soluble lysate delivered more promising results, where it appeared protein treatment may have increased reporter expression. While the increases observed were small, this result further brought doubt to the functionality of transcription factors purified from the insoluble fraction of the cell lysate.

It became clear that to successfully generate neurons using a protein-delivery based approach, we would need large quantities of soluble transcription factors. Our hypothesis was that protein insolubility was due, at least in part, to the nuclear importation of the

protein following production. Since pilot work with small molecule inhibition of nuclear importation was not promising, we next aimed to remove the nucleus from the production system altogether using *in vitro* translation systems. While *in vitro* translation systems are much more expensive methods to produce protein and not nearly as scalable as transient transfection, they were the most direct way to test the hypothesis. Furthermore, two new commercially available *in vitro* translation systems looked especially promising, advertising the potential to produce milligram quantities of protein. The Expressway Cell-Free IVT system (Invitrogen) used an *E. coli* cell lysate. While the Fishman Lab previously had poor luck with bacterial expression of transcription factors, a cell-free system had never been attempted. Furthermore, this *E. coli* lysate system was reasonably affordable advertised as capable of producing ~1mg protein for ~400 dollars. The One-Step Human High-Yield IVT Kit (Pierce) also reported the potential to make milligram quantities of protein. Although the projected cost was higher, at ~1mg for ~1100 dollars, mammalian cell lysate had a better chance of producing full-length, soluble transcription factors.

Appropriate Tat-Mash1 and Tat-Mash1-GFP expression vectors were created for each of the IVT systems using the pEXP5 and pT7CFE1 plasmids for the *E. coli* and HeLa lysate systems, respectively. IVT reactions were performed for each system and the HeLa cell lysate produced a much higher concentration of full length soluble protein (Figure 3.12). While the *E. coli* lysate did produce some full-length Tat-Mash1 and Tat-Mash1-GFP, overall yield was much lower and a portion of the expressed protein was insoluble. Furthermore, there were a number of myc-positive bands observed in the Tat-Mash1-GFP reaction, indicating expression of some truncated final products. The large-scale One-Step

Human High Yield IVT kit showed potential for the production of transcription factors for neuronal differentiation.

The available published literature describing the production of recombinant transcription factors is small, likely reflecting the considerable protein expression challenges described at length in this chapter. Published recombinant transcription factor delivery papers fall into one of two categories: the creation of protein induced pluripotent stem cells (piPSCs) and all other papers where gene expression or cell differentiation is modified for a variety of applications. The creation of piPSCs is the largest specific application of the technology and has been a valuable resource for better understanding the potential and limitations of transcription factor delivery.

Reprogramming CPP-linked transcription factors Oct4, Klf4, Sox2, and c-Myc have been expressed both in *E. coli* (Nemes et al., 2014; Pan et al., 2010; Zhou et al., 2009) and mammalian HEK 293 cells (Kim et al., 2009). Reports regarding solubility of the reprogramming factors were variable. The first report of piPSC generation used factors solubilized from the insoluble lysate and refolded them before purification (Zhou et al., 2009). Conversely, a recent paper did not mention any inclusion body production or denaturing purification conditions implying that *E. coli* expressed soluble protein (Nemes et al., 2014). The biological activity of transcription factors purified from the insoluble lysate has been disputed; Pan et al. found that recombinant reprogramming transcription factors they purified from inclusion bodies had minimal biological activity (Pan et al., 2010). There is no published work comparing the activity of transcription factors purified from both the soluble and insoluble fractions of the lysate. While there is some published work indicating that denatured Tat-linked proteins are refolded and active after cellular

100

uptake, this work did not directly involve transcription factors (Jin et al., 2001). One publication used soluble transcription factors produced in HEK 293 cells. Interestingly, they did not purify the factors, but only lysed the cells in a buffer appropriate for cell treatment. As a result, the transcription factor dose was not clear. While Kim et al. did not state the reasons for not purifying the transcription factor from the lysate, it very well could have been due to the insolubility of protein and low purification yields following traditional lysis methods (Kim et al., 2009). The approach used by Kim and colleagues is fairly similar to one of our approaches to deliver soluble Tat-Mash1 and Tat-Mash1-GFP (Figure 3.11).

The concentration of delivered protein was a major pitfall of our work; it is possible that for our Tat-Mash1 and Tat-Mash1-GFP delivery work, we needed a much higher treatment dose. The two successful publications describing piPSC generation with bacteria-expressed proteins used 8 μg/mL purified protein, 8x more that we were able to use (Zhou et al., 2009; Nemes et al., 2014). Pan et al. reported minimal biological activity for their purified factors; they treated with 40nM. For reference, 1 μg/mL Tat-Mash1 or Tat-Mash1-GFP would equal ~30nM or ~15nM respectively. It cannot be ruled out that poor activity observed in our work, and the work of Pan and colleagues, could have been due to low treatment doses. Despite the success by multiple laboratories in creating piPSCs, all report that protein-based methods are less efficient than viral methods, with one report giving iPSC generation efficiency at 0.001% of input cells for protein-based methods compared to 0.01% for genetic methods (Kim et al., 2009).

Aside from piPSC generation, most other transcription factor delivery work is spread over a number of fields. The first published report of direct protein delivery of a transcription factor involved the production of a soluble artificial transcription factor (ATF)

linked to a cell-penetrating peptide. The CPP-ATF was produced in *E. coli* and was extracted and purified in its soluble form. Following delivery of a high CPP-ATF dose of 500nM, VEGF-A expression was increased, indicating the factor was biologically active (Tachikawa et al., 2004). In 2008, soluble pancreatic homeobox-1 transcription factor Pdx1 was expressed in *E. coli*. No additional CPP was included as Pdx1 already contained a protein transduction domain. Using a promoter/reporter system, Koya et al. demonstrated that 1 μM Pdx1 was able to induce reporter expression similarly to lentiviral infection. *In vivo*, Koya and colleagues found that delivered Pdx1 could promote β-cell regeneration and differentiation of liver cells to insulin-producing cells (Koya et al., 2008).

Aside from the work of Tachikawa et al. and Koya et al., no additional transcription factor delivery papers were published until 2014, when several appeared. Estrogen-related receptor β (ESRRB) containing a R7 CPP was expressed as a soluble protein in *E. coli* and delivered to human mesenchymal stem cells at a 50 μg/mL dose. RT-PCR was used to confirm the increase in expression of several pluripotency markers with addition of the ESRRB protein (Jo et al., 2014). Tat-conjugated Nanog was expressed in *E. coli* and purified from the soluble lysate. While the protein was soluble at production, the treatment scheme implies there were solubility issues. The protein transduction procedure was atypical; protein-containing medium was incubated at 37C for two hours, centrifuged, and the precipitate free medium was filtered before protein transduction. Final Nanog-Tat concentration was 100nM but initial concentrations could have been much higher. Protein functionality was demonstrated two ways: the ability to bind a consensus DNA sequence and showing that treatment with Nanog-Tat was able to support ESC self-renewal independent of critical factor LIF (Peitz et al., 2014). In another example of recombinant

transcription factor delivery, TAZ was expressed in *E. coli* conjugated to an arginine-rich CPP. The recombinant TAZ was purified from the insoluble lysate and desalted; it was used to treat cells at a 100nM concentration without any specific refolding procedure. Activity of the CPP-TAZ was demonstrated *in vitro* through osteogenic differentiation of human mesenchymal stem cells and *in vivo* using a rabbit bone formation assay (Suh et al., 2014).

Two papers where protein delivery was used to promote transdifferentiation have been published. In the first, pancreatic acinar cells were transdifferentiated into insulin-positive cells. Tat-linked islet transcription factors Ngn3, Pdx1, and NeuroD/β2 were expressed in *E. coli* and purified from the insoluble lysate. After purification, proteins were dialyzed in a step-wise fashion to facilitate protein renaturation. Protein treatment with 1μM Tat-Pdx1 or Tat-NeuroD/β2 induced luciferase reporter gene expression 2X over a control. Also, and more importantly, rat acinar cell line AR42 was converted to insulin-positive cells after 3 days of treatment with all 3 factors (Lan et al., 2014).

In March 2015, the first paper employing transcription factors for neuronal transdifferentation was published. Recombinant Tat-Sox2 and Tat-Lmx1a, with a cocktail of small molecules, were used to transdifferentiate human foreskin fibroblasts to induced dopaminergic progenitor cells. The recombinant proteins were expressed in *E. coli* and purified from the insoluble lysate. Fibroblasts were transdifferentiated in a complex procedure involving seven 48 hour protein and small molecule-treatment cycles. In each treatment, cells were given 10 μg/mL of both Tat-Sox2 and Tat-Lmx1a. Although efficiency was not discussed in the manuscript, indicating that it may have been quite low, the induced dopaminergic progenitors were capable of expansion (Mirakhori et al., 2015).

3.6.   Conclusions

Although there has long been interest in protein-based neuronal differentiation, evidence that this is technically feasible has only been recently presented (Mirakhori et al., 2015), and even then, was aided by a cocktail of small molecules. Another substantial accomplishment in the direct delivery of transcription factors has been the creation of multiple piPSC lines. Despite the success, there were multiple drawbacks of the approach, particularly that piPSC generation is even less efficient than iPSC generation via genetic approaches. Beginning in 2014, successful transcription factor protein delivery has been accomplished in fields besides piPSC generation. However, these studies typically used very high protein concentrations and had relatively low efficiency. Most transcription factor expression literature indicates that protein solubility upon lysis is relatively poor and that purifying active transcription factor is a significant biotechnology challenge.

Many of the methods employed in this chapter have been used in the literature. Transcription factors have been purified from the insoluble lysate or added to cells in a crude soluble lysate. Both nuclear importation and promoter/reporter systems are tests for transcription factor functionality. Despite these approaches, the overall goal of this study was not achieved for two main reasons: biological activity of the proteins and the treatment dose. Both of these pitfalls can be potentially addressed by the described *in vitro* translation method used to successfully generate high concentrations of soluble protein. Although not particularly cost effective, *in vitro* translation likely represents the best method currently available for transcription factor production. IVT for transcription factor production has not been described or employed anywhere else in the literature. With efficient soluble production, this project could be revisited using many of the same methods attempted.

With more biologically active protein, the dose could be increased to 100 nM - 1 µM, the treatment concentrations where successful functional outcomes were typically observed. Creative approaches in protein expression and purification will be critical to achieving protein-based neuronal differentiation and potentially making these procedures as efficient as genetic methods.

Chapter 4: A Peptide Linked Recombinant Glucocerebrosidase for Targeted Neuronal Delivery: Design, Production, and Assessment

4.1.   Abstract

Although recombinant glucocerebrosidase (GCase) is the standard therapy for Gaucher's disease, the commonest inherited lysosomal storage disease, enzyme replacement is not effective when the central nervous system is affected. Linkage to a membrane binding peptide is a strategy to enhance neuronal uptake of proteins such as GCase, where the native protein is not well internalized by neurons. We created a series of recombinant genes/proteins where GCase was linked to different membrane binding peptides including the Tat peptide, the rabies glycoprotein derived peptide (RDP), the binding domain from tetanus toxin (TTC), and a tetanus-like peptide (Tet1). The majority of these proteins showed adequate expression in a mammalian producer cell line (HEK 293F), and most were secreted in soluble form into the media as predicted by the inclusion of a secretary domain.   Purified recombinant Tat-GCase and RDP-GCase showed similar GCase protein delivery to neuronal cells in culture and superior delivery to native GCase. This initial result was unexpected based on observations of superior protein delivery to neurons with RDP as a vector. A recombinant protein where a fragment of the flexible hinge region from IgA (IgAh) was introduced between RDP and GCase showed substantially enhanced GCase neuronal delivery (2.5 times over Tat-GCase), suggesting that the original construct resulted in interference with RDP's capacity to bind neuronal membranes. Incubation with both RDP-IgAh-GCase and Tat-GCase proteins for 18 hours resulted in a significant increase in GCase activity in a mutant neuronal cell line with little untreated GCase activity. This cell line also accumulates large amounts of the pathologic

Gaucher's disease lipid substrate glucosylsphingosine. Extended treatment of these mutant neuronal cells with either Tat-GCase or RDP-IgAh-GCase resulted in a >90% reduction in glucosylsphingosine content, approaching normal levels. RDP-IgAh-GCase, as well as Tat-GCase, merit study *in vivo* to assess their potential as treatment for neuronopathic forms of GD. Both peptide vectors are reported to also be capable of carrying a protein across the blood brain barrier, suggesting the possibility of avoiding invasive direct brain delivery.

*Chapter 4 is reproduced, in part, from a paper submitted for peer review. Permission information from the reviewing journal can be found on page 184.

4.2   Introduction

Nearly 35 years ago, the discovery that glycan engineering of glucocerebrosidase could target the enzyme efficiently to non-parenchymal liver cells facilitated the development of the first FDA-approved biologic for Gaucher's disease therapy. It was found that the exposure of terminal mannose residues on the N-glycans of glucocerebrosidase (GCase) dramatically increased enzyme targeting to macrophages (Busterbosch et al., 1996; Friedman et al., 1999; Furbish et al., 1981) due to their mannose-binding lectin (Stahl et al., 1978). This facilitated the practical application of enzyme replacement therapy for type 1 Gaucher's disease (GD). Gaucher's disease is an inherited lysosomal storage disease where homozygous mutations in the gene for glucocerebrosidase result in accumulation of glycosphingolipid substrates glucosylceramide and glucosylsphingosine. GD is classified by its three subtypes: non-neuronopathic type 1, acute neuronopathic type 2, and chronic neuronopathic type 3 (Branco Novo et al., 2012; Cabrera-Salazar et al., 2010; Lee et al., 2005).

In 1991, Ceredase (alglucerase, Genzyme Corp) became the first FDA-approved sequentially deglycosylated GCase (Branco Novo et al., 2012). Although Ceredase was purified from human placental tissue, three recombinant GCase enzymes have since been introduced for enzyme replacement therapy (ERT). All expose mannose-terminal residues on N-glycans using a variety of strategies. Cerezyme (imiglucerase, Genezyme) is produced in Chinese Hamster Ovary (CHO) cells and enzymatically deglycosylated to expose mannose residues like Ceredase. VPRIV (velaglucerase alfa, Shire) is a recombinant GCase produced in human fibroblast carcinoma cells and treated with mannosidase I inhibitor kifunesine during production to produce mannose terminal glycans. Finally, Elelyso (taliglucerase alfa, Protalix) is produced in carrot cells and targeted to storage vacuoles where mannose-terminal residues are exposed (Shaaltiel et al., 2007; Tekoah et al., 2013). The four N-glycosylation sites that are occupied in wild-type GCase are all occupied in the recombinant GCase enzymes (Brumshtein et al., 2010). Imiglucerase and taliglucerase alfa have an average glycan mass of 1160 daltons while velaglucerase alfa has an average glycan mass of 1790 daltons (Tekoah et al., 2013). The effect of mannose-chain length has been somewhat controversial, being reported to both have no effect on macrophage binding (Van Patten et al., 2007) and improve macrophage binding (Brumshtein et al., 2010).

Along with the recombinant enzyme therapies, two small molecule glucosylceramide synthase inhibitors have been approved for type 1 GD therapy. Zavesca (miglustat, Actelion Pharmaceuticals), was approved in 2002 for type 1 therapy when ERT is not an option (Ficicioglu et al., 2008; Pastores, 2010). Cerdelga (eliglustat, Genzyme) was FDA-approved in 2014 and has been shown to have similar efficacy to Cerezyme and

notably, does not have the unpleasant gastrointestinal and neurological side effects of Zavesca (Poole et al., 2014). Initially, there was hope that Zavesca could be useful for neuronopathic GD therapy. However, it was not shown to improve the neurologic symptoms of type 3 GD patients in a clinical trial (Schiffmann et al., 2008). Currently, no type 3 GD clinical trials are in progress for Cerdelga. Research has also focused on chaperones that can competitively bind glucocerebrosidase in the endoplasmic reticulum and improve lysosomal trafficking and enzyme activity. Isofagomine has shown neuronopathic GD therapeutic potential in a type 2 GD mouse model (Sun et al., 2011; Sun et al., 2012). While it has never been tested for neuronopathic GD, chaperone ambroxol could also have potential (Zimran et al., 2013). Genzyme has published data on a propriety small molecule GZ 161 that extended the life of type 2 GD mice (Cabrera-Salazar et al., 2012). Although ERT is the standard of care for GD therapy, small molecule therapeutics are valuable treatment options with potential for future growth.

Although three recombinant GCase enzymes and the two glucosylceramide synthase inhibitors are commercially available, all treat only the non-neuronopathic type 1 GD. None of these GCase enzymes will cross the blood brain barrier due to their size and the lack of mannose receptors on brain endothelia (Grubb et al., 2010), nor do they have any predicted preferential neuronal-targeting properties. Efficiency of uptake in neuronal cell lines is significantly less than in macrophages and has been shown to be variable based on the cell line used (Schueler et al., 2002). Currently, there is no available therapy for neuronopathic types 2 or 3 GD. As a result, there is a distinct need for an engineered recombinant GCase enzyme for neuronal delivery enabling the possibility of enzyme replacement therapy for types 2/3 GD, analogous to how glycan modification facilitated

the development of an enzyme for type 1 therapy. A neuron-targeted GCase would need to preferentially bind neurons and ideally, would cross the blood-brain barrier (BBB) increasing the options for therapeutic delivery.

There are a wide variety of peptide delivery vectors capable of facilitating the endocytosis of GCase in neurons. These peptides can be generally separated into two classes: receptor-independent peptides that lack cell type specificity and receptor-dependent peptides that have retained cell-type specificity. These delivery vectors also vary with additional parameters including their ability to cross the BBB and feasibility for use *in vivo*. The first category of receptor-independent peptides includes cell-penetrating peptides (CPPs) that have the ability to deliver proteins to any cell type (Reviews: Chauhan et al., 2007; Deshayes et al., 2005; Heitz et al., 2009; Zorko et al., 2005). While originally controversial, it is now widely accepted that these peptides are taken into cells through endocytosis. CPPs have been shown to deliver cargo proteins across the BBB (Schwarze et al., 1999) although this has been reported to be very low efficiency (Xia et al., 2001). While a large number of different CPPs exist, Tat, an 11 amino acid peptide originally derived from the transactivator protein of HIV (Tat), was the first to be described (Frankel et al., 1988) and remains one of the more widely used varieties. Tat is taken up by receptor-independent macropinocytosis and following uptake, most of the Tat-linked cargo protein is sequestered in endosomes (Chauhan et al., 2007; Gillmeister et al., 2011).

Tat has been used, in a limited capacity, to enhance the delivery of lysosomal enzymes *in vitro*. Types 1 and 2 Gaucher fibroblasts were treated with GCase-Tat resulting in approximately 4 and 10 fold more intracellular enzyme activity compared to control GCase, for types 1 and 2 fibroblasts respectively (Lee et al., 2005). Tat has also been

linked to another lysosomal enzyme, galactocerebrosidase (GALC), for delivery to a wider variety of cell types with variable results. Tat improved delivery to COS-7 cells ~1.5x compared to the control proteins. No improvement in GALC delivery was observed with primary fibroblasts and Tat decreased delivery of GALC to primary mouse cortical neurons (Zhang et al., 2008).

Another class of receptor-dependent cell type-specific peptides derived from neuron binding virus and toxins may prove to be more promising candidates for neuronal delivery of GCase. Tetanus toxin fragment C (TTC), the non-toxin ~50kDa neuronal binding domain of tetanus toxin, is one of the most well characterized binding domains from this class. TTC has been used extensively to deliver cargo proteins (Francis et al., 2000; Francis et al., 2004; Li et al., 2009) and has a strong affinity for neurons through its binding of complex gangliosides and protein receptors P15 and SV2A/B (Calvo et al., 2012; Miana-Mena et al. 2002; Yeh et al., 2010). While it could dramatically enhance the binding of GCase to neurons, TTC does not cross the blood brain barrier and could raise concerns regarding an *in vivo* immune response. As a result, the potential of TTC as an *in vivo* delivery domain is likely also limited. Smaller toxin or virus-derived peptides with less immunogenic potential would be preferable to TTC. Tet1, a 12 amino acid peptide identified for ganglioside properties similar to TTC, is a small peptide option (Federici et al., 2007). Until recently, the ability of Tet1 to deliver cargo protein was never directly compared to TTC or a CPP such as Tat (Mello et al., in preparation). As a result, the ability of Tet1 to facilitate neuronal binding of GCase is uncertain. Furthermore, Tet1 will not mediate translocation across the BBB.

For the delivery of GCase to the brain, rabies-derived peptide (RDP) may have the most potential. Several varieties of RDP have been derived from either of the two regions of the rabies virus glycoprotein (RVG) responsible for nerve binding (Fu and Zhang et al., 2013). Both varieties have been reported to cross the BBB and bind neurons. A 29 amino acid portion derived from RVG amino acid sequence 175-203 has been used for delivery with a nonarginine attached by a sequence of three glycines (Gong et al., 2012; Kumar et al., 2007; Xiang et al., 2011) and by itself (Gao et al., 2014; Liu et al., 2009). Both DNA and protein have been delivered with a 39 amino acid peptide where a 27 amino acid portion derived from RVG sequence 330-356 is connected to a nonarginine by a sequence of 3 glycines (Fu et al., 2012; Fu et al., 2013a; Fu et al., 2013b). RDP has been shown to deliver model protein GFP to neural progenitor cells (NPCs) better than Tat, Tet1, or TTC (Mello et al., in preparation). A number of proteins have been successfully delivered across the BBB using RDP including luciferase, β-galactosidase, BDNF, GDNF, and GFP (Fu et al., 2012; Fu et al., 2013b).

With the goal of producing a neuronal cell type targeted recombinant GCase enzyme, 17 variants were designed, expressed, and if expressed successfully, purified and assessed for enzyme activity and neuronal binding and internalization. For recombinant GCase, binding domains including Tat, RDP, Tet1, and TTC were assessed and compared to each other and FDA-approved Cerezyme (Genzyme Corp). Combinations of Tat and the receptor-dependent peptides were also investigated as the combination of Tat and TTC has been shown to work better than either Tat or TTC alone (Gramlich et al., 2013). Design of the candidate genes and enzymes reflected goals of high level expression, enzyme activity, and neuronal binding. GFP was also included in some of the constructs to allow

for histologic assessment of binding and internalization. Following initial screening, enzyme internalization of promising GCase variants was assayed quantitatively by lysing cells after protein treatment and quantitating the concentrations of active enzyme in the cell lysate. Substrate reduction capabilities for Tat-linked GCase and the most promising neuron-targeted recombinant GCase were also quantitatively tested.

4.3. Methods and Materials

4.3.1. Construction of glucocerebrosidase expression vectors

All glucocerebrosidase expression vectors were creating using the base plasmid pSecTag2a (Life Technologies) containing an IgK leader sequence to promote secretion upstream of the multiple cloning site, and both a myc epitope tag and 6x His purification tag downstream of the multiple cloning site. The wild-type glucocerebrosidase gene (*GBA1*) sequence was amplified from a lentiviral expression vector generously provided by Dr. Ricardo Feldman, University of Maryland Baltimore (Panicker et al., 2012). *GBA1* was cloned into the pSecTag2a backbone using EcoRI and EcoRV restriction sites creating pTag_GBA. For cloning of additional domains, AgeI and BsiWI restriction sites were introduced in frame at the 5' and 3' ends respectively of *GBA1*. Enhanced green fluorescent protein (EGFP) sequence was amplified by PCR and cloned into the pTag_GBA sequence 3' of the *GBA1* gene using BsiWI and XhoI restriction sites. This plasmid, named, pTag_GBA_GFP was used for the construction of all *GFP*-containing *GBA1* expression vectors. The *EGFP* sequence was derived from Clontech plasmid pEGFP-1.

All cell-penetrating peptides or neuronal-targeting domains were cloned into either pTag_GBA or pTag_GBA_GFP via AscI and AgeI restriction sites. Unless a linker region

was specifically designed into the expression vector, only the AgeI restriction site separated the 5' domain and *GBA1*. The *TTC* and *Tat-TTC* sequences were amplified from the pGEX4T3_Tat_TTC_GFP vector (Gramlich et al., 2013) using PCR. Each of the *Tat*, *Tet1*, and *Tat-Tet1* sequences were made as duplex oligos by Integrated DNA Technologies (IDT) and cloned into either pTag_GBA or pTag_GBA_GFP. *Tet1* was cloned 3' of *GFP* in one expression vector using the XhoI restriction site. All other sequences were created using the IDT gblock synthetic gene construction service. Sequences constructed as gblocks included *Tat_5xTet1*, *5xTet1*, *RDP*, *RDP_GFP*, *RDP_Tat*, *RDP_Flex*, *RDP_IgAh*, and *RDP_Rigid*. All gblocks were first cloned into the PCR Blunt (Life Technologies) vector for sequence confirmation before introduction into either pTag_GBA or pTag_GBA_GFP via the AscI and AgeI restriction sites.

4.3.2. Cell culture

HEK 293F suspension cells were maintained at a 40mL working volume in 125mL vented non-baffled shake flasks (Corning) and passaged three times per week. For standard passaging, cultures were seeded at 2E5-4E5 cells/mL and not allowed to exceed 2E6 cells/mL to avoid excessive cell aggregation. All suspension cultures were grown at 37ºC and 8% CO_2 with shaking at 125 RPM on an innova 2000 shaker (New Brunswick Scientific).

Human neural progenitor cells (hNPCs, Lonza) were grown in hNPC starting medium (3). Passage 4 vials of neurospheres were thawed into hNPC starting medium and allowed to attach over 2-4 days at which time the plated neurospheres were dissociated with Accutase (Sigma) and replated in 50% hNPC starting medium and 50% MEM medium containing 5% horse serum. Re-plated hNPCs were maintained until dense

enough for experimental use and fed 5mL medium once per week. For protein transduction and imaging, hNPCs were plated in poly-L-lysine coated 8-well chambered coverglasses (Nunc) and expanded for 4 days until cells reached the density of ~25,000 cells/cm^2.

Glucocerebrosidase-knockout (GCKO) and wild-type (WT) SV40-immortalized mouse neuronal cell lines were generously provided by Dr. Wendy Westbroek and Dr. Ellen Sidransky (National Institutes of Health). These cells were maintained in Neurobasal medium supplemented with 1X B27, 1mM L-glutamine, and 1X Penicillin/Streptomycin (Life Technologies). Cultures were passaged once per week and medium was changed the day after passaging and every three days afterwards. All culture vessels were coated with poly-L-lysine (Sigma P9155) to facilitate cell attachment. For protein transduction, cells were plated in poly-L-lysine coated 6-well plates and allowed to expanded 4-6 days until 80-90% confluent. The iPSC-derived Gaucher and WT neurons were generously provided by the lab of Ricardo Feldman and were differentiated and cultured as previously described (Panicker et al., 2012; Panicker et al., 2014).

4.3.3. Expression of recombinant glucocerebrosidase

All recombinant GCase enzymes were expressed using transient transfection of HEK 293F suspension cells (Life Technologies). Four expression and harvesting schemes were utilized varying length of protein expression and culture scale. HEK 293F cells were transfected at 1E6 cells/mL with 30mL in 125mL vented non-baffled shake flasks (Corning) and 120mL in 500mL vented non-baffled shake flasks (Corning). Large scale plasmid preps were performed using the Endotoxin-Free Megaprep Kit (Qiagen). Cultures were transfected with 1μg plasmid DNA for each 1E6 cells in culture. Plasmid DNA was complexed with 2μL 293fectin reagent (Life Technologies) per μg DNA for 30 minutes at

room temperature before addition to the culture. Complexes were prepared using OptiMEM serum-free medium containing GlutaMax (Life Technologies). All HEK 293F culture work was performed using Freestyle 293 medium (Life Technologies).

Transiently transfected batch cultures were maintained at 37°C and 8% CO_2 for 48 hours or 96 hours. Samples of culture medium and cells were taken during batch culture expression to determine ideal harvest time and whether the extracellular medium, soluble lysate, or insoluble lysate contained the most GCase. Batch cultures were harvested by centrifuging at 3500 RPM for 10 minutes at which time cell-free culture medium was removed and stored at 4°C until purification. The cell pellet was washed with 1X PBS pH = 7.4, centrifuged again, and frozen at -80C until ready for cell lysis and protein purification. All 30mL expression batch cultures were purified directly. Unless otherwise stated, medium from the 120mL cultures was first concentrated ~5-10x using Amicon Ultra 50,000 dalton molecular weight cutoff centrifugal filters. This medium concentration was done to facilitate resin binding with a reasonable volume for the resin bed volume. Medium was not concentrated before the scaled-up purification performed to assess substrate accumulation and reduction.

4.3.4. Purification of recombinant glucocerebrosidase

Following protein expression, culture medium or concentrated culture medium containing the expressed GCase was stored at 4°C until ready for purification. For select GCase enzymes that were not secreted, cell pellets were lysed with 1mL MPER non-denaturing lysis buffer (Pierce) for each 100mg cell pellet according the manufacturer's recommended protocol. Proteins were purified using Ni-NTA Resin (Pierce) and three buffers, all with the same 1X PBS pH=7.4 base (20mM sodium phosphate, 300mM sodium

chloride). Equilibration buffer, Wash Buffer, and Elution Buffer were each pH = 7.4 and contained 10mM, 25mM, and 250mM imidazole respectively.

The protein purification method used was a combination of standard batch and column purification methods. An equal volume of cold Equilibration Buffer was added to medium or soluble lysate, up to a 44mL final volume, and the solution was added to a washed 0.5mL bed volume of Ni-NTA resin and bound overnight at 4ºC for ~20-21 hours. Following overnight binding in batch mode, the resin suspension was equilibrated to room temperature, at which time the resin suspension was slowly poured into a 5mL column to pack the resin bed. The flow-through solution was poured over the resin bed two additional times and allowed to empty by gravity flow at a rate of approximately 1mL/min. Each resin bed was washed three times with 1mL, two resin bed volumes, of Wash Buffer. The GCase was eluted off the column with three separate 1mL volumes of Elution Buffer. Before flowing off the column by gravity flow, each column was capped and the Elution Buffer was allowed to sit on the resin bed for five minutes. All purification samples were run on 4-12% SDS-PAGE gels and stained with SimplyBlue Safestain (Life Technologies). Total protein in GCase-containing elutions was quantitated by Bradford Assay (Thermo Scientific). The specific GCase concentration was determined by densitometry using the ImageLab 3.0 (Biorad) software. All elutions containing reasonable amounts of purified GCase were supplemented with 1mg/mL BSA and stored at 4ºC until use.

4.3.5. Glucocerebrosidase activity assay

GCase enzyme activity was determined using a 0.1M acetate assay buffer pH = 5.0 containing 3mM 4-MUG (4-Methylumbelliferyl β-D-glucopyranoside), 0.15% (v/v) Triton X-100, and 0.15% (w/v) taurodeoxycholic acid sodium salt (Calbiochem). Purified GCase

or cell lysate was added to the activity assay buffer and incubated at 37°C for one hour. The reaction was stopped with the addition of a 2X volume of 0.2M glycine buffer pH = 10.8. Product 4-methylumbelliferone was detected using the Victor 3 fluorimeter (filter set excitation = 355nm, emission = 460nm). Black 96-well plates were typically used although initial work was performed with white 96-well plates. The 4-methylumbelliferone detection is highly linear between 10nM-10μM in the black 96-well plate and between 10nm-5μM in the white 96-well plate. Enzyme activity units are defined as nmol 4-methylumbelliferone released per hour.

4.3.6. Assessing glucocerebrosidase binding and internalization

Due to the large number of recombinant GCase vectors constructed, initial screening of GFP-containing recombinant GCase binding and internalization was accomplished with protein transduction of GCase following by live-cell imaging of the GFP fluorescence. NPCs were treated with 1μg/mL enzyme in NPC starting medium for 18 hours. After the overnight incubation, cells were washed 3X in NPC starting medium without growth factors or heparin and immediately imaged using the Axio Observer Z1 Motorized fluorescent microscope (Carl Zeiss Inc., Oberkochen, Germany). An analogous procedure was performed for the iPSC-derived Gaucher neurons with the exception that all washing was performed with complete medium.

Quantitative assessment of GCase binding and internalization was performed using GCase-knockout mouse neurons (Sidransky Lab) for recombinant GCase enzymes that showed promise in initial screening. All experiments included the appropriate wild-type controls for each of the two cell types. GCKO and WT mouse neurons were plated in poly-

L-lysine coated 6-well plates and cells were allowed to expand 4-6 days until 80-90% confluent. Duplicate wells were used for each treatment condition.

Cells were treated with 12μg/mL recombinant enzyme overnight for 18 hours at which time the cells were extensively washed with 1X PBS to remove excess protein. Cells were harvested from well plates using TrypLE Express (Life Technologies) and lysed using MPER non-denaturing cell lysis buffer (Pierce). Lysate protein concentrations were determined by Bradford Assay (Thermo Scientific). Enzyme activity in the cell lysates was determined by adding lysate to the 0.1M acetate assay buffer and incubating at 37ºC for one hour. Experiments used different amounts of lysate depending on lysate concentration. Final concentrations ranged from 10-20μg/100μL with a total volume of 200-300μL per reaction. Standard curves for each recombinant enzyme were generated to quantitate the concentration of enzyme detected in the lysate. Units of enzyme activity in the lysate were calculated using a 4-methylumbelliferone standard curve.

4.3.7. Assessment of glucosylsphingosine reduction using LC-MS/MS

To assess glucosylsphingosine accumulation and potential reduction with protein treatment, immortalized GCKO and WT mouse neuronal cultures were plated in poly-L-lysine coated 6-well plates and allowed to expand four days until ~80% confluent. To perform the complete experiment, 18 wells of GCKO cells and 6 wells WT cells were plated. Four treatment conditions were planned: Tat-GCase treatment of GCKO cells, RDP-IgAh-GCase treatment of GCKO cells, an untreated GCKO control, and an untreated WT control. Each treatment condition was performed in duplicate with each of the duplicates consisting of three pooled wells to ensure there was enough material collected to detect glucosylsphingosine accumulation.

Tat-GCase and RDP-IgAh-GCase were expressed and purified using a scaled-up version of the procedure performed for assessing recombinant enzyme binding/internalization (previous section). The transiently transfected flask was scaled up 4X; 120mL culture was transfected in a 500mL non-baffled shake flask. Purification scale up was performed to keep protein concentration similar to the small scale procedure throughout the purification process. This was done since concentration of protein had been found to reduce enzyme activity (Figure 4.3). BioRad Econo-Pac polypropylene chromatography columns with a 15mm internal diameter were chosen so a 2mL resin bed would have the same bed height compared to when the 5mL columns were used in the smaller scale procedure.

Aside from the 4x scale-up of production and purification processes, one additional step was performed for the protein purification to investigate substrate accumulation and reduction; final 4mL elutions were desalted using Zeba 7kDa MWCO desalting columns with a 10mL resin bed (Pierce). Buffer exchange was performed into 1X PBS pH = 7.4 (Life Technologies). Pilot experiments showed that while treatment of the GCKO mouse neuronal cultures with protein elution buffer for <24 hours was acceptable, cell loss was high with longer protein treatments. The cell loss with extended treatment was found to result from the components of the elution buffer, likely the 250mM imidazole. In a mock treatment experiment, dilution of medium with 1X PBS alone did not lead to any appreciable cell detachment and/or death.

After four days of cell growth, duplicate sets of wells were treated with either 10 µg/mL protein diluted in fresh medium or fresh medium alone for untreated controls. Duplicate treatment conditions were performed for each of Tat-GCase and RDP-IgAh-

GCase. Every 24 hours, for 72 hours total, medium was exchanged, adding fresh protein or fresh medium only. Following 72 hours of treatment, cells were washed 2X with 1X PBS pH = 7.4 and harvested by scraping. PBS was removed by centrifugation and cell pellets were frozen at -80C. Frozen cell pellets were shipped on dry ice to Cincinnati Children's Hospital for glycosphingolipid analysis. Lipid extraction and LC-MS/MS analysis of glucosylceramide and glucosylsphingosine accumulation was performed as previously described (Sun et al., 2012; Sun et al., 2013). All quantitative glycosphingolipid data was normalized to total protein detected in the cell lysate.

4.4. Results

4.4.1. Protein expression and purification

A total of seventeen GCase expression vectors were created evaluating a number of different parameters including: the presence of a cell-penetrating peptide or neuronal delivery vector, the presence of GFP, the order of protein domains, and the linker regions between domains. Besides varying design in one of the aforementioned categories, all expression vectors used pSecTag2a as the base and contained an IgK leader sequence at the 5' end and a myc epitope tag and 6xHis tag at the 3' end. Of the 17 recombinant GCase enzymes expressed, only 3 failed to express correctly (Table 4.1). Tat-TTC-GCase-GFP and RDP-GFP-GCase were expressed as smaller truncated forms at a high level. A low level of full-length Tat-TTC-GCase-GFP was observed via western blot while no full-length RDP-GFP-GCase was observed. Tat-GCase-GFP-5xTet1 was the only enzyme to not be expressed at all. GFP fluorescence was not even observed in the producer cells and no myc-containing bands were found in the supernatant or soluble lysate of the producer cells.

The IgK signal peptide facilitated the secretion of all enzymes (Figure 4.1) except for the TTC-containing TTC-GCase-GFP and Tat-TTC-GCase-GFP. Interestingly, the ~100 kDa truncated Tat-TTC-GCase-GFP fragment was secreted while the full length Tat-TTC-GCase-GFP was found only in the soluble lysate. TTC-GCase-GFP was expressed at a high level but found only in the soluble lysate of the producer HEK 293F cells. Secreted GCase was several kilodaltons larger than non-secreted GCase (Figure 4.1), a size difference consistent with differences in glycosylation (Berg-Fussman et al., 1993; Grace et al., 1994). A size difference between secreted and intracellular GCase has been observed (Branco Novo et al., 2012). GCase has five N-glycosylation sites, four of which are typically occupied in wild-type GCase (Shaaltiel et al., 2007; Tekoah et al., 2013). Proper glycosylation at only the N19 position is critical for GCase activity (Berg-Fussman et al., 1993).
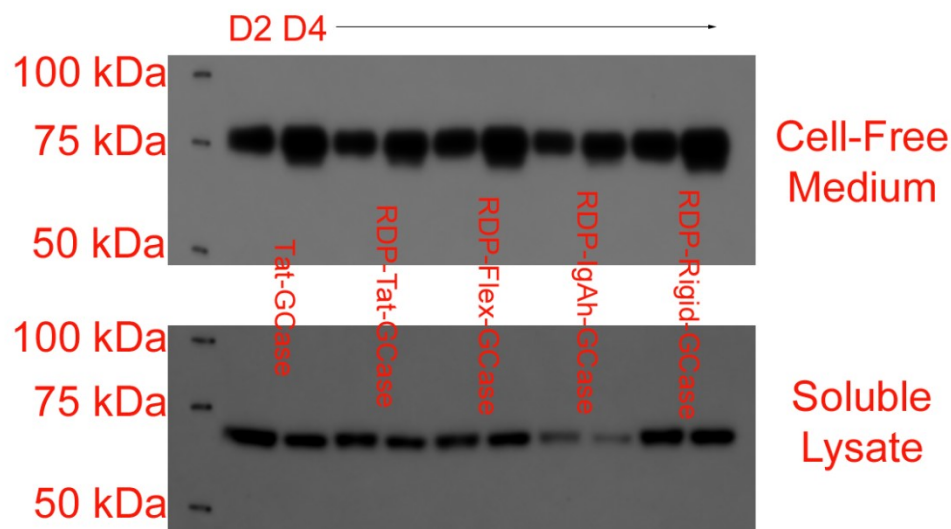
Figure 4.1: The IgK signal peptide facilitated efficient GCase secretion for most engineered enzymes. Predicted molecular weights (polypeptide only): Tat-GCase: 66.1 kDa, RDP-Tat-GCase: 70.7 kDa, RDP-Flex-GCase: 69.7 kDa, RDP-IgAh-GCase: 71.1 kDa, and RDP-Rigid-GCase: 71.2 kDa. Following transient transfection, cell-free medium and HEK 293F soluble lysate were run on 4-12% NuPage Bis-Tris gels and a western blot was performed for the myc epitope tag. For each condition, samples collected both two and four days after transfection were run. Three-fold more cell-free supernatant was run on the gels compared to soluble lysate to account for the at least 3x more concentrated soluble lysate. The results shown for the five enzymes were typical for all the secreted glucocerebrosidases. Extending batch duration increases the quantity of secreted protein in the extracellular medium but does not increase the quantity of protein in the soluble lysate.

All proteins were purified using HisPur Ni-NTA resin (Pierce). While all proteins co-purified with a number of other proteins, the band of interest was dramatically concentrated (Figure 4.2A). Recombinant GCase is not visible in the supernatant via SDS-PAGE and Simply Blue Safestain (Life Technologies) before purification. Along with the assessment of enzyme activity, product quality for all purified proteins was confirmed via SDS-PAGE and Simply Blue Safestain (Figure 4.2A) and anti-myc western blot (Figure 4.2B). Final yield of purified GCase was calculated by first performing a Bradford assay to determine total protein and then densitometry to account for the impurities in the final elution.
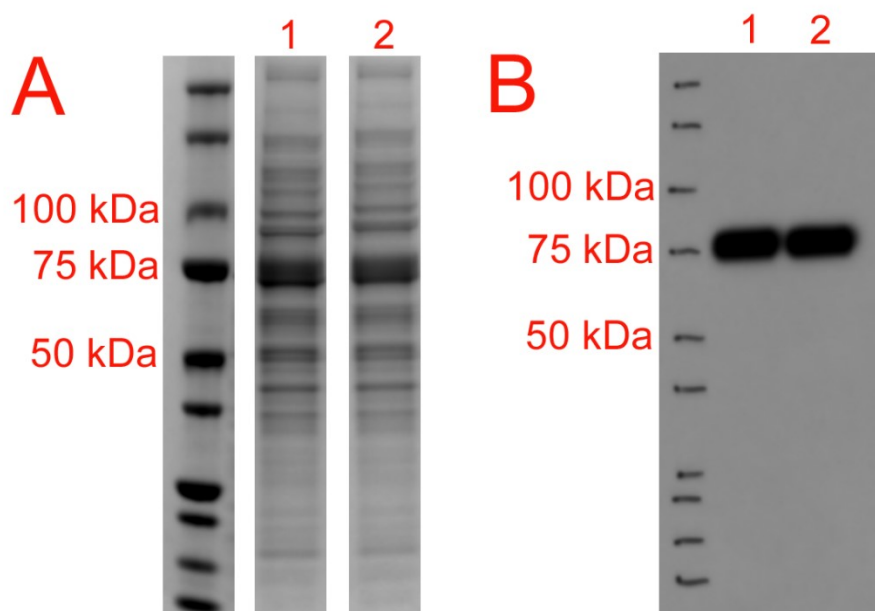
Figure 4.2: Purification of Tat-GCase and RDP-IgAh-GCase. The main elutions for Tat-GCase (1) and RDP-IgAh-GCase (2) were run on 4-12% NuPage Bis-Tris SDS-PAGE gels. SimplyBlue Safestain was used to examine total protein in the elution (A) and an anti-myc western blot (B) was utilized to confirm the location of the purified GCase on the gels. Both Tat-GCase and RDP-IgAh-GCase were found ~75 kDa, a size consistent with their predicted molecular weight and glycosylation. Comparable SDS-PAGE gels exist for all purified proteins referenced in Table 4.1.

For practical reasons, all parameters were not varied with all delivery domains and linker regions utilized in the construction of the recombinant enzymes. However, since there is quite a bit of overlap among the design of the recombinant GCase enzymes (Table 1), a number of inferences regarding the effect of enzyme design on expression level and activity can be made. First, commercial product Cerezyme (Genzyme Corp.) had a specific enzyme activity that was ~3.5X higher than the most active novel enzyme described here. The higher activity of Cerezyme is due, at least in part, to its increased purity (Van Patten et al., 2007). Second, the presence of CPP Tat or the CPP-containing neuronal delivery domain RDP at the N-terminal end of an expressed glucocerebrosidase appeared to

improve the level of expression consistent with previously described attempts at recombinant GCase expression (Lee et al., 2005; Vaags et al., 2005). CPP VP22 has also been shown to enhance GCase expression (Jin et al., 2012). Third, the only full-length GCase to not be secreted, TTC-GCase-GFP, was the least active enzyme by far. Fourth, while most enzymes were expressed fairly well, a select few were expressed at lower levels with final elutions containing <10 µg/mL purified protein. Fifth, there does not seem to be any correlation between protein expression level and enzyme specific activity. Finally, the presence of GFP decreased both production yields and specific activity. Specific activity was decreased by a greater degree than what would be expected due to the difference in molecular weight alone. Due to the decrease in activity and yield, after the design of the initial set of expression vectors, GFP was typically not included in later constructs.

Summary of Recombinant GCase Activity and Expression Level		
GCase	Specific Activity (U/mg)	Expression Level
Cerezyme	1.28E+05	N/A
RDP-GCase	3.67E+04	Acceptable
Tat-GCase-GFP-Tet1	3.26E+04	Low
Tat-GCase	3.24E+04	Acceptable
Tat-5xTet1-GCase-GFP	2.79E+04	Low
RDP-Rigid-GCase	2.53E+04	Acceptable
RDP-Flex-GCase	2.46E+04	Acceptable
RDP-Tat-GCase	2.24E+04	Acceptable
GCase (Fishman Lab)	2.04E+04	Low
Tat-GCase-GFP	1.99E+04	Acceptable
Tat-Tet1-GCase-GFP	1.81E+04	Acceptable
RDP-IgAh-GCase	1.78E+04	Acceptable
RDP-GCase-GFP	1.53E+04	Acceptable
Tet1-GCase-GFP	1.23E+04	Low
TTC-GCase-GFP	5.95E+03	Acceptable
Tat-TTC-GCase-GFP	N/A	Expressed in Truncated Form
RDP-GFP-GCase	N/A	Expressed in Truncated Form
Tat-GCase-GFP-5xTet1	N/A	Not Expressed

Table 4.1: Summary of GCase enzyme activity and protein expression efficiency data.
Seventeen recombinant GCase enzymes plus commercially available Cerezyme (Genzyme Corp) are listed in the table. Enzymes are listed in order of specific activity given as units enzyme per mg recombinant protein. One U is defined as the amount of enzyme to release 1 nmol 4-methylumbelliferone per hour. Except for the three enzymes that were not appropriately expressed, expression levels were found to be approximately bimodal where a select group of enzymes were expressed at a low level with final yields of 10 μg/mL or less. Other recombinant GCase enzymes were typically purified at yields several fold higher. Specific activity values represent the average of all preparations of each listed enzyme.

4.4.2. Production scheme impacted enzyme yield and activity

Four different production schemes utilizing transient transfection of HEK 293F suspension cells were used to express the recombinant GCase enzymes. For practical reasons, all production schemes were not tested for all enzymes. Figure 4.3 illustrates how production scheme affected the yield and activity of Tat-GCase. Production schemes

included: 1) Two days of batch growth for a 30mL culture, 2) Two days of batch growth for a 120mL culture, 3) Four days of batch growth for a 30mL culture, and 4) Four days of batch growth for a 120mL culture. The larger scale cultures were concentrated 5-11x by centrifugal filtration before binding the Ni-NTA resin. At harvest, culture viabilities were consistently ~90% for the 48 hour batches and ~60-70% for the 96 hour batches.
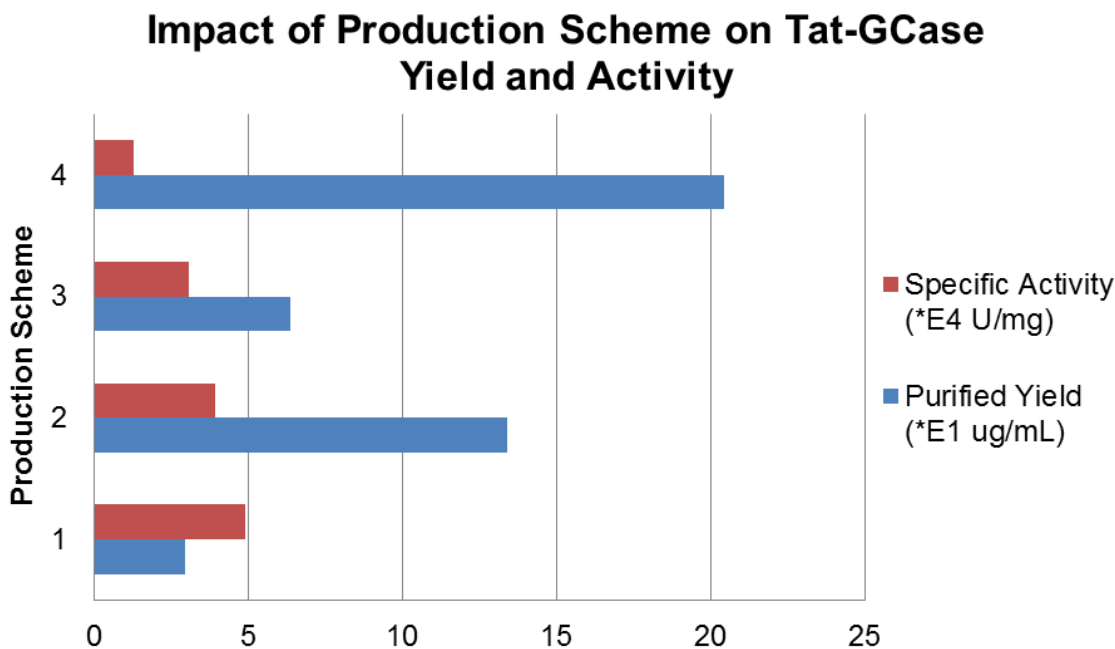
Figure 4.3: The effect of production scheme on Tat-GCase production yields and specific activity. Production schemes included: 1) Two days for a 30mL culture, 2) Two days for a 120mL culture, 3) Four days for a 30mL culture, and 4) Four days for a 120mL culture. Before purification, the medium from 120mL batch cultures was concentrated 5-11x by centrifugal filtration.

For small scale experiments, production scheme #3 was found to be preferable. While the final product was less active than scheme #1 or #2, far less transfection reagent was used and more than enough enzyme was obtained to screen enzyme activity and cell binding/internalization. However, the highest quality and most active final product was achieved with the shorter production time. Longer production time with the medium

concentration led to a much less active final product; as a result, production scheme #4 was deemed unacceptable for use despite delivering the highest yields by far.

4.4.3. Assessment of recombinant GCase binding/internalization using fluorescent microscopy

Since initial purification yields were low and the number of recombinant GCase candidates was numerous, initial screening of neuronal binding and internalization was performed by treating NPCs with 1 µg/mL purified protein and using fluorescent microscopy to compare GFP fluorescence (Figure 4.4). Qualitatively, NPCs bound similar amounts of Tat-GCase-GFP and TTC-GCase-GFP. For NPC binding, Tet1 alone was insufficient, nor did Tet1 provide any enhancement in combination with Tat. In fact, combinations of Tat and Tet1 were bound/internalized by NPCs less than Tat-GCase-GFP itself.

Protein transduction and imaging of GFP fluorescence was repeated in iPSC-derived Gaucher neurons generously provided by Dr. Ricardo Feldman, University of Maryland Baltimore. While imaging individual neurons was challenging due to the cell clustering, a qualitative comparison was possible. Proportionally to Tat-GCase-GFP, Tet1-GCase-GFP was bound by neurons better than it had been by NPCs. However, Tet1 alone was not better than Tat, nor was any combination of Tat and Tet1. GFP fluorescence in the TTC-GCase-GFP treated Gaucher neurons was qualitatively the brightest. However, TTC-GCase-GFP was not secreted and had much lower enzyme activity than the other enzymes produced (Table 4.1). Additionally, TTC would be highly immunogenic *in vivo*; as a result further work with TTC-GCase-GFP was not pursued.

	NPCs	Gaucher Neurons
Tat-GCase-GFP		
Tat-Tet1-GCase-GFP		
Tat-GCase-GFP-Tet1		
Tet1-GCase-GFP		
TTC-GCase-GFP		
Tat-GCase		
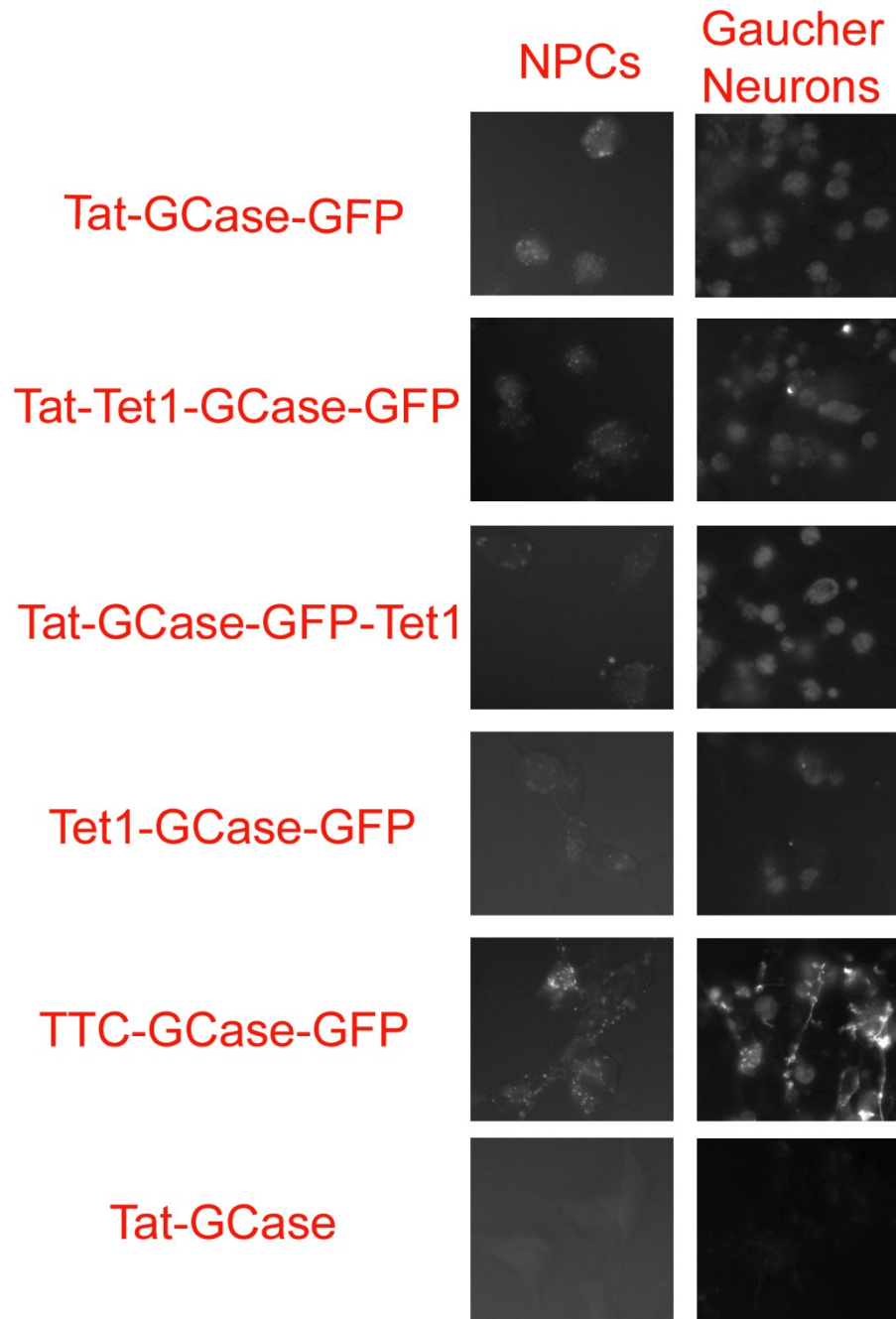
Figure 4.4: Qualitative comparison of recombinant glucocerebrosidase binding and internalization in both Neural Progenitor Cells (NPCs) and iPSC-derived Gaucher neurons. Cells were treated for 18 hours with 1 µg/mL purified protein, thoroughly washed, and imaged live using the Zeiss Axio Observer Z1 fluorescent microscope. 400X fluorescent images were taken with a Zeiss AxioCam MRm monochrome camera (1.3 megapixel, 12 bits/pixel) using the C-Apochromat 40x/1.2 W Korr objective. The exposure time for all images was 500ms.

A Tet1-containing construct, Tat-5xTet1-GCase-GFP, tested the hypothesis that multiple repeats of the 12 amino acid Tet1 peptide might lead to enhanced neuronal cell binding. NPCs were treated with Tat-Tet1-GCase-GFP and Tat-5xTet1-GCase-GFP in parallel and GFP fluorescence was qualitatively compared. In combination with Tat, additional Tet1 repeats did not appear to offer any binding advantage (data not shown). Furthermore, additional Tet1 repeats led to several-fold lower levels of protein expression.

4.4.4. Quantitative assessment of RDP-containing GCase binding and internalization in a GCase-knockout mouse neuronal cell line

While initial screening using the qualitative comparison of GFP fluorescence following the protein transduction of GFP-containing GCase enzymes successfully ruled out Tet1 as a GCase delivery vector, it was clear that a more quantitative method was required for future work. The advantage of the imaging studies was the low concentration of protein needed; 1 µg/mL treatment concentrations led to visible GFP fluorescence after 18 hours. To quantitate intracellular GCase activity, both higher purified protein yields and a cell line with low wild-type GCase activity were required.

Quantitatively, recombinant GCase enzymes without GFP and with either Tat or RDP at the N-terminus were evaluated as these attributes tended to give high protein expression, enabling treatment of cells with at least 12 µg/mL purified protein. Initial pilot studies tested whether NPCs were a suitable cell line for quantitative work and they were not due to high background wild-type GCase activity. While iPSC-derived Gaucher neurons had very low wild-type activity and were an interesting scientific model, the number of cells required made this cell option expensive and less ideal. The ideal cell type for this work proved to be a SV40-transformed glucocerebrosidase-knockout mouse

neuronal cell line generously provided by Wendy Westbroek and Ellen Sidransky (NIH, Bethesda, MD). Pilot studies indicated that this cell line had very low wild-type GCase activity and preferentially bound RDP and TTC-linked recombinant GFP proteins.

For the first RDP-GCase enzyme created, the 39 amino acid RDP peptide was inserted in place of Tat in the Tat-GCase construct. RDP and GCase were separated by only two amino acids, Thr-Gly, due to the presence of the AgeI restriction site used in subcloning. The first quantitative experiment performed with the GCKO mouse neurons compared the uptake of Tat-GCase, RDP-GCase, and Cerezyme following an 18 hour treatment with 12 µg/mL purified protein. Enzyme uptake was compared two ways: the concentration of active GCase harvested in cell lysate and the activity of GCase found in the cell lysate. The concentration of enzyme internalized was determined using standard curves of each purified GCase. While standard curves were approximately linear between 50-400 ng/mL purified enzyme, a second or third order polynomial best fit the curve. Specifically a second order polynomial fit was used for this initial experiment while, with more data points, a third-order polynomial fit was used for all subsequent experiments. Due to the higher activity of Cerezyme, comparing concentration of active internalized enzyme is the fairest comparison of enzyme delivery.

Unexpectedly, RDP-GCase was not delivered preferentially compared to Tat-GCase, and by concentration, both RDP-GCase and Tat-GCase were internalized only marginally better than Cerezyme in the GCKO mouse neuronal line (Table 4.2). Both were able to deliver 3% of wild-type SV40-converted mouse neuron GCase activity. This result was inconsistent with our observation that, in neuronal cell types, RDP improves recombinant protein delivery considerably compared to Tat (Mello et al., in preparation),

leading to the hypothesis that, in this first generation RDP-GCase recombinant enzyme, RDP folding or binding was sterically hindered.

Comparison of Delivered GCase Activity in GCKO Mouse Neuronal Cell Lysate			
Protein	GCase Detected (ng/mL)	Normalized to Tat-GCase	Percent WT Activity Delivered
Tat-GCase	135.74	1.00	3.07
RDP-GCase	118.90	0.88	3.02
Cerezyme	98.53	0.73	23.09

Table 4.2: Comparison of GCase detected in GCKO mouse neuronal cell lysate following protein treatment with 12 µg/mL recombinant GCase. RDP was not found to improve GCase binding and internalization. Neither Tat nor RDP facilitated significantly better protein transduction efficiency compared to commercially available Cerezyme (Genzyme Corp). For all enzyme assays, 20 µg lysate was added per 100 µL.

4.4.5. Linker region design is critical to facilitate RDP-mediated neuronal delivery of glucocerebrosidase

Since we had thoroughly established that RDP-GFP preferentially binds neuronal cell types compared to Tat-GFP without a linker region, it was clear that while a linker region between RDP and the recombinant protein of interest is not required in all circumstances, it might be imperative for GCase. The first attempt at relieving this hypothesized steric hindrance was to create RDP-GFP-GCase, where GFP would be utilized as the linker region. While the eventual goal would have been to engineer a small peptide linker region, effective RDP-GFP delivery predicted that GFP would be an effective linker region to test the steric hindrance hypothesis. However, since RDP-GFP-GCase was expressed only in a truncated form (Table 4.1), the small peptide linker region design was attempted.

The four linker regions inserted between the Thr-Gly two amino acid sequence and RDP were Tat, a flexible linker region (Flex), a linker region derived from the flexible hinge region of IgA (IgAh), and a highly alpha-helical linker region (Rigid). The RDP-Tat-GCase enzyme was created since Tat has the length of a typical linker region, 11 amino acids, and most importantly, there was a high degree of confidence that Tat would not interfere with protein expression. The flexible linker region selected was GGGSGGGS. Although shorter than most flexible linkers, this 8-amino acid linker was used successfully in the construction of RDP-linked recombinant proteins (Fu et al., 2012). The IgAh linker region is a typical example of proline-rich semi-rigid linker regions that are commonly used (Bhandari et al., 1986; Evans et al., 1986; Li et al., 2009; Low et al., 1976; Turner et al., 1993). Finally, the rigid $A(EAAK)_4A$ 22 amino acid linker was selected for its highly alpha-helical structure, ensuring a known amount of space between RDP and GCase (Arai et al., 2001).

Along with Tat-GCase as the control, each of RDP-Tat-GCase, RDP-Flex-GCase, RDP-IgAh-GCase, and RDP-Rigid-GCase were expressed and purified. Using production scheme #3 with four days of expression, all expressed well with final yields from ~40-70 μg/mL. All new RDP-linked enzymes had comparable specific activities ranging from 1.78E4 to 2.53E4 U/mg (Table 4.1).

Duplicate wells containing GCKO mouse neuronal cells were treated with 12μg/mL of purified Tat-GCase or one of the RDP-Linker-GCase enzymes for 18 hours at which time the cells were harvested, lysed, and protein content of the lysates was quantitated. Identical quantities of lysate were added to MUG-containing assay buffer and 4-methylumbelliferone fluorescence was compared. Fluorescence from GCase-treated

samples was normalized using untreated GCKO cell lysate. The percentage of wild-type activity delivered was calculated using untreated wild-type mouse neuronal cell line lysate. The concentration of GCase found in the lysate was calculated by preparing standard curves of each purified GCase.

The concentration of GCase detected in the cell lysate was compared for all RDP-Linker-GCase enzymes (Figure 4.5). RDP-IgAh-GCase performed the best, as 2.65X more RDP-IgAh-GCase was delivered to the GCKO neurons compared to Tat-GCase. Tat-GCase was bound/internalized better than both RDP-Flex-GCase and RDP-Rigid-GCase. Although RDP-IgAh-GCase is a less active enzyme than Tat-GCase, 2.52X more enzyme activity was delivered to the GCKO cells representing ~10% of wild-type activity. This result was replicated with a second independent experiment (Table 4.3).
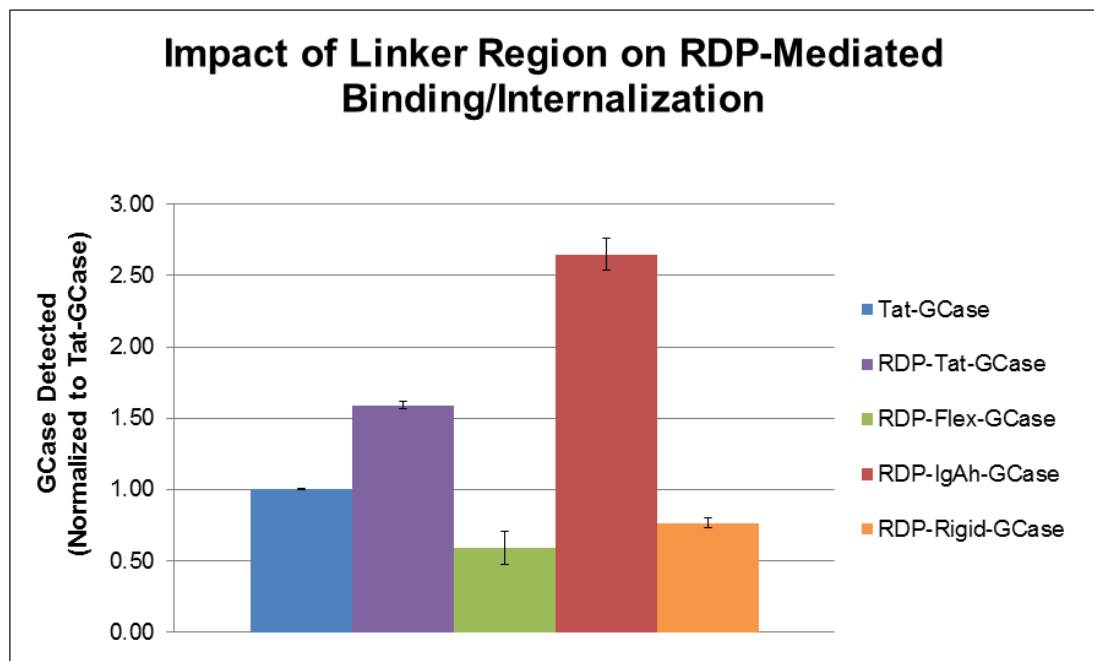
Figure 4.5: The impact of linker region on RDP-Linker-GCase binding and internalization in GCKO mouse neurons. The concentrations of GCase detected in the cell lysates for each treatment condition were quantitated and subsequently normalized to Tat-GCase to facilitate comparison. RDP-IgAh-GCase was internalized 2.65X more than Tat-GCase. All bars in the above graph represent the average of duplicate treatment conditions.

Comparison of Delivered GCase Activity in GCase-Knockout Mouse Neuronal Cell Lysate (Experiment #1)				
Protein	GCase Detected (ng/mL)	GCase Detected (Normalized to Tat-GCase)	Percent WT Activity Delivered	Percent WT Activity Delivered (Normalized to Tat-GCase)
Tat-GCase	67.08	**1.00**	3.94	**1.00**
RDP-Tat-GCase	106.71	1.59	5.89	1.50
RDP-Flex-GCase	39.77	0.59	1.32	0.34
RDP-IgAh-GCase	177.68	**2.65**	9.92	**2.52**
RDP-Rigid-GCase	51.29	0.76	1.74	0.44

Comparison of Delivered GCase Activity in GCase-Knockout Mouse Neuronal Cell Lysate (Experiment #2)				
Protein	GCase Detected (ng/mL)	GCase Detected (Normalized to Tat-GCase)	Percent WT Activity Delivered	Percent WT Activity Delivered (Normalized to Tat-GCase)
Tat-GCase	29.75	**1.00**	1.87	**1.00**
RDP-IgAh-GCase	66.18	**2.22**	4.45	**2.38**

Table 4.3: Data compilation for the two independent experiments quantitating GCase activity in GCKO mouse neuronal cell lysate following a 18 hour protein treatment with 12μg/mL purified protein. All data points in the above tables represent the average of duplicate treatment conditions. Duplicate conditions all gave similar results.

4.4.6. Reduction of glucosylsphingosine accumulation with Tat-GCase and RDP-IgAh-GCase treatment

Production and purification processes were scaled up 4X to produce enough Tat-GCase and RDP-IgAh-GCase to perform the substrate accumulation and reduction assessment. Each scaled up production process was performed in duplicate to produce 8x the final protein typically generated. This was accomplished; final protein concentrations and purity were similar to the smaller scale process. Desalting and buffer exchange did not lead to any loss of purified enzyme however activity was reduced. Although the reduction in activity was unexpected and unwanted, removal of the 250mM imidazole was necessary for treatments spanning multiple days.

The GCKO mouse neuronal cell line was expected to accumulate glucosylsphingosine but not glucosylceramide (W. Westbroek, personal communication). This expected result was confirmed; GCKO cells accumulated GlcSph ~60X more than WT cells while no accumulation of GlcCer or any GlcCer species was observed in the GCKO cells (Figure 4.6). Treatment with both Tat-GCase and RDP-IgAh-GCase was found to reduce accumulated glucosylsphingosine to essentially wild-type levels (Figure 4.6).
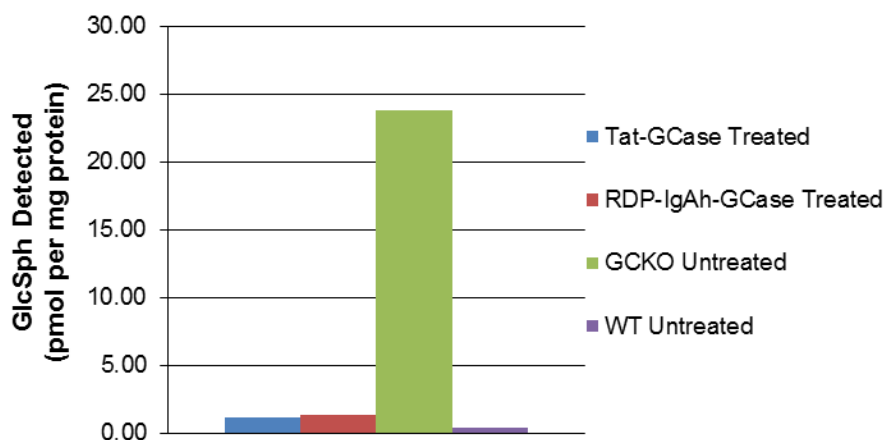
Effect of Protein Treatment on Glucosylsphingosine and Glucosylceramide Accumulation			
Treatment Condition	Sample	Glucosylsphingosine (pmol/mg)	Glucosylceramide (pmol/mg)
Tat-GCase	1	1.18	64.33
Tat-GCase	2	1.17	262.33
RDP-IgAh-GCase	1	1.25	258.89
RDP-IgAh-GCase	2	1.43	211.62
GCKO Untreated	1	14.44	192.01
GCKO Untreated	2	33.22	311.32
WT Untreated	1	0.44	423.56
WT Untreated	2	0.35	455.79

Figure 4.6: Treatment of GCase-Knockout (GCKO) immortalized mouse neuronal cell line with Tat-GCase or RDP-IgAh-GCase dramatically reduces glucosylsphingosine (GlcSph) accumulation. Duplicate sets of three wells were treated with 10μg/mL purified protein or fresh medium only for 72 hours with complete medium changes every 24 hours. For each triplicate treatment condition, wells were pooled for analysis. Accumulated GlcSph was quantitated using LC-MS/MS analysis and data was normalized to the total protein detected in the cell lysate. Duplicate GlcSph data points presented in the table were averaged for graphical display.

4.5.   Discussion

The development of RDP-IgAh-GCase potentially represents a significant advance in recombinant protein therapeutics for neuronopathic Gaucher's disease therapy. In pursuit of developing an effective neuron-targeted recombinant GCase, seventeen different recombinant enzymes were designed and expressed. Parameters that were varied in

recombinant protein design included the type of cell penetrating peptide or neuronal membrane binding vector, the presence of GFP, the order of the different functional domains N-terminus to C-terminus, and the type of linker region used between protein domains. Recombinant proteins were designed in stages where results from each set where employed to optimize the design of subsequent sets of proteins. There was enough overlap in the sequences of the recombinant enzymes to make a number of observations regarding recombinant GCase design and expression. All of the recombinant GCase enzymes expressed and successfully purified had specific activities at least 3x lower than commercially available Cerezyme (Genzyme) using the *in vitro* activity assay with synthetic substrate 4-MUG. Due to this difference in enzyme activity, all protein incubation conditions of cells were set up by enzyme concentration instead of enzyme activity, a treatment paradigm that has been used with some GCase delivery work (Lee et al., 2005). It is highly likely that increasing the purity of our GCase would improve enzyme specific activity as protein aggregation would be reduced (Van Patten et al., 2007). Improving production yields and purity after protein purification are two important future goals in this work.

The second observation made was that the presence of cell-penetrating peptide Tat or cell-penetrating peptide-containing RDP improved protein expression. The improvement of GCase expression with inclusion of CPPs Tat and VP22 has been previously observed (Jin et al., 2012; Lee et al., 2005; Vaags et al., 2005) although the mechanism involved is not currently known. Comparing the production of the GFP-containing recombinant GCase enzymes can provide insight on this observation. Interestingly, while Tat-GCase-GFP, Tat-Tet1-GCase-GFP, and RDP-GCase-GFP all

expressed well, Tet1-GCase-GFP did not. Although Tet1 is similar to the size of the Tat peptide, it is not highly cationic. In fact, Tat-Tet1-GCase-GFP was the only Tet1-containing enzyme to be expressed at comparable levels to Tat-GCase-GFP or RDP-GCase-GFP. The only Tat or RDP-containing enzymes to express poorly also contained Tet1 (Table 4.1). Wild-type GCase did not express nearly as well as any of the Tat-GCase or RDP-GCase enzymes. Overall, at this time, it can only be concluded that a CPP N-terminal to GCase improves production. Although the absence of Tat or RDP at the N-terminus leads to lower production, it does not lead to lower enzyme activity. There does not appear to be any clear relationship between expression level and enzyme activity (Table 4.1).

Many of the initial GCase expression vectors were designed with a GFP at the C-terminus of the GCase sequence. The motivation for this design was the desire to perform initial screening for cell binding with low concentrations of protein, using fluorescent microscopy before using more quantitative methods to assess binding and internalization. While initial screening was performed for the first set of variants (Figure 4.4), most subsequently designed enzymes were made without a GFP. This decision was based on two observations: GFP-containing enzymes had lower expression levels compared to their counterparts without GFP and GFP-containing enzymes had lower specific activities than even predicted by their greater molecular weights.

While the initial evaluation of GCase binding and internalization via GFP fluorescence was not a perfect system, it was suitable for eliminating Tet1 from further evaluation for GCase delivery. Qualitatively, Tet1-GCase-GFP was not delivered as well as Tat-GCase-GFP nor did the addition of Tet1 with Tat give any appreciable advantage

over Tat alone in either NPCs or iPSC-derived Gaucher neurons (Figure 4.4). Furthermore, work in our lab using model protein GFP indicated that Tet1 could not facilitate delivery to NPCs as well as Tat, TTC, or RDP (Mello et al., in preparation).

While TTC-GCase-GFP did not appear to be bound or internalized better than Tat-GCase-GFP in NPCs qualitatively, it did improve binding with the iPSC-derived Gaucher neurons. While this was an interesting observation regarding the neuronal properties of NPCs, it did not make TTC our preferred delivery vector for GCase. TTC-GCase-GFP is also potentially problematic for *in vivo* delivery due to the presence of highly immunogenic TTC. Furthermore, TTC-GCase-GFP was not secreted during production. While purifying the protein from soluble lysate was not an issue, we observed that proteins harvested from the soluble lysate were several kDa smaller than their secreted counterparts. TTC-GCase-GFP was by far the least active enzyme purified, possibly due to decreased post-translational modification. N-glycosylation at the first of the four occupied sites, at amino acid #19, is critical for full catalytic activity (Berg-Fussman et al., 1993).

RDP seemed to be the most promising protein delivery vector for the neuronal targeting of GCase on the basis of its small size, low potential antigenicity, and high level of neuronal binding. Along with the published literature (Fu et al., 2012; Fu et al., 2013b), experience in our lab indicated that model protein RDP-GFP could be delivered to neural progenitor cells ~9X better than Tat-GFP and ~46X better than Tet1-GFP (Mello et al., in preparation). Along with the promising pilot binding studies, expression of RDP-GCase was high, nearly identical to Tat-GCase. However, our initial recombinant RDP-GCase was unexpectedly not bound or internalized preferentially to Tat-GCase (Table 4.2). The first pTagRDP_GBA expression vector was constructed like the pTagTat_GBA, where the

RDP sequence replaced the Tat sequence with only a two amino acid linker region separating the delivery peptide from the GCase sequence. We hypothesized that RDP was sterically hindered by GCase, and that introduction of a linker region would allow RDP to appropriately bind its receptor(s). Four additional RDP-GCase enzymes were designed, each with a differently linker region. The flexible, semi-rigid IgAh, and rigid linker regions were chosen based upon potential structure, while Tat was selected as a linker region to ensure that at least one of the RDP-Linker-GCase enzymes expressed well. We were unsure what affect the addition of space between RDP and GCase would have on expression level. Although expression levels did vary for the RDP-Linker-GCase variants, all expressed fairly well. Enzyme activity was comparable for all variants ranging between 1.78E4 – 2.53E4 U/mg (Table 4.1). Linker region length did not appear to affect enzyme activity as RDP-IgAh-GCase and RDP-Rigid-GCase were the least and most active linker-containing enzymes respectively. Overall, RDP-IgAh-GCase was found to be bound and internalized preferentially compared to Tat-GCase and all the other RDP-Linker-GCase variants. While there are review articles describing the effect of linker region on recombinant protein design (Chen et al., 2013; George et al., 2003; Zhang et al., 2009) this work with RDP-GCase is a rare description of the impact of a variety of linker region classes on enzyme functionality and delivery. This work also indicates what while RDP has a lot of potential to mediate the neuronal targeting of cargo proteins, steric hindrance of RDP by the cargo protein is an issue. While the IgAh linker could be useful for all RDP-based delivery, it is possible that linker region will need to be evaluated on a protein-specific basis.

The 19 amino acid IgAh linker, PVPSTPPTPSPSTPPTPSM, was first used by Hallewell and colleagues in 1989 to link superoxide dismutase (SOD) subunits for the purpose of making functional polymers. The IgAh linker was chosen in an attempt to reproduce the partially flexible linkage between Fab and Fc portions of IgA (Hallewell et al., 1989). Our collaborators have used it previously to facilitate the expression of a recombinant TTC-GDNF in a baculovirus expression system (Li et al., 2009). The IgAh linker closely mimics a class of relatively common proline-rich linker regions (Bhandari et al., 1986; Evans et al., 1986; Turner et al., 1993). Proline has been found to be the most preferred amino acid in linkers during linker region analysis. Proline-rich sequences adopt less secondary structure since proline does not hydrogen bond with other amino acids leading to a more extended confirmation (George et al., 2003).

The development of RDP-IgAh-GCase is the creation of the first recombinant glucocerebrosidase capable of effectively binding neurons with the potential to cross the blood brain barrier. There have only been two publications describing the delivery of GCase using methods other than mannose-directed endocytosis. As described, Lee et al. created GCase-Tat and demonstrated that it was delivered preferentially to type 1 and type 2 Gaucher fibroblasts. While it was suggested that GCase-Tat could be used for types 2 and 3 GD therapy, delivery of GCase-Tat to neurons was not demonstrated. This publication is the first to describe the binding and internalization of Tat-GCase in a neuronal cell type. The well-known ability of Tat to move cargo proteins across the BBB makes Tat-GCase more promising for neuronopathic Gaucher's disease therapy than mannose-terminal recombinant GCase (Schwarze et al., 1999). However, results presented here indicate that Tat might not provide much of a binding advantage. Besides the creation

142

of Tat-GCase, a receptor-dependent delivery strategy was employed for facilitating the passage of GCase across the BBB. Apolipoproteins B and E capable of mediating lysosomal enzyme delivery across the BBB have been tested and compared to Tat (Böckenhoff et al., 2014; Spencer et al., 2007). Specifically, ApoB has been used to deliver GCase across the BBB. ApoB can bind the low-density lipoprotein receptor (LDLR) and mediate transcytosis of cargo protein across the BBB (Spencer et al., 2013). While it can transport proteins across the BBB, it does not target the GCase to neurons once in the CNS.

RDP-IgAh-GCase has the potential to not only target neurons, but to transport GCase across the BBB. The potential to cross the BBB adds a straightforward and non-invasive treatment scheme in addition to direct infusion. In an effort to improve delivery of enzyme to deep brain structures such as the basal ganglia, direct IC injection of GCase using the low pressure infusion parameters of convection enhanced delivery (CED) have been investigated in large animals. This method results in high concentrations in brain regions adjacent to the infusion site; evidence of enzyme in a vesicular location was observed (Lonser et al., 2005; Lonser et al., 2007). CED was employed to attempt to treat an infant with acute neuronopathic GD. Although the patient tolerated the treatment with some degree of stabilization, distribution of the injectate suggested that multiple intra-cerebral injections would be needed to for widespread brain treatment even using CED (Lonser et al., 2007). In a small study, 3 patients with GD underwent intra-cerebroventricular infusion of GCase. As with intra-cerebral injection, failure of this therapy was due to lack of neuronal binding of this unmodified commercial enzyme (Erickson et al., 1997).

The final goal of the presented work was to demonstrate that the active GCase we delivered to the GCase-knockout mouse neuronal cell line was functional and capable of reducing accumulated substrate. While enzymatically active RDP-IgAh-GCase and Tat-GCase were detected in cell lysate, we aimed to show that following receptor-mediated endocytosis, sufficient enzyme was trafficked to the lysosome to reduce GlcSph accumulation. Proteins were treated for 72 hours, a treatment time chosen based on both *in vitro* and *in vivo* GCase treatment literature (Cabrera-Salazar et al., 2010; Panicker et al., 2012). When the protein-treated and control cells were analyzed by LC-MS/MS to quantitate GlcSph, the GCKO neuronal cell line was found to accumulate ~60X more GlcSph than the WT cells and both RDP-IgAh-GCase and Tat-GCase treatment reduced GlcSph accumulation to essentially wild-type levels. This result fully confirmed that we had delivered active, functional recombinant enzyme. In 2010, Cabrera-Salazar and colleagues demonstrated that three consecutive daily intra-cerebroventicular injections of reformulated Cerezyme reduced GlcCer and GlcSph levels to wild-type concentrations in the neuronopathic Gaucher's disease K14 mouse model (Cabrera-Salazar et al., 2010). Substrate reduction *in vivo* has the potential to be even more efficient with a neuron-targeted recombinant GCase instead of one that is internalized via mannose-directed endocytosis.

4.6. Conclusions

Recombinant RDP-IgAh-GCase has exciting potential as a therapeutic for neuronopathic Gaucher's disease due to both its neuron-targeting properties and potential to cross the BBB. RDP-IgAh-GCase was bound/internalized ~2.5 fold over control protein Tat-GCase and both enzymes were found to reduce substrate glucosylsphingosine

concentrations to wild-type levels in a GCase-knockout mouse neuronal cell line. In future work, both RDP-IgAh-GCase and Tat-GCase merit *in vivo* testing to determine their therapeutic potential in Gaucher's disease animal models. Additionally, while a transient expression system was invaluable for the production of multiple GCase variants in the work presented here, moving forward, improved production and purification processes will be pursued both to support *in vivo* testing and facilitate scale-up to meet increased protein needs.

Chapter 5: Conclusions

5.1. Review of Findings

This thesis dissertation work aimed to develop novel protein therapeutics for neurological diseases including Parkinson's disease and neuronopathic Gaucher's disease. The two most important achievements of this research were the discovery and characterization of the Tat-TTC protein delivery vector and the development of RDP-IgAh-GCase, the first neuron-targeted recombinant glucocerebrosidase with the potential to cross the BBB. While our goal to develop a protein-treatment method for dopaminergic neuronal differentiation was not met, that research project generated a number of interesting results including the finding that a new *in vitro* translation system can express soluble transcription factors at a high level.

The motivation for Chapter 2 was to develop an improved neuron-specific protein delivery vector. Although such a vector could have multiple uses, one particular idea and motivation for the work was to improve the delivery of transcription factors for the differentiation of NPCs. The hypothesis was that because cell-penetrating peptide Tat and neuronal binding polypeptide TTC bind neuronal membranes through different mechanisms, the combination of the two could facilitate more efficient protein delivery than either Tat or TTC alone. Model protein GFP was used since its fluorescence leads to straightforward methods of detection. Tat-GFP, TTC-GFP, and Tat-TTC-GFP were delivered to NPCs, N18-RE-105 neuroblastoma cells, and 3T3 mouse fibroblasts to determine whether Tat-TTC-GFP was preferentially bound or internalized, and whether or not this binding was neuronal cell type-specific. Binding and internalization was quantitated in NPCs using direct fluorimetry. After 18 hours of 20 µg/mL protein

146

treatment, cells were lysed and protein found in the lysate was quantitated. Tat-TTC-GFP fluorescence was easily detected while Tat-GFP and TTC-GFP fluorescence was below the limit of detection. Using conservative estimates and assuming the maximum amount of Tat-GFP and TTC-GFP were in the lysate, below the limit of detection, Tat-TTC-GFP was found to be bound or internalized at least 83 fold better than Tat-GFP and at least 33 fold better than TTC-GFP. This result was confirmed using fluorescent image quantitation. In NPCs and N18-RE-105 neuroblastoma cells, Tat-TTC-GFP was taken up at least an order of magnitude better than Tat-GFP or TTC-GFP where as in 3T3 cells, no preferential binding was observed. This result indicated that Tat-TTC-GFP is both an improved protein delivery vector and neuronal cell type-specific.

Future plans for our protein delivery vectors, including Tat-TTC, included a variety of intracellular compartments. The protein delivery vectors were taken up by endocytosis and the majority of delivered cargo was retained in endosomes following uptake. Although this is fine for lysosomal protein delivery, to deliver cargo to cytosolic or nuclear targets, we needed to find a way to facilitate cargo redistribution. Using the TPPS$_{2a}$ photosensitizer and light delivered by the 4X objective of a Zeiss fluorescent microscope, PCI was mediated leading to clear release of GFP into the cytosol. Some cytotoxicity was expected with PCI because it involved the rupture of membranes, therefore, LDH assays were performed to ensure that PCI could be mediated with reasonable cytoxicity. While full endosomal rupture was too cytotoxic, a substantial quantity of protein could be released without excessive cell death.

Chapter 3 covered the attempt to produce functional transcription factors to mediate dopaminergic neuronal differentiation. The long-term plan for this project was to develop

147

a library of reprogramming factors that could be used with a variety of source cells. To start, we chose to produce Mash1, Lmx1a, and Nurr1 based on a paper that used lentiviral delivery of these three factors to transdifferentiate human fibroblasts to dopaminergic neurons (Caiazzo et al., 2011). A number of technologies developed in the Tat-TTC project were utilized in Chapter 3. Since our initial goal was to deliver recombinant factors to fibroblasts, the Tat delivery vector was chosen over Tat-TTC. Furthermore, since the intracellular target was the nucleus, PCI was used to redistribute endocytosed cargo from the endosomes.

Both Tat-Nurr1 and Tat-Nurr1-GFP expressed at very low levels; the quantity of protein produced was insufficient for any experimentation. Unpublished attempts in the Fishman Lab to express Nurr1 were unsuccessful, so our issues with Nurr1 expression in mammalian cells were not unexpected. Tat-Mash1, Tat-Mash1-GFP, Tat-Lmx1a, and Tat-Lmx1a-GFP were all expressed, and the majority of the protein was found in the insoluble lysate. Proteins were purified and shown to be taken up by NPCs via protein transduction. Using PCI, Tat-Lmx1a-GFP was delivered to the nucleus while for Tat-Mash1-GFP, nuclear delivery results were inconsistent. Promoter-reporter vectors were utilized to show transcription factor functionality. Only Tat-Mash1 was shown to be functional with co-transfection of 3T3 fibroblasts, but all factors increased luciferase expression in SK-N-BE(2)C cells. This indicated that Tat-Mash1-GFP was less active than Tat-Mash1 and the Lmx1a reporter vector is cell type-specific. Two protein treatment paradigms were attempted to demonstrate Tat-Mash1 protein functionality following reporter gene transfection. While no increase in luciferase expression was observed following 1 µg/mL purified protein treatment, small increases were observed when Tat-Mash1-containing

soluble lysate was added. This finding called the functionality of the resolubliized transcription factors into question. Following this result, our efforts shifted to identifying a method to produce soluble transcription factor. I identified the Pierce one-step HeLa *in vitro* translation kit as the best option; it was able to produce high concentrations of soluble Tat-Mash1 and Tat-Mash1-GFP. This method will be critical for future work as it has the potential to address the two main roadblocks that limited the work in Chapter 3: the yield of soluble transcription factor produced and consequently, the dose that was given.

My work with protein delivery of transcription factors gave me an appreciation for the attributes of a recombinant protein that would be best for therapeutic delivery. If a protein could be expressed in a soluble form, required endosomal/lysosomal targeting, and had a clear functional output, it would lend itself well to delivery using many of the protein delivery vectors I had either developed or gained experience with in the lab. An interesting candidate for neuronal-targeted protein delivery emerged from an interest in developing PD therapeutics. Mutations for the *GBA1* gene encoding the enzyme glucocerebrosidase are the greatest genetic risk factor for PD. Furthermore, many individuals with *GBA1* mutations have GCase deficiencies that lead to Gaucher's disease. While there are multiple FDA-approved large and small molecule therapeutics for the non-neuronopathic type 1 GD, there is currently no therapy for types 2 and 3 with nervous system involvement. As a result, I aimed to develop the first neuron-targeted GCase that would have potential for neuronopathic GD therapy.

Tat-GCase had previously been shown to be internalized by Gaucher fibroblasts several fold better than commercially available Cerezyme (Lee et al., 2005). However, this result had never been shown in neuronal cell types. In Chapter 4, I demonstrated that Tat-

GCase was not bound or internalized by a GCase-knockout neuronal cell line much better than Cerezyme. Numerous GCase-variants were produced before I identified and developed RDP-IgAh-GCase, a GCase variant that was found to be internalized ~2.5x more than Tat-GCase in the GCKO neuronal cells. A 19 amino acid linker from the flexible hinge region of IgA was found to be critical to relieve steric hindrance of RDP by GCase itself. Both Tat-GCase and RDP-IgAh-GCase were shown to reduce glucosylsphingosine accumulation in the GCKO neurons to wild-type levels. RDP has been shown the ability to cross the BBB (Fu et al., 2012). Moving forward, RDP-IgAh-GCase has considerable potential as a protein treatment for neuronopathic types 2 and 3 GD, and has the potential to be delivered non-invasively because the protein would be predicted to cross the BBB.

5.2. Future Work

5.2.1. Tat-TTC protein delivery vector

Research presented in Chapter 2 and in Gramlich et al., 2013 demonstrated that Tat-TTC is one of the highest capacity neuron-specific protein delivery vectors that has been described in the literature. However, since TTC is highly immunogenic, Tat-TTC is limited to future *in vitro* applications. Tat-TTC warrants consideration for *in vitro* protein delivery where the maximum intracellular dose is desired. Although the larger size of Tat-TTC may limit its protein expression, its dramatically improved binding would make its evaluation in any *in vitro* setting worthwhile. There has already been a fair amount of interest in Tat-TTC from other labs for protein delivery, and other applications. Recently, the lab of Jeffrey Friedman at Rockefeller University contacted the Fishman Lab for the plasmid DNA so they can use Tat-TTC's improved binding for neuronal mapping.

Tat-TTC could be modified in the future to enable it to be used as an *in vivo* protein delivery vector. The most straightforward way to do this would be to substitute the 51 kDa C-terminal fragment of the heavy chain of Botulinum toxin for TTC. While this 51 kDa fragment is still large and potentially immunogenic, individuals are not vaccinated against Botulinum toxin, a fact that makes TTC a non-starter for *in vivo* work. The better option for *in vivo* delivery is likely RDP, a rabies-derived peptide that we have worked with extensively in this thesis research. As it is a combination of a virus-derived neuronal binding domain and a polyarginine cell-penetrating peptide, RDP functions analogously to Tat-TTC except that RDP is much smaller and likely far less immunogenic than TTC. The combination of a cell-type specific peptide and a receptor-independent cell-penetrating peptide is likely a promising formula for construction of cell type-specific protein delivery vectors for many cell types.

5.2.2. Neuronal differentiation using protein delivery of transcription factors

As discussed at length in chapter 3, I was not successful in expressing and purifying recombinant transcription factors capable of reproducing the reporter gene induction observed with traditional co-transfection. In chapter 3, I concluded that this was likely the direct result of not having a method to produce sufficient quantities of soluble transcription factor, and therefore, treating cells with only low protein doses. Indeed, when I treated reporter-transfected 3T3 fibroblasts with Tat-Mash1 and Tat-Mash1-GFP containing soluble producer cell lysate, there was a small increase in reporter gene expression. Future work mediating neuronal differentiation with purified recombinant factors must start with an expression system capable of high levels of soluble protein production. In this thesis, I identified a mammalian *in vitro* translation system with the potential to meet this distinct

need. While cell-free expression systems have limited scalability, they would be sufficient to support the development of protein-based neuronal differentiation technology. Besides needing high concentrations of soluble transcription factor, the efficiency of differentiation is a critical issue. Even if a protein-based differentiation procedure was developed, if it was too inefficient, it would not be able to generate the large number of cells needed for cell replacement therapy.

Two months before the completion of this thesis, the first paper describing a form of neuronal differentiation using recombinant transcription factors was published (Mirakhori et al., 2015). In this article, a complex cocktail of small molecules, along with recombinant Tat-Sox2 and Tat-Lmx1a, was utilized to transdifferentiate human foreskin fibroblasts to dopaminergic progenitor cells capable of expanding and spontaneously differentiating into dopaminergic neurons. This article, while extremely interesting, did have a few limitations. First, there was no information given regarding efficiency, likely indicating efficiency was very low. It is possible that this was due to limited functionality of their resolubilized transcription factors. Second, the method was complex and involved a cocktail of small molecules as well.

The ideal method to generate replacement neurons or specialized dopaminergic neurons would be efficient, straightforward, and lead to high concentrations of fully differentiated neurons that would be safe for transplantation. Two methods described in Chapter 3 have the potential to improve process efficiency: the *in vitro* translation system, and PCI to improve the nuclear delivery of the transcription factors following endocytosis. The feasibility of these two methods has been demonstrated in this thesis, but significant

work will need to be required to use them to develop an efficient protein-based differentiation scheme.

5.2.3. The potential of RDP-IgAh-GCase as a therapy for neuronopathic Gaucher's disease

RDP-IgAh-GCase is the first neuron-targeted recombinant GCase ever developed, and as a result, the enzyme has significant potential for use in enzyme replacement therapy for neuronopathic GD. Chapter 4 described the preferential delivery and *in vitro* functionality of the enzyme. Future work can facilitate the continued development of RDP-IgAh-GCase including improving the production and purification schemes and demonstrating *in vivo* functionality.

The first goal of this work is to finish the *in vitro* characterization of RDP-IgAh-GCase delivery. One interesting result from the substrate reduction work is that both Tat-GCase and RDP-IgAh-GCase reduced glucosylsphingosine accumulation to approximately wild-type levels. Since I have reproducibly shown that RDP-IgAh-GCase treatment delivers more GCase and enzyme activity intracellularly, this result likely indicates that we delivered more Tat-GCase or RDP-IgAh-GCase than was necessary. The GCKO mouse neuronal cell line needs to be treated with several concentrations of either Tat-GCase or RDP-IgAh-GCase to generate dose response curves. The expected and probable result will be that a lower RDP-IgAh-GCase dose can clear the glucosylsphingosine substrate.

After the *in vitro* delivery work is completed and dose-response curves are generated, the next major goal of the project will be to evaluate the therapeutic effects of RDP-IgAh-GCase in neuronopathic GD mouse models. Before the *in vivo* effects can be

evaluated, improved production and purification methods need to be developed. As is done in the biopharmaceutical industry, I would propose that a stable mammalian cell line expressing high levels of RDP-IgAh-GCase be generated to maximize secreted protein production. With a stable cell line, production could be scaled up and traditional bioprocess techniques could be utilized to considerably improve enzyme yields. With higher yields, multiple purification steps could be performed to improve final product purity, and as a result, improve final product activity (Van Patten et al., 2007). When the purified RDP-IgAh-GCase and Tat-GCase stocks were desalted, protein was not lost but activity was. With higher yield and purity, purification schemes that do not reduce activity could be developed. The design of the RDP-IgAh-GCase could be further optimized as well. The Fishman Lab has shown that RDP can enhance GFP internalization ~9x more than Tat, indicating that perhaps the potential of RDP-mediated binding with GCase has not been fully realized (Mello et al., in preparation).

With more pure and higher RDP-IgAh-GCase yields, *in vivo* evaluation of RDP-IgAh-GCase's therapeutic potential could be performed. The ideal mouse model for *in vivo* evaluation is the 4L;C* neuronopathic mouse GD model that has homozygous V394L *GBA1* mutation and is null for GCase activator saposin C. This mouse model was generated by our collaborator Dr. Ying Sun. This mouse model has 4-10% of wild-type GCase activity that is particularly unstable due to the lack of saposin C. The mice develop neurological symptoms at day 30 and die by day 48 (Sun et al., 2011). Although their lifespan seems relatively short, it is considerably longer than the neuronopathic K14 GD model that has been used in phenotype correction research (Cabrera-Salazar et al., 2010; Cabrera-Salazar et al., 2012). The 4L;C* model accumulates both glucosylceramide and

glucosylsphingosine and will allow the assessment of substrate reduction. It will be critical to test multiple dosing strategies. Intravenous delivery will need to be assessed since RDP has the potential to cross the BBB. Also, direct brain infusion that has been performed with mannose-terminal GCase (Lonser et al., 2005), should be attempted. It would be interesting to test whether RDP-IgAh-GCase therapeutic effects could be enhanced with the addition of small molecules therapies that were described at length in Chapter 1. It has been suggested that small molecule therapies may be most effective in combination with some sort of enzyme replacement therapy (Cabrera-Salazar et al., 2012).

The final future direction for the RDP-IgAh-GCase work is to investigate alternate delivery strategies that still take advantage of the enhanced neuronal binding of the enzyme. Work has already begun in the Fishman Lab in pursuit of this goal. With the IgK signal peptide, the RDP-IgAh-GCase expression vector could be transfected into neuronal cells, secreted by producer cells, and taken up by a large proportion of surrounding cells due to the presence of RDP. To this end, we have already constructed a third generation lentiviral expression system to test the feasibility of this idea. The pursuit of genetic techniques to deliver RDP-IgAh-GCase does not mean that the protein delivery approach is not feasible or valuable. RDP-IgAh-GCase has great potential for neuronopathic GD therapy and this potential merits the investigation of multiple delivery strategies.

References Cited

(1)   Anderson DC, Nichols E, Manger R, Woodle D, Barry M, Fritzberg AR. 1993. Tumor cell retention of antibody FAB fragments is enhanced by an attached HIV Tat protein-derived peptide. *Biochem Biophys Res Comm*, 194, 876-884.

(2)   Arai R, Ueda H, Kitayama A, Kamiya N, Nagamune T. 2001. Design of the linkers which effectively separate domains of a bifunctional fusion protein. *Protein Eng*, 14, 529-532.

(3)   Barati S, Chegini F, Hurtado P, Rush RA. 2002. Hybrid tetanus toxin C fragment-diphtheria toxin translocation domain allows specific gene transfer into PC12 cells. *Exp Neurol*, 177, 75-87.

(4)   Barzilay R, Ben-Zur T, Bulvik S, Melamed E, Offen D. 2009. Lentiviral delivery of LMX1a enhances dopaminergic phenotype in differentiated human bone marrow mesenchymal stem cells. *Stem Cells Dev.*, 18, 591-601.

(5)   Berg K, Selbo PK, Prasmickaite L, Tjelle TE, Sandvig K, Moan J, Gaudernack G, Fodstad O, Kjølsrud S, Anholt H, Rodal GH, Rodal SK, Høgset A. 1999. Photochemical internalization: a novel technology for delivery of macromolecules into cytosol. *Cancer Res*, 59, 1180-3.

(6)   Berg K, Weyergang A, Prasmickaite L, Bonsted A, Høgset A, Strand MT, Wagner E, Selbo PK. 2010. Photochemical internalization (PCI): a technology for drug delivery. *Methods Mol Biol*, 635, 133-45.

(7)   Berg-Fussman A, Grace ME, Ioannou Y, Grabowski GA. 1993. Human acid beta-glucosidase: N-glycosylation site occupancy and the effect of glycosylation on enzymatic activity. *J Biol Chem*, 268, 14861-14866.

(8)   Bhandari DG, Levine BA, Trayer IP, Yeadon ME. 1986. 1H-NMR study of motility and conformational constraints within the proline-rich N-terminal of the LC1 alkali light chain of skeletal myosin. *Eur J Biochem*, 160, 349-356.

(9)   Böckenhoff A, Cramer S, Wölte P, Knieling S, Wohlenberg C, Gieselmann V, Galla HJ, Matzner U. 2014. Comparison of five peptide delivery vectors for improved brain delivery of the lysosomal enzyme arylsulfatase A. *J Neurosci*, 34, 3122-3129.

(10)   Boussif O, Lezoualc'h F, Zanta MA, Mergny MD, Scherman D, Demeneix B, Behr JP. 1995. A versatile vector for gene and oligonucleotide transfer into cells in culture and in vivo: polyethylenimine. *Proc Natl Acad Sci U S A*, 92, 7297-7301.

(11)   Box M, Parks DA, Knigh A, Hale C, Fishman PS, Fairweather NF. 2003. A multi-domain protein system based on the HC fragment of tetanus toxin for targeting DNA to neuronal cells. *J Drug Target*, 11, 333-343.

(12)   Branco Novo J, Morganit L, Maria Moro A, Paes Leme AF, de Toledo Serrano SM, Raw I, Ho PL. 2012. Generation of Chinese Hamster Ovary cell line producing recombinant human glucocerebrosidase. *J Biomed Biotechnol*, 875383.

(13)   Brumshtein B, Salinas P, Peterson B, Chan V, Silman I, Sussman JL, Savickas PJ, Robinson GS, Futerman AH.. 2010. Characterization of gene-activated human acid-β-glucosidase: Crystal structure, glycan composition, and internalization into macrophages. *Glycobiology*, 20, 24-32.

(14)   Busterbosch MK, Donker W, Van De Bilt H, Van Weely S, Van Berkel TJC, Aerts JMFG. 1996. Quantitative analysis of the targeting of mannose-terminal

glucocerebrosidase predominant uptake by liver endothelial cells. *Eur J Biochem*, 237, 344-349.

(15)   Cabrera-Salazar MA, Bercury SD, Ziegler RJ, Marshall J, Hodges BI, Chuang WL, Pacheco J, Li L, Cheng SH, Scheule RK. 2010. Intracerebroventricular delivery of glucocerebrosidase reduces substrates and increases lifespan in a mouse model of neuronopathic Gaucher disease. *Exp Neurol*, 225, 436-444.

(16)   Cabrera-Salazar MA, DeRiso M, Bercury SD, Li L, Lydon JT, Weber W, Pande N, Cromwell MA, Copeland D, Leonard J, Cheng SH, Scheule RK. 2012. Systemic delivery of a glucosylceramide synthase inhibitor reduces CNS substrates and increases lifespan in a mouse model of type 2 Gaucher disease. *PLoS One*, 7, e43310.

(17)   Cai J, Donaldson A, Yang M, German MS, Enikolopov G, Iacovitti L. 2009. The role of Lmx1a in the differentiation of human embryonic stem cells into midbrain dopamine neurons in culture and after transplantation into a Parkinson's Disease model. *Stem Cells*, 27, 220-229.

(18)   Caiazzo M, Dell Anno MT, Dvoretskova E, Lazarevic D, Taverna S, Leo D, Sotnikova TD, Menegon A, Roncaglia P, Colciago G, Russo G, Carninci P, Pezzoli G, Gainetdinov RR, Gustincich S, Dityatev A, Broccoli V. 2011. Direct generation of functional dopaminergic neurons from mouse and human fibroblasts. *Nature*, 476, 224-229.

(19)   Calvo AC, Oliván S, Manzano R, Zaragoza P, Aguilera J, Osta R. 2012. Fragment C of Tetanus Toxin: New Insights into Its Neuronal Signaling Pathway. *Int J Mol Sci*, 13, 6883-6901.

(20)   Capablo JL, Franco R, Sáenz de Cabezón A, Alfonso P, Pocovi M, Giraldo P.
         2007. Neurologic improvement in a type 3 Gaucher disease patient treated with
         imiglucerase/miglustat combination. *Epilepsia*, 48, 1406-1408.

(21)   Chauhan A, Tikoo A, Kapur AK, Singh M. 2007. The taming of the cell
         penetrating domain of the HIV Tat: myths and realities. *J Control Release*, 17,
         148-162.

(22)   Chen C, Fu Z, Kim JJ, Barbieri JT, Baldwin MR. 2009. Gangliosides as high
         affinity receptors for tetanus neurotoxin. *J Biol Chem*, 284, 26569-26577.

(23)   Chen X, Zaro JL, Shen WC. 2013. Fusion protein linkers: property, design, and
         functionality. *Adv Drug Deliv Rev*, 65, 1357-1369.

(24)   Chung S, Kim CH, Kim KS. 2012. Lmx1a regulates dopamine transporter gene
         expression during ES cell differentiation and mouse embryonic development. *J
         Neurochem*, 122, 244-250.

(25)   Ciftci K, Levy RJ. 2001. Enhanced plasmid DNA transfection with
         lysosomotropic agents in cultured fibroblasts. *Int J Pharm*, 218, 81-92.

(26)   Cromey DW. 2010. Avoiding twisted pixels: ethical guidelines for the appropriate
         use and manipulation of scientific digital images. *Sci Eng Ethics*, 16, 639-667.

(27)   Davis AS, Federici T, Ray WC, Boulis NM, O'Connor D, Clark KR, Bartlett JS.
         2015. Rational design and engineering of a modified Adeno-Associated Virus
         (AAV1)-based vector system for enhanced retrograde delivery. *Neurosurgery*, 76,
         216-225.

(28)   Decressac M, Volakaksis N, Björklund A, Perlmann T. 2013. Nurr1 in Parkinson
         disease-from pathogenesis to therapeutic potential. *Nat Rev Neurol*, 9, 629-636.

(29)   Derossi D, Joliot AH, Chassaing G, Prochiantz A. 1994. The third helix of the antennapedia homeodomain translocates through biological membranes. *J Biol Chem*, 269, 10444-10450.

(30)   Deshayes S, Morris MC, Divita G, Heitz F. 2005. Cell-penetrating peptides: tools for intracellular delivery of therapeutics. *Cell Mol Life Sci*, 62, 1839-1849.

(31)   Drachman DB, Adams RN, Balasubramanian U, Lu Y. 2010. Strategy for treating motor neuron diseases using a fusion protein of botulinum toxin binding domain and streptavidin for viral vector acess: work in progress. *Toxins*, 2, 2872-2889.

(32)   Dvir H, Harel M, McCarthy AA, Toker L, Silman I, Futerman AH, Sussman JL. 2003. X-ray structure of human acid β-glucosidase, the defective enzyme in Gaucher disease. *EMBO Rep*, 4, 704-709.

(33)   Ebert AD, McMillan EL, Svendsen CN. 2008. Isolating, expanding, and infecting human and rodent fetal neural progenitor cells. *Curr Protoc Stem Cell Biol*, Chapter 2, Unit 2D.2.

(34)   Eiríksdóttir E, Mäger I, Lehto T, El Andaloussi S, Langel U. 2010. Cellular internalization kinetics of (luciferin-)cell-penetrating peptide conjugates. *Bioconjug Chem*, 21, 1662-1672.

(35)   Elliot G, O'Hare P. 1997. Intercellular trafficking and protein delivery by a herpesvirus structural protein. *Cell*, 88, 223-233.

(36)   El-Sayed A, Futaki S, Harashima H. 2009. Delivery of macromolecules using arginine-rich cell-penetrating peptides: ways to overcome endosomal entrapment. *AAPS J*, 11, 13-22.

(37)   Endoh T, Sisido M, Ohtsuki T. 2008. Cellular siRNA delivery mediated by a cell-
        permeant RNA-binding protein and photoinduced RNA interference. *Bioconjug
        Chem*, 19, 1017-1024.

(38)   Erickson A, Bembi B, Schiffmann R. 1997. Neuronopathic forms of Gaucher's
        disease. *Baillieres Clin Haematol*. 10, 711-723.

(39)   Evans JS, Levine BA, Trayer IP, Dorman CJ, Higgins CF. 1986. Sequence-imposed
        structural constraints in the TonB protein of *E. coli*. *FEBS Lett*, 208, 211-216.

(40)   Farfel-Becker T, Vitner EB, Futerman AH. 2011. Animal models for Gaucher
        disease research. *Dis Model Mech*, 4, 746-752.

(41)   Fawell S, Seery J, Daikh Y, Moore C, Chen LL, Pepinsky B, Barsoum J. 1994.
        Tat-mediated delivery of heterologous proteins into cells. *Proc Natl Acad Sci U S
        A*, 91, 664-668.

(42)   Federici T, Liu JK, Teng Q, Yang J, Boulis NM. 2007. A means for targeting
        therapeutics to peripheral nervous system neurons with axonal damage.
        Neurosurgery, 60, 911-918.

(43)   Felgner PL, Gadek TR, Holm M, Roman R, Chan HW, Wenz M, Northrop JP,
        Ringold GM, Danielsen M. 1987. Lipofection: a highly efficient, lipid-mediated
        DNA-transfection procedure. *Proc Natl Acad Sci U S A*, 84, 7413-7417.

(44)   Ficicioglu C. 2008. Review of miglustat for clinical management in Gaucher
        disease type 1. *Ther Clin Risk Manag*, 4, 425-431.

(45)   Figueiredo DM, Hallewell RA, Chen LL, Fairweather NF, Dougan G, Savitt JM,
        Parks DA, Fishman PS. 1997. Delivery of recombinant tetanus-superoxide

dismutase proteins to central nervous system neurons by retrograde axonal transport. *Exp Neurol*, 145, 546-554.

(46)   Figueiredo DM, Matthews CC, Parks DA, Fairweather NF, Dougan G, Wilt SG, Fishman PS. 2000. Interaction of tetanus toxin derived hybrid proteins with neuronal cells. *J Nat Toxins*, 4, 363-379.

(47)   Fishman PS, Savitt JM. 1989. Transsynaptic transfer of retrogradely transported tetanus protein-peroxidase conjugates. *Exp Neurol*, 106, 197-203.

(48)   Fishman PS, Parks DA, Patwardhan AJ, Matthews CC. 1999. Neuronal binding of tetanus toxin compared to its ganglioside binding fragment (H(c)). *Nat Toxins*, 4, 151-156.

(49)   Fishman PS. (2009). Tetanus Toxin. In: Jankovic J, ed. Botulinum Toxin: Therapeutic Clinical Practice & Science. Philadelphia: Saunders, 406-424.

(50)   Francis JW, Hosler BA, Brown Jr. RH, Fishman PS. 1995. CuZn superoxide dismutase (SOD-1): tetanus toxin fragment C hybrid protein for targeted delivery of SOD-1 to neuronal cells. *J Biol Chem*, 270, 15434-15442.

(51)   Francis JW, Brown Jr. RH, Figueiredo D, Remington MP, Castillo O, Schwarzschild MA, Fishman PS, Murphy JR, vanderSpek JC. 2000. Enhancement of diphtheria toxin potency by replacement of the receptor binding domain with tetanus toxin C-fragment: a potential vector for delivering heterologous proteins to neurons. *J Neurochem*, 74, 2528-2536.

(52)   Francis JW, Bastia E, Matthews CC, Parks DA, Schwarzschild MA, Brown Jr. RH, Fishman PS. 2004. Tetanus toxin fragment C as a vector to enhance delivery of proteins to the CNS. *Brain Res*, 1011, 7-13.

162

(53)   Frankel AD, Pabo CO. 1988. Cellular uptake of the tat protein from human

immunodeficiency virus. *Cell*, 55, 1189-1193.

(54)   Fretz MM, Høgset A, Koning GA, Jiskoot W, Storm G. 2007. Cytosolic delivery

of liposomally targeted proteins induced by photochemical internalization. *Pharm

Res*, 24, 2040-2047.

(55)   Friedman B, Vaddi K, Preston C, Mahon E, Cataldo JR, McPherson JM. 1999. A

comparison of the pharmacological properties of carbohydrate remodeled

recombinant and placental-derived β-glucocerebrosidase: Implications for clinical

efficacy in treatment of Gaucher Disease. *Blood*, 93, 2807-2816.

(56)   Fu A, Wang Y, Zhan L, Zhou R. 2012. Targeted delivery of proteins into the

central nervous system mediated by rabies virus glycoprotein-derived peptide.

Pharm Res, 29, 1562-1569.

(57)   Fu A, Zhang M, Gao F, Xu X, Chen Z. 2013a. A novel peptide delivers plasmids

across blood-brain barrier into neuronal cells as a single-component transfer

vector. *PLoS One*, 8, e59642.

(58)   Fu A, Zhao Z, Gao F, Zhang M. 2013b. Cellular uptake mechanism and

therapeutic utility of a novel peptide in targeted-delivery of proteins into neuronal

cells. *Pharm Res*, 30, 2108-2117.

(59)   Furbish FS, Steer CJ, Krett NL, Barranger JA. 1981. Uptake and distribution of

placental glucocerebrosidase in rat hepatic cells and effects of sequential

deglycosylation. *Biochim Biophys Acta*, 673, 425-434.

(60)   Gao Y, Wang ZY, Zhang J, Zhang Y, Huo H, Wang T, Jiang T, Wang S. 2014. RVG-peptide-linked trimethylated chitosan for delivery of siRNA to the brain. *Biomacromolecules*, 15, 1010-1018.

(61)   Geisler IM, Chmielewski J. 2011. Dimeric cationic amphiphilic polyproline helices for mitochondrial targeting. *Pharm Res*, 28, 2797-2807.

(62)   George RA, Heringa J. 2003. An analysis of protein domain linkers: their classification and role in protein folding. *Protein Eng*, 15, 871-879.

(63)   Gianolio E, Arena F, Strijkers GJ, Nicolay K, Högset A, Aime S. 2011. Photochemical activation of endosomal escape of MRI-Gd-agents in tumor cells. *Magn Reson Med*, 65, 212-219.

(64)   Gillmeister MP. 2009. Additions to recombinant proteins for delivery and function. Doctoral dissertation, Johns Hopkins University.

(65)   Gillmeister MP, Betenbaugh MJ, Fishman PS. 2011. Cellular trafficking and photochemical internalization of cell penetrating peptide linked cargo proteins: a dual fluorescent labeling study. *Bioconjug Chem*, 22, 556-566.

(66)   Gong C, Li X, Xu L, Zhang YH. 2012. Target delivery of a gene into the brain using the RVG29-oligoarginine peptide. *Biomaterials*, 33, 3456-3463.

(67)   Grace ME, Newman KM, Scheinker V, Berg-Fussman A, Grabowski GA. 1994. Analysis of human acid β-glucosidase by site-directed mutagenesis and heterologous expression. *J Biol Chem*, 269, 2283-2291.

(68)   Gramlich PA, Remington MP, Amin J, Betenbaugh MJ, Fishman PS. 2013. Tat-Tetanus Toxin Fragment C: a novel protein delivery vector and its use with photochemical internalization. *J Drug Target*, 21, 662-674.

(69)   Griesel G, Krug C, Yurlova L, Diaconu M, Mansouri A. 2011. Generation of
        knockout mice expressing a GFP-reporter under the control of the *Lmx1a* locus.
        Gene Expr Patterns, 11, 345-348.

(70)   Grubb JH, Volger C, Sly WS. 2010. New strategies for enzyme replacement
        therapy for lysosomal storage diseases. *Rejuvenation Res*, 13, 229-236.

(71)   Hallewell RA, Laria I, Tabrizi A, Gunnar C, Getzoff ED, Tainer JA, Cousena LS,
        Mullenbach GT. 1989. Genetically engineered polymers of human CuZn
        superoxide dismutase. *J Biol Chem*, 264, 5260-5268.

(72)   Hart O, Westphal H. 2000. Functions of LIM-homeobox genes. *Trends Genet*, 16,
        75-83.

(73)   Hassane FS, Abes R, El Andaloussi S, Lehto T, Sillard R, Langel U, Lebleu B.
        2011. Insights into the cellular trafficking of splice redirecting oligonucleotides
        complexed with chemically modified cell-penetrating peptides. *J Control Release*,
        153, 163-172.

(74)   Heitz F, Morris MC, Divita G. 2009. Twenty years of cell-penetrating peptides:
        from molecular mechanisms to therapeutics. *Br J Pharmacol*, 157, 195-206.

(75)   Hruska KS, LaMarca ME, Scott CR, Sidransky E. 2008. Gaucher disease:
        mutation and polymorphism spectrum in the glucocerebrosidase gene (*GBA*).
        Hum Mutat, 29, 567-583.

(76)   Huang H, Kubish GM, Redmond TM, Turner DL, Thompson RC, Murphy GG,
        Uhler MC. 2010. Direct transcriptional activation of Gadd45γ by AsclI during
        neuronal differentiation. *Molecular and Cellular Neuroscience*, 44, 282-296.

(77) Jiang C, Wan X, He Y, Pan T, Jankovic J, Le W. 2005. Age-dependent dopaminergic dysfunction in Nurr1 knockout mice. *Exp Neurol*, 191, 154-162.

(78) Jin LH, Bahn JH, Eum WS, Kwon HY, Jang SH, Han KH, Kang TC, Won MH, Kang JH, Cho SW, Park J, Choi SY. 2001. Transduction of human catalase mediated by an HIV-1 Tat protein basic domain and arginine-rich peptides into mammalian cells. *Free Radical Biology Medicine*, 31, 1509-1519.

(79) Jin G, Zhu G, Zhao Z, Liu F. 2012. VP22 enhances the expression of glucocerebrosidase in human gaucher II fibroblast cells mediated by lentiviral vectors. *Clin Exp Med*, 12, 135-143.

(80) Jo J, Hong S, Choi WY, Lee DR. 2014. Cell-penetrating peptide (CPP)-conjugated proteins is an efficient tool for manipulation of human mesenchymal stromal cells. *Scientific Reports*, 4, 1-8.

(81) Johnson MM, Michelhaugh SK, Bouhamdan M, Schmidt CJ, Bannon MJ. 2011. The transcription factor NURR1 exerts concentration-dependent effects on target genes mediating distinct biological processes. *Front Neurosci*, 5, 135.

(82) Jones SW, Christison R, Bundell K, Voyce CJ, Brockbank SM, Newham P, Lindsay MA. 2005. Characterisation of cell-penetrating peptide-mediated peptide delivery. *Br J Pharmacol*, 145, 1093-1102.

(83) Kadkhodaei B, Ito T, Joodmardi E, Mattsson B, Rouillard C, Carta M, Muramatsu SI, Sumi-Ichinose C, Nomura T, Metzger D, Chambon P, Lindqvist E, Larrson NG, Olson L, Björklund A, Ichinose H, Perlmann T. 2009. Nurr1 is required for maintenance of maturing and adult midbrain dopamine neurons. *J Neurosci*, 29, 15923-15932.

(84)   Kaplan IM, Wadia JS, Dowdy SF. 2005. Cationic TAT peptide transduction domain enters cells by macropinocytosis. *J Control Release*, 102 247-253. Erratum in: *J Control Release*, 107 (2005), 184-185. *J Control Release*, 107 (2005), 571-572.

(85)   Kassa R, Monterroso V, David LL, Tshala-Katumbay D. 2013. Diagnostic and therapeutic potential of tetanus toxin-derivatives in neurological disease. *J Mol Neurosci*, 51, 788-791.

(86)   Kern SM, Feig AL. 2011. Adaptation of Clostridium difficile toxin A for use as a protein translocation system. *Biochem Biophys Res Commun*, 405, 570-574.

(87)   Khanna R, Benjamin ER, Pellegrino L, Schilling A, Rigat BA, Soska R, Nafar H, Ranes BE, Feng J, Lun Y, Powe AC, Palling DJ, Wustman BA, Schiffmann R, Mahuran DJ, Lockhart DJ, Valenzano KJ. 2010. The pharmacological chaperone isofagomine increases activity of the Gaucher disease L444P mutant form of β-glucosidase. *FEBS J*, 277, 1618-1638.

(88)   Kim D, Kim CH, Moon JI, Chung YG, Chang MY, Han BS, Ko S, Yang E, Cha KY, Lanza R, and Kim KS. 2009. Generation of Human Induced Pluripotent Stem Cells by Direct Delivery of Reprogramming Proteins. *Cell Stem Cell*, 4, 472-476.

(89)   Kim HS, Kim J, Jo Y, Jeon D, Cho YS. 2014. Direct lineage reprogramming of mouse fibroblasts to functional midbrain dopaminergic neuronal progenitors. *Stem Cell Res*, 12, 60-68.

(90)   Koo SK, Hill JK, Hwang CH, Lin ZS, Millen KJ, Wu DK. 2009. *Lmx1a* maintains proper neurogenic, sensory, and non-sensory domains in the mammalian inner ear. *Dev Biol*, 333, 14-25.

(91)   Koya V, Lu S, Sun YP, Purich DL, Atkinson MA, Li SW, Yang LJ. 2008.
         Reversal of streptozotocin-induced diabetes in mice by cellular transduction with
         recombinant pancreatic transcription factor Duodenal Homeobox-1. *Diabetes*, 57,
         757-769.

(92)   Kumar P, Wu H, McBride JL, Jung KE, Kim MH, Davidson BL, Lee SK,
         Shankar P, Manjunath N. 2007. Transvascular delivery of small interfering RNA
         to the central nervous system. *Nature*, 448, 39-45.

(93)   Kwon YW, Chung YJ, Kim J, Lee HJ, Park J, Roh TY, Cho HJ, Yoon CH, Koo
         BK, Kim KS. 2014. Comparative study of efficacy of dopaminergic neuron
         differentiation between embryonic stem cell and protein-based induced
         pluripotent stem cell. *PLoS One*, 9, e85736.

(94)   Lan MS, Chen C, Saunee NA, Zhang T, Breslin MB. 2014. Expression of
         biologically active TAT-fused recombinant islet transcription factors. *Life
         Sciences*, 114, 45-50.

(95)   Lee CY, Li JF, Liou JS, Charng YC, Huang YW, Lee HJ. 2011. A gene delivery
         system for human cells mediated by both a cell-penetrating peptide and a
         piggyBac transposase. *Biomaterials*, 32, 6264-6276.

(96)   Lee KO, Luu N, Kaneski CR, Schiffmann R, Brady RO, Murray GJ. 2005.
         Improved intracellular delivery of glucocerebrosidase mediated by the HIV-1 Tat
         protein transduction domain. *Biochem Biophys Res Commun*, 337, 701-707.

(97)   Lentz TL. 1990. Rabies virus binding to an acetylcholine receptor α-subunit
         peptide. *J Mol Recognit*, 3, 82-88.

(98) Li Y, Cong B, Ma C, Qi Q, Fu L, Zhang G, Min Z. 2011. Expression of Nurr1 during rat brain and spinal cord development. *Neurosci Letters*, 488, 49-54.

(99) Li Y, Foran P, Fairweather NF, de Paiva A, Weller U, Dougan G, Dolly JO. 1994. A single mutation in the recombinant light chain of tetanus toxin abolishes its proteolytic activity and removes the toxicity seen after reconstitution with native heavy chain. *Biochemistry*, 33, 7014-7020.

(100) Li J, Chian RJ, Ay I, Celia SA, Kashi BB, Tamrazian E, Matthews JC, Remington MP, Pepinsky RB, Fishman PS, Brown Jr RH, Francis JW. 2009. Recombinant GDNF: Tetanus toxin fragment C fusion protein produced from insect cells. *Biochem Biophys Res Commun*, 385, 380-384.

(101) Li J, Chian RJ, Ay I, Kashi BB, Celia SA, Tamrazian E, Pepinsky RB, Fishman PS, Brown Jr. RH, Francis JW. 2009. Insect GDNF:TTC fusion protein improves delivery of GDNF to mouse CNS. *Biochem Biophys Res Commun*, 390, 947-951.

(102) Liu Y, Huang R, Han L, Ke W, Shao K, Ye L, Lou J, Jiang C. 2009. Brain-targeting gene delivery and cellular internalization mechanisms for modified rabies virus glycoprotein RVG29 nanoparticles. *Biomaterials*, 30, 4195-4202.

(103) Lonser RR, Walbridge S, Murray GJ, Aizenberg MR, Vortmeyer AO, Aerts JMFG, Brady RO, Oldfield EO. 2005. Convection perfusion of glucocerebrosidase for neuronopathic Gaucher's disease. *Ann Neurol*, 57, 542-548.

(104) Lonser RR, Schiffman R, Robison RA, Butman JA, Quezado Z, Walker ML, Morrison PF, Walbridge S, Murray GJ, Park DM, Brady RO, Oldfield EO. 2007.

Image-guided, direct convective delivery of glucocerebrosidase for neuronopathic Guacher disease. *Neurology*, 68, 254-261.

(105) Low T, Liu YSV, Putnam FW. 1976. Structure, funciton, and evolutionary relationships of Fc domains of human immunoglobulins A, G, M, and E. *Science*, 191, 390-392.

(106) Maiolo JR, Ferrer M, Ottinger EA. 2005. Effects of cargo molecules on the cellular uptake of arginine-rich cell-penetrating peptides. *Biochim Biophys Acta*, 1712, 161-172.

(107) Makoff AJ, Oxer MD, Romanos MA, Fairweather NF, Ballantine S. 1989. Expression of tetanus toxin fragment C in E. coli: high level expression by removing rare codons. *Nucleic Acids Res*, 17, 10191-10202.

(108) Maillard AP, Gaudin Y. 2002. Rabies virus glycoprotein can fold into two alternate, antigenically distinct conformations depending on membrane-anchor type. *J Gen Virol*, 83, 1465-1476.

(109) Manosroi A, Lohcharoenkal W, Götz F, Werner RG, Manosroi W, Manosroi J. 2011. Cellular uptake enhancement of Tat-GFP fusion protein loaded in elastic niosomes. *J Biomed Nanotechnol*, 7, 366-376.

(110) Marro S, Pang ZP, Yang N, Tsai MC, Qu K, Chang HY, Südhof TC, Wernig M. 2011. Direct lineage conversion of terminally differentiated hepatocytes to functional neurons. *Cell Stem Cell*, 9, 374-382.

(111) Marshall J, McEachern KA, Cavanagh Kyros JA, Nietupski JB, Budzinski TL, Ziegler RJ, Yew NS, Sullivan J, Scaria A, van Rooijen N, Barranger JA, Cheng

SH. 2002. Demonstration of feasibility of *in vivo* gene therapy for Gaucher disease using a chemically induced mouse model. *Mol Ther*, 6, 179-189.

(112) Martinat C, Bacci JJ, Leete T, Kim J, Vanti WB, Newman AH, Cha JH, Gether U, Wang H, Abeliovich A. 2006. Cooperative transcription activation by Nurr1 and Pitx3 induces embryonic stem cell maturation to the midbrain dopamine neuron phenotype. *Proc Natl Acad Sci U S A*, 103, 2874-2879.

(113) Matsushita M, Noguchi H, Lu YF, Tomizawa K, Michiue H, Li ST, Hirose K, Bonner-Weir S, Matsui H. 2004. Photo-acceleration of protein release from endosome in the protein transduction system. *FEBS Lett*, 572, 221-226.

(114) Meerovich I, Muthukrishnan N, Johnson GA, Erazo-Oliveras A, Pellois JP. 2014. Photodamage of lipid bilayers by irradiation of a fluorescently labeled cell-penetrating peptide. *Biochim Biophys Acta*, 1840, 507-515.

(115) Mello N, Gramlich PA, Remington MP, Fishman PS. 2015. Rabies glyocprotein derived peptide shows enhanced neuronal internalization of GFP compared to tetnaus toxin fragment C, Tat, and Tet-1. In preparation.

(116) Miana-Mena FJ, Roux S, Benichou J, Osta R, Brulet P. 2002. Neuronal activity-dependent membrane traffic at the neuromuscular junction. *Proc Natl Acad Sci U S A*, 99, 3234-3239.

(117) Mirakhori F, Zeynali B, Rassouli H, Salekdeh GH, Baharvand H. 2015. Direct conversion of human fibroblasts into dopaminergic neural progenitor-like cells using Tat-mediated protein transduction of recombinant factors. *Biochem Biophys Res Comm*, 459, 655-661.

(118) Nakase I, Niwa M, Takeuchi T, Sonomura K, Kawabata N, Koike Y, Takehashi M, Tanaka S, Ueda K, Simpson JC, Jones AT, Sugiura Y, Futaki S. 2004. Cellular uptake of arginine-rich peptides: roles for macropinocytosis and actin rearrangement. *Mol Ther*, 10, 1011-1022.

(119) Nakase I, Tadokoro A, Kawabata N, Takeuchi T, Katoh H, Hiramoto K, Negishi M, Nomizu M, Sugiura Y, Futaki S. 2007. Interaction of arginine-rich peptides with membrane-associated proteoglycans is crucial for induction of actin organization and macropinocytosis, *Biochemistry*, 46, 492-501.

(120) Nemes C, Varga E, Polgar Z, Klincumhorn N, Pirity MK, Dinnyes A. 2014. Generation of mouse induced pluripotent stem cells by protein transduction. *Tissue Engineering: Part C*, 20, 383-392.

(121) Nishimura S, Takahashi S, Kamikatahira H, Kuroki Y, Jaalouk DE, O'Brien S, Koivunen E, Arap W, Pasqualini R, Nakayama H, Kuniyasu A. 2008. Combinatorial targeting of the acropinocytotic pathway in leukemia and lymphoma cells. *J Biol Chem*, 283, 11752-11762.

(122) Oliveira H, Fernandez R, Pires LR, Martins MC, Simões S, Barbosa MA, Pêgo AP. 2010. Targeted gene delivery into peripheral sensorial neurons mediated by self-assembled vectors composed of poly(ethylene imine) and tetanus toxin fragment C. *J Control Release*, 143, 350-358.

(123) Pan C, Lu B, Chen H, Bishop CE. 2010. Reprogramming human fibroblasts using HIV-1 TAT recombinant proteins OCT4, SOX2, KLF2 and c-MYC. *Mol Biol Rep*, 37, 2117-2124.

(124)   Panicker LM, Miller D, Park TS, Patel B, Azevedo JL, Awad O, Masood MA, Veenstra TD, Goldin E, Stubblefiedl BK, Tayebi N, Polumuri SK, Vogel SN, Sidransky E, Zambidis ET, Feldman RA. Induced pluripotent stem cell model recapitulates pathologic hallmarks of Gaucher disease. *Proc Natl Acad Sci U S A*, 109, 18054-18059.

(125)   Panicker LM, Miller D, Awad O, Bose V, Lun Y, Park TS, Zambidis ET, Sgambato JA, and Feldman RA. 2014. Gaucher iPSC-derived macrophages produce elevated levels of inflammatory mediators and serve as a new platform for therapeutic development. *Stem Cells,* 32, 2338-2349.

(126)   Park IK, Lasiene J, Chou SH, Horner PJ, Pun SH. 2007. Neuron-specific delivery of nucleic acids mediated by Tet1-modified poly(ethylenimine). *J Gene Med*, 9, 691-702.

(127)   Pastores GM. 2010. Recombinant glucocerebrosidase (imiglucerase) as a therapy for Gaucher disease. *Biodrugs*, 24, 41-47.

(128)   Peitz M, Münst B, Thummer RP, Helfen M, Edenhofer F. 2014. Cell-permeant recombinant Nanog protein promotes pluripotency by inhibiting endodermal specification. *Stem Cell Res*, 12, 680-689.

(129)   Pepinsky RB, Androphy EJ, Corina K, Brown R, Barsoum J. 1994. Specific inhibition of Human Papillomavirus E2 trans-activator by intracellular delivery of its repressor. *DNA Cell Biol*, 13, 1011-1019.

(130)   Perlmann T, Wallén-Mackenzie Å. 2004. Nurr1, an orphan nuclear receptor with essential functions in developing dopamine cells. *Cell Tissue Res*, 318, 45-52.

(131)   Perrier AL, Tabar V, Barberi T, Rubio ME, Bruses J, Topf N, Harrison NL, Studer L. 2004. Derivation of midbrain dopamine neurons from human embryonic stem cells. *Proc Natl Acad Sci U S A*, 101, 12543-12548.

(132)   Pfisterer U, Kirkeby A, Torper O, Wood J, Nelander J, Dufour A, Björklund A, Lindvall O, Jakobsson J, Parmar M. 2011. Direct conversion of human fibroblasts to dopaminergic neurons. *Proc Natl Acad Sci U S A*, 108, 10343-10348.

(133)   Pooga M, Hällbrink M, Zorko M, Langel Ü. 1998. Cell penetration by transportan. *FASEB*, 12, 67-77.

(134)   Poole, RM. 2014. Eliglustat: first global approval. *Drugs*, 74, 1829-1836.

(135)   Qiang L, Fujita R, Yamashita T, Angulo S, Rhinn H, Rhee D, Doege C, Chau L, Aubry L, Vanti WB, Moreno H, Abeliovich A. 2011. Direct conversion of Alzheimer's Disease patient skin fibroblasts into functional neurons. *Cell*, 146, 359-371.

(136)   Rekha KR, Inmozhisivakamasundari R. 2014. Nurr1: a new insight to protect dopaminergic neurodegeneration in Parkinson's disease. *Ther Targets Neurol Dis*, 1, e436.

(137)   Renigunta A, Krasteva G, König P, Rose F, Klepetko W, Grimminger F, Seeger W, Hänze J. 2006. DNA transfer into human lung cells is improved with Tat-RGD peptide by caveoli-mediated endocytosis. Bioconjug Chem, 17, 327-334.

(138)   Rhee YH, Ko JY, Chang MY, Yi SH, Kim D, Kim CH, Shim JW, Jo AY, Kim BW, Lee H, Lee SH, Suh W, Park CH, Koh HC, Lee YS, Lanza R, Kim KS, Lee SH. 2011. Protein-based human iPS cells efficiently generate functional dopamine

neurons and can treat a rat model of Parkinson disease. *J Clin Invest*, 121, 2326-2335.

(139) Richard JP, Melikov K, Vives E, Ramos C, Verbeure B, Gait MJ, Chernomordik LV, Lebleu B. 2003. Cell-penetrating peptides: a reevaluation of the mechanism of cellular uptake. *J Biol Chem*, 278, 585-590.

(140) Rinne J, Albarran B, Jylhävä J, Ihalainen TO, Kankaanpää P, Hytönen VP, Stayton PS, Kulomaa MS, Vihinen-Ranta M. 2007. Internalization of novel non-viral vector TAT-streptavidin into human cells. *BMC Biotechnol*, 7: 1.

(141) Saleh AF, Arzumanov A, Abes R, Owen D, Lebleu B, Gait MJ. 2010. Synthesis and splice-redirecting activity of branched, arginine-rich peptide dendrimer conjugates of peptide nucleic acid oligonucleotides. *Bioconjug Chem*, 21, 1902-1911.

(142) Salvioli R, Tatti M, Scarpa S, Moavero SM, Ciaffoni F, Felicetti F, Kaneski CR, Brady RO, Vaccaro AM. 2005. The N370S (Asn^{370}-Ser) mutation affects the capacity of glucosylceramidase to interact with anionic phospholipid-containing membranes and saposin C. *Biochem J*, 390, 95-103.

(143) Sandvig K, Torgersen ML, Engedal N, Skotland T, Iversen TG. 2010. Protein toxins from plants and bacteria: probes for intracellular transport and tools in medicine. *FEBS Lett*, 584, 2626-2634.

(144) Schiffmann R, FitzGibbon EJ, Harris C, DeVile C, Davies EH, Abel L, van Schaik IN, Benko WS, Timmons M, Ries M, Vellodi A. 2008. Randomized, controlled trial of miglustat in Gaucher's disease type 3. *Ann Neurol*, 64, 514-522.

(145) Schönhuber W, Fuchs B, Juretschko S, Amannl R. 1997. Improved sensitivity of whole-cell hybridization by the combination of horseradish peroxidase-labeled oligonucleotides and tyramide signal amplification. *Appl Environ Microbiol*, 63, 3268-3273.

(146) Schueler U, Kaneski C, Murray G, Sandhoff K, Brady RO. 2002. Uptake of mannose-terminal glucocerebrosidase in cultured human cholinergic and dopaminergic neuron cell lines. *Neurochem Res*, 27, 325-330.

(147) Schwarze SR, Ho A, Vocero-Akbani A, Dowdy SF. 1999. In vivo protein transduction: delivery of a biologically active protein into the mouse. *Science*, 285, 1569-1572.

(148) Selbo PK, Weyergang A, Høgset A, Norum OJ, Berstad MB, Vikdal M, Berg K. 2010. Photochemical internalization provides time- and space-controlled endolysosomal escape of therapeutic molecules. *J Control Release*, 148, 2-12.

(149) Shaaltiel Y, Bartfield D, Hashmueli S, Baum G, Brill-Almon E, Galili G, Dym O, Boldin-Adamsky SA, Silman I, Sussman JL, Futerman AH, Aviezer D. 2007. Production of glucocerebrosidase with terminal mannose glycans for enzyme replacement therapy of Gaucher's disease using a plant cell system. *Plant Biotechnol J*, 5, 579-590.

(150) Shiraishi T, Nielsen PE. 2006. Enhanced delivery of cell-penetrating peptide-peptide nucleic acid conjugates by endosomal disruption. *Nat Protoc*, 1, 633-636.

(151) Shiraishi T, Nielsen PE. 2011. Enhanced cellular delivery of cell-penetrating peptide-peptide nucleic acid conjugates by photochemical internalization. *Methods Mol Biol*, 683, 391-397.

(152) Shiraishi T, Nielsen PE. 2011. Improved cellular uptake of antisense peptide nucleic acids by conjugation to a cell-penetrating peptide and a lipid domain. *Methods Mol Biol*, 751, 209-221.

(153) Sidransky E. 2012. Gaucher disease: insights from a rare mendelian disorder. *Discov Med*, 14, 273-281.

(154) Siebert M, Sidransky E, Westbroek W. 2014. Glucocerebrosidase is shaking up the synucleinopathies. *Brain*, 137, 1304-1322.

(155) Sinha, G. 2014. Gaucher's disease oral therapy gets nod from FDA. *Nat Biotechnol*, 32, 970-971.

(156) Soderholm, JF, Bird SL, Kalab P, Sampathkumar Y, Hasegawa K, Uehara-Bingen M, Weis K, Heald R. 2011. Importazole, a small molecule inhibitor of the transport receptor importin-β. *ACS Chemical Biology*, 6, 700-708.

(157) Son EY, Ichida JK, Wainger BJ, Toma JS, Rafuse VF, Woolf CJ, Eggan K. 2011. Conversion of mouse and human fibroblasts into functional spinal motor neurons. *Cell Stem Cell*, 9, 205-218.

(158) Spencer BJ, Verma IM. 2007. Targeted delivery of proteins across the blood-brain barrier. *Proc Natl Acad Sci U S A*, 104, 7594-7599.

(159) Srinivasan D, Muthukrishnan N, Johnson GA, Erazo-Oliveras A, Lim J, Simanek EE, Pellois JP. 2011. Conjugation to the cell-penetrating peptide TAT potentiates the photodynamic effect of carboxytetramethylrhodamine. *PLoS One*, 6, e17732.

(160) Stahl PD, Rodman JS, Miller MJ, Schlesinger PH. 1978. Evidence for receptor-mediated binding of glycoproteins, glycoconjugates, and lysosomal glycosidases by aveolar macrophages. *Proc Natl Acad Sci U S A*, 75, 1399-1403.

(161) Suh JS, Lee JY, Choi YJ, You HK, Hong SD, Chung CP, Park YJ. 2014. Intracellular delivery of cell-penetrating peptide-transcriptional factor fusion protein and its role in selective osteogenesis. *International Journal of Nanomedicine*, 9, 1153-1166.

(162) Sun Y, Ran H, Liou B, Quinn B, Zamzow M, Zhang W, Bielawski J, Kitatani K, Setchell KDR, Hannun YA, Grabowski GA. 2011. Isofagomine *in vivo* effects in a neuronopathic Gaucher disease mouse. *PLoS One*, 6, e19037.

(163) Sun Y, Liou B, Xu YH, Quinn B, Zhang W, Hamler R, Setchell KDR, Grabowski GA. 2012. *Ex vivo* and *in vivo* effects of isofagomine on acid β-glucosidase variants and substrate levels in Gaucher disease. *J Biol Chem*, 287, 4275-4287.

(164) Sun Y, Zhang W, Xu YH, Quinn B, Dasgupta N, Liou B, Setchell KDR, Grabowski GA. 2013. Substrate compositional variation with tissue/region and *Gba1* mutations in mouse models- implications for Gaucher Disease. *PLoS One*, 8, e57560.

(165) Swistowski A, Peng J, Liu Q, Mali P, Rao MS, Zeng X. 2010. Efficient generation of functional dopaminergic neurons from human induced pluripotent stem cells under defined conditions. *Stem Cells*, 28, 1893-1904.

(166) Tachikawa K, Scröder O, Frey G, Briggs SP, Sera T. Regulation of the endogenous VEGF-A gene by exogenous designed regulatory proteins. *Proc Natl Acad Sci U S A*, 101, 15225-15230.

(167) Takahashi K, Yamanaka S. 2006. Induction of pluripotent stem cells from mouse embryonic and adult fibroblast cultures by defined factors. *Cell*, 126, 652-655.

(168)   Takayama K, Nakase I, Michiue H, Takeuchi T, Tomizawa K, Matsui H, Futaki S. 2009. Enhanced intracellular delivery using arginine-rich peptides by the addition of penetration accelerating sequences (Pas). *J Control Release*, 138, 128-133.

(169)   Tamargo RJ, Velayati A, Goldin E, Sidransky E. 2012. The role of saposin C in Gaucher disease. *Mol Genet Metab*, 106, 257-263.

(170)   Tekoah Y, Tzaban S, Kizhner T, Hainrichson M, Gantman A, Golembo M, Avioezer D, Shaaltiel Y. 2013. Glycosylation and functionality of recombinant β-glucocerebrosidase from various production systems. *Biosci Rep*, 33, e0071.

(171)   Thomas M. 2010. Role of transcription factors in cell replacement therapies for neurodegenerative diseases. *Regen Med*, 5, 441-450.

(172)   Turner SL, Russell GC, Williamson MP, Guest GR. 1993. Restructuring an interdomain linker in the dihydrolipoamide acetyltransferase component of the pyruvate dehydrogenase complex of *Escherichia coli*. *Protein Eng*, 6, 101-108.

(173)   Vaags AK, Campbell TN, Choy FYM. 2005. HIV Tat variants differentially influence the production of glucocerebrosidase in *Sf9* cells. *Genet Mol Res*, 4, 491-495.

(174)   Van Patten SM, Hughes H, Huff MR, Piepenhagen PA, Waire J, Qiu H, Chandrashekar G, Reczek D, Ward PV, Kutzko JP, Edmunds T. 2007. Effect of mannose chain length on targeting of glucocerebrosidase for enzyme replacement therapy of Gaucher disease. *Glycobiology*, 17, 467-478.

(175)   Vasconcelos FF, Castro DS. 2014. Transcription control of vertebrate neurogenesis by the proneural factor AsclI. *Front Cell Neurosci*, 8, 1-6.

(176) Vierbuchen T, Ostermeier A, Pang ZP, Kokubu Y, Südhof TC, Wernig M. 2010. Direct conversion of fibroblasts to functional neurons by defined factors. *Nature*, 463, 1035-1041.

(177) Vivès E, Brodin P, Lebleu B. 1997. A truncated HIV-1 Tat protein basic domain rapidly translocates through the plasma membrane and accumulates in the cell nucleus. *J Biol Chem*, 272, 16010-16017.

(178) Wadia JS, Stan RV, Dowdy SF. 2004. Transducible TAT-HA fusogenic peptide enhances escape of TAT-fusion proteins after lipid raft macropinocytosis. *Nat Med*, 10, 310-315.

(179) Walton KM, Sandberg K, Rogers TB, Schnaar RL. 1988. Complex ganglioside expression and tetanus toxin binding by PC12 pheochromocytoma cells. *J Biol Chem*, 263, 2055-2063.

(180) Waters JC. 2009. Accuracy and precision in quantitative fluorescence microscopy. *J Cell Biol*, 185, 1135-1148.

(181) Wang H, Zhong CY, Wu JF, Huang YB, Liu CB. 2010. Enhancement of TAT cell membrane penetration efficiency by dimethyl sulphoxide. *J Control Release*, 143, 64-70.

(182) Wang J, Zurawski TH, Meng J, Lawrence GW, Aoki KR, Wheeler L, Dolly JO. 2012. Novel chimeras of botulinum and tetanus neurotoxins yield insights into their distinct sites of neuroparalysis. *FASEB J*, 26, 5035-5048.

(183) Wang JT, Giuntini F, Eggleston IM, Bown SG, Macrobert AJ. 2012. Photochemical internalisation of a macromolecular protein toxin using a cell penetrating peptide-photosensitiser conjugate. *J Control Release*, 157, 305-313.

(184) Wender PA, Mitchell DJ, Pattabiraman K, Pelkey ET, Steinman L, Rothbard JB. 2000. The design, synthesis, and evaluation of molecules that enable or enhance cellular uptake: peptoid molecular transporters. *Proc Natl Acad Sci U S A*, 97, 13003-13008.

(185) Weyergang A, Berstad MEB, Bull-Hansen B, Olsen CE, Selbo PK, Berg K. 2015. Photochemical activation of drugs for the treatment of therapy-resistant cancers. *Photochem Photobiol Sci*, 10.1039/c5pp00029g.

(186) Xia H, Mao Q, Davidson BL. 2001. The HIV Tat protein transduction domain improves the biodistribution of β-glucuronidase expressed from recombinant viral vectors. *Nat Biotechnol*, 19, 640-644.

(187) Xiang L, Zhou R, Fu A, Xu X, Huang Y, Hu C. 2011. Targeted delivery of large fusion protein into hippocampal neurons by systemic administration. *J Drug Target*, 19, 632-636.

(188) Yeh FL, Dong M, Yao J, Tepp WH, Lin G, Johnson EA, Chapman ER. 2010. SV2 mediates entry of tetanus neurotoxin into central neurons. *PLoS Pathog*, 6, e1001207.

(189) Yoo AS, Sun AX, Shcheglovitov A, Portmann T, Li Y, Lee-Messer C, Dolmetsch RE, Tsien RW, Crabtree GR. 2011. MicroRNA-mediated conversion of human fibroblasts to neurons. *Nature*, 476, 228-232.

(190) Zhan C, Yan Z, Xie C, Lu W. 2010. Loop 2 of *Ophiophagus hannah toxin b* binds with neuronal nicotinic acetylcholine receptors and enhances intracranial drug delivery. *Mol Pharm*, 7, 1940-1947.

(191) Zhang J, Yun J, Shang Z, Zhang X, Pan B. 2009. Design and optimization of a linker for fusion protein construction. *Prog Nat Sci*, 19, 1197-1200.

(192) Zhang L, Le W, Xie W, Dani JA. 2012a. Age-related changes in dopamine signaling in Nurr1 deficient mice as a model of Parkinson's disease. *Neurobiol Aging*, 33, 1001.e7-16.

(193) Zhang XY, Dinh A, Cronin J, Li SC, Reiser J. 2008. Cellular uptake and lysosomal delivery of galactocerebrosidase tagged with the HIV Tat protein transduction domain. *J Neurochem*, 104, 1055-1064.

(194) Zhang Y, Zhang W, Johnston AH, Newman TA, Pyykkö I, Zou J. 2012b. Targeted delivery of Tet1 peptide functionalized polymersomes to the rate cochlear nerve. *Int J Nanomedicine*, 7, 1015-1022.

(195) Zhou H, Wu S, Joo J, Zhu S, Han D, Lin T, Trauger S, Bien G, Yao S, Zhu Y, Siuzdak G, Schöler HR, Duan L, Ding S. 2009. Generation of induced pluripotent stem cells using recombinant proteins. *Cell Stem Cell*, 4, 381-384.

(196) Zimran A, Altarescu G, Elstein D. 2013. Pilot study using ambroxol as a pharmacological chaperone in type 1 Gaucher disease. *Blood Cells Mol Dis*, 50, 134-137.

(197) Zirzow GC, Sanchez A, Murray GJ, Brady RO, Oldfield EO. 1999. Delivery, distribution, and neuronal uptake of exogenous mannose-terminal glucocerebrosidase in the intact rat brain. *Neurochem Res*, 24, 301-305.

(198) Zorko M, Langel U. 2005. Cell-penetrating peptides: mechanism and kinetics of cargo delivery. Adv Drug Deliv Rev, 57, 529-45.

Copyright Permission, Journal of Drug Targeting:

Permission Question; Use of Article in PhD Thesis

Academic Journals Society Permissions   Thu, Mar 5, 2015 at

<society.permissions@tandf.co.uk>   9:28 AM

To: "paul.gramlich@gmail.com" <paul.gramlich@gmail.com>

Our Ref: MD/GDRT/H25

5th March 2015

Dear Paul Gramlich,

Thank you for your correspondence requesting permission to reproduce the following article published in our journal in your thesis.

'Tat-Tetanus Toxin Fragment C: a novel protein delivery vector and its use with photochemical internalization' By Gramlich PA, Remington MP, Amin J, Betenbaugh MJ, Fishman PS Journal of Drug Targeting ,Vol.21. 662-674

We will be pleased to grant permission on the sole condition that you acknowledge the original source of publication and insert a reference to the article on the Journals website:

This is the authors accepted manuscript of an article published as the version of record in Journal of Drug Targeting 2013http://informahealthcare.com/

Please note that this license does not allow you to post our content on any third party websites or repositories.

Thank you for your interest in our Journal.

Yours sincerely

Michelle Dickson – Permissions & Licensing Executive, Journals.
Routledge, Taylor & Francis Group.
4 Park Square, Milton Park, Abingdon, Oxon, OX14 4RN, UK.
Tel: +44 (0)20 7017 7413
Fax:+44 (0)20 7017 6336
Web:www.tandfonline.com
e-mail:Michelle.Dickson@tandf.co.uk
Taylor & Francis is a trading name of Informa UK Limited,
registered in England under no. 1072954

Copyright Permission, Bioconjugate Chemistry:

Chapter 4 is reproduced, in part, from a manuscript submitted to Bioconjugate Chemistry for peer review. The American Chemical Society (ACS) automatically grants permission for use in a student's thesis. The full ACS policy is available at the listed web address. A portion of the policy is included below as well:

http://pubs.acs.org/userimages/ContentEditor/1218205107465/dissertation.pdf

American Chemical Society's Policy on Theses and Dissertations:
If your university requires you to obtain permission, you must use the RightsLink permission system. See RightsLink instructions at http://pubs.acs.org/page/copyright/permissions.html. This is regarding request for permission to include your paper(s) or portions of text from your paper(s) in your thesis. Permission is now automatically granted; please pay special attention to the implications paragraph below.

The Copyright Subcommittee of the Joint Board/Council Committees on Publications approved the following:

Copyright permission for published and submitted material from theses and dissertations
ACS extends blanket permission to students to include in their theses and dissertations their own articles, or portions thereof, that have been published in ACS journals or submitted to ACS journals for publication, provided that the ACS copyright credit line is noted on the appropriate page(s).

Publishing implications of electronic publication of theses and dissertation material
Students and their mentors should be aware that posting of theses and dissertation material on the Web prior to submission of material from that thesis or dissertation to an ACS journal may affect publication in that journal. Whether Web posting is considered prior publication may be evaluated on a case-by-case basis by the journal's editor. If an ACS journal editor considers Web posting to be "prior publication", the paper will not be accepted for publication in that journal. If you intend to submit your unpublished paper to ACS for publication, check with the appropriate editor prior to posting your manuscript electronically.

CURRICULUM VITAE

Paul A. Gramlich

602 N. Eutaw St.
2nd Floor Apt.
Baltimore, MD 21201

(908) 868-8501
paul.gramlich@gmail.com
 www.linkedin.com/pub/paul-gramlich/a5/310/b48/

Education:

Johns Hopkins University
PhD, Chemical and Biomolecular Engineering

Baltimore, MD
August 2010- July 2015

- "Design, Development, and Delivery of Novel Recombinant Proteins for Neuron-Targeted Therapy and Neuronal Differentiation"
- Research Advisors: Michael J. Betenbaugh, PhD; Paul S. Fishman, MD/PhD
- Cumulative GPA: 3.96/4.0

The Pennsylvania State University
BS, Biochemistry and Molecular Biology

University Park, PA
August 2001-May 2005

- Graduated with honors from Schreyer Honors College
- Cumulative GPA: 3.75/4.0

Awards and Honors:

- Interfraternity Council Academic Achievement Award (2005)
- Gibbons-Farrell Trustee Scholarship (2005)
- Theta Delta Chi Educational Foundation Scholarship (2004-2005)
- Schreyer Honors College Academic Excellence Scholarship (2001-2005)
- Adam Henry Memorial Scholarship (2001)

Academic Research Experience:

Betenbaugh Laboratory, Johns Hopkins Univ.
Fishman Laboratory, VA Medical Center
Graduate Research Assistant

Baltimore, MD
December 2010-Present

- Designed, produced, purified, and delivered a neuron-targeted recombinant glucocerebrosidase intended for neuronopathic Gaucher's disease therapy
  - 17 novel glucocerebrosidase variants designed, transiently expressed, purified, and assessed
  - Performed all molecular biology for expression vector construction and assessment
  - Developed well-format cell-based assays to evaluate enzyme binding/internalization
  - Performed sphingolipid extractions and assisted in the setup of a LC-MS/MS assay to monitor glucosylsphingosine accumulation and reduction
  - Reduced accumulated substrate to wild-type levels with protein treatment
- Created a collection of recombinant transcription factors for neuronal differentiation
  - Evaluated multiple expression systems to maximize transcription factor solubility
- Discovered Tat-TTC, a novel neuronal cell type-specific protein delivery vector
  - Binding and internalization analyzed by direct fluorimetry and fluorescent microscopy

- Optimized a photochemical internalization (PCI) procedure for the release of endosomally-entrapped recombinant proteins and assessed cell viability using LDH assays
- Mentored 11 graduate and undergraduate students

Seeger Laboratory, Fox Chase Cancer Center   Philadelphia, PA
    Biological Lab Technician   June 2005-July 2006
- Gained extensive molecular biology experience; created and modified expression vectors to support Seeger Lab Hepatitis C Virus and West Nile Virus research
- Assessed HCV protein NS3 function using site-directed mutagenesis and novel assays

Pugh Laboratory, Pennsylvania State Univ.   University Park, PA
    Undergraduate Researcher   August 2002-May 2005
- Performed undergraduate research in yeast transcriptional regulation
  - Created haploid *Mot1* mutants for microarray analysis
- Evaluated the effect of physical and chemical stresses on yeast strain survival

Industry Research Experience:

Merck & Co., Inc.   Union, NJ
Schering-Plough Corp.   October 2006-August 2010
Assistant Scientist, Bioprocess Development
- Developed and optimized novel mammalian and bacterial cell culture production processes
- Evaluated and selected CHO clones for high-yield and stable production of recombinant proteins including monoclonal antibodies
- Scaled-up mammalian production processes from shake flasks to 2L bioreactors and subsequently to wave bioreactors and 500L bioreactors for preclinical production
- Evaluated CHO cell line production stability and medium stability
- Supported novel base and feed medium development using the Hitachi HPLC Amino Acid Analyzer
- Collaborated with cell line development, purification, and bioanalytical groups to improve processes
- Prepared over a dozen technical reports

Teaching Experience:

Johns Hopkins University   Baltimore, MD
Teaching Assistant, Transport Phenomena I   Spring 2012 & Spring 2013
- Managed numerous responsibilities including planning and running the recitation sections, teaching class when the instructor was unavailable, grading all exams, and meeting students for extra instruction

Huntington Learning Center   Doylestown, PA
SAT Math and Chemistry Tutor   February 2006-September 2006
- Tutored students using the HLC SAT Math lesson plans and served as the learning center's only chemistry tutor where I generated all lessons and teaching materials

Publications:

Gramlich PA, Westbroek W, Feldman R, Awad O, Mello N, Remington MP, Sun Y, Zhang W, Sidransky E, Betenbaugh MJ, Fishman PS. A peptide-linked recombinant glucocerebrosidase for targeted neuronal delivery: design, production, and assessment. Submitted for peer review.

Mello N, **Gramlich PA**, Remington MP, Fishman PS. Rabies glycoprotein derived peptide shows enhanced neuronal internalization of GFP compared to tetanus toxin fragment C, Tat, and Tet1. In preparation.

Gramlich PA, Remington MP, Amin J, Betenbaugh MJ, Fishman PS. Tat-Tetanus Toxin Fragment C: a novel protein delivery vector and its use with photochemical internalization. *J Drug Targeting* **2013**, 21, 662-674.

Selected Posters and Presentations:

Gramlich, PA et al. Novel neuronal cell type-specific protein delivery vectors: development and application for the delivery of recombinant glucocerebrosidase to neurons. Presented at National Institutes of Health Porter Neuroscience Research Center, Bethesda, MD, 20 November 2014.

Gramlich, PA et al. Use of ganglioside-binding Tet1 peptide and cell-penetrating peptide Tat to deliver glucocerebrosidase to the CNS. Poster presented at the Interagency Botulism Research Coordinating Committee (IBRCC) 2013 Meeting Poster Session, Annapolis, MD, October 2013.

Gramlich, PA et al. Tat-Tetanus Toxin Fragment C: a novel protein delivery vector and its use with photochemical internalization. Poster presented at the Interagency Botulism Research Coordinating Committee (IBRCC) 2012 Meeting Poster Session, Baltimore, MD, October 2012.

Professional Training Courses:

Cellular Bioprocess Technology, University of Minnesota, 2008
Animal Cell Culture Methods and Scale-Up, Pennsylvania State University, 2007